

## INFORMATION TO USERS

This manuscript has been reproduced from the microfilm master. UMI films the text directly from the original or copy submitted. Thus, some thesis and dissertation copies are in typewriter face, while others may be from any type of computer printer.

**The quality of this reproduction is dependent upon the quality of the copy submitted.** Broken or indistinct print, colored or poor quality illustrations and photographs, print bleedthrough, substandard margins, and improper alignment can adversely affect reproduction.

In the unlikely event that the author did not send UMI a complete manuscript and there are missing pages, these will be noted. Also, if unauthorized copyright material had to be removed, a note will indicate the deletion.

Oversize materials (e.g., maps, drawings, charts) are reproduced by sectioning the original, beginning at the upper left-hand corner and continuing from left to right in equal sections with small overlaps. Each original is also photographed in one exposure and is included in reduced form at the back of the book.

Photographs included in the original manuscript have been reproduced xerographically in this copy. Higher quality 6" x 9" black and white photographic prints are available for any photographs or illustrations appearing in this copy for an additional charge. Contact UMI directly to order.

**UMI<sup>®</sup>**

Bell & Howell Information and Learning  
300 North Zeeb Road, Ann Arbor, MI 48106-1346 USA  
800-521-0600



**Contributions of GABA to Reorganization in Raccoon Primary  
Somatosensory Cortex.**

**by**

**Liisa A. Tremere**

**Submitted in partial fulfillment of the requirements  
for the degree of Doctor of Philosophy**

**at**

**Dalhousie University  
Halifax, NS  
May 2000**

**© Copyright by Liisa A. Tremere, 2000**



National Library  
of Canada

Acquisitions and  
Bibliographic Services

395 Wellington Street  
Ottawa ON K1A 0N4  
Canada

Bibliothèque nationale  
du Canada

Acquisitions et  
services bibliographiques

395, rue Wellington  
Ottawa ON K1A 0N4  
Canada

*Your file Votre référence*

*Our file Notre référence*

The author has granted a non-exclusive licence allowing the National Library of Canada to reproduce, loan, distribute or sell copies of this thesis in microform, paper or electronic formats.

The author retains ownership of the copyright in this thesis. Neither the thesis nor substantial extracts from it may be printed or otherwise reproduced without the author's permission.

L'auteur a accordé une licence non exclusive permettant à la Bibliothèque nationale du Canada de reproduire, prêter, distribuer ou vendre des copies de cette thèse sous la forme de microfiche/film, de reproduction sur papier ou sur format électronique.

L'auteur conserve la propriété du droit d'auteur qui protège cette thèse. Ni la thèse ni des extraits substantiels de celle-ci ne doivent être imprimés ou autrement reproduits sans son autorisation.

0-612-57372-9

Canada

**DALHOUSIE UNIVERSITY**

**FACULTY OF GRADUATE STUDIES**

The undersigned hereby certify that they have read and recommend to the Faculty of Graduate Studies for acceptance a thesis entitled "Contribution of GABA to Reorganization in Raccoon Primary Somatosensory Cortex"

---

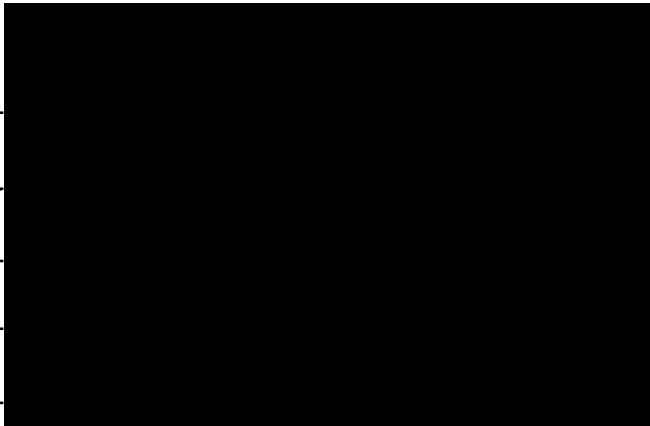
by Liisa Tremere

---

in partial fulfillment of the requirements for the degree of Doctor of Philosophy.

Dated: May 29, 2000

External Examiner \_\_\_\_\_  
Research Supervisor \_\_\_\_\_  
Examining Committee \_\_\_\_\_  
\_\_\_\_\_  
\_\_\_\_\_



# Dalhousie University

**Date:** May 29, 2000.

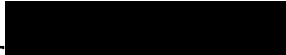
**Author:** Liisa Anne Tremere

**Title:** Contributions of GABA to Reorganization in Raccoon Primary Somatosensory Cortex.

**Department or School:** Physiology and Biophysics

**Degree:** Ph.D.      **Convocation:** October 2000

Permission is herewith granted to Dalhousie University to circulate and to have copied for non-commercial purposes, at its discretion, the above title upon the request of individuals or institutions.

  
Signature of Author

The author reserves other publication rights, and neither the thesis nor extensive extracts from it may be printed or otherwise reproduced without the author's written permission.

The author attests that permission has been obtained for the use of any copyrighted material appearing in this thesis (other than brief excerpts requiring only proper acknowledgement in scholarly writing), and that all such use is clearly acknowledged.

**Dedicated to the memory of Clarence Fritz and Ruth Anderson**

## **Table of Contents**

<b>1. Introduction.....</b>	<b>1</b>
1.1 Reorganization and plasticity.....	1
1.2 Somatosensory Pathways.....	5
1.2 a. Anatomical organization.....	5
1.2.b Activation of the somatosensory cortex from the periphery.....	10
1.3 CNS reorganization following digit amputation in the adult raccoon.....	12
1.3.a Primary Somatosensory Cortex.....	12
1.3.b Thalamic reorganization.....	16
1.3.c Cuneate reorganization.....	20
1.4 Somatosensory reorganization with digit amputation: comparison across species.....	21
1.4.a Reorganization and the somatosensory cortex in primate.....	22
1.4.b Reorganization and the somatosensory cortex in bat.....	24
1.4.c Reorganization and the somatosensory cortex in rat.....	26
1.5 Altered sensory input: comparison of different methods of deafferentation on cortical reorganization.....	27
1.5.a Nerve cut.....	27
1.5.b Nerve crush.....	30
1.5.c Local anesthesia.....	32
1.5.d Crossed median nerve repair, syndactyly and transplant.....	34
1.6 Time course of cortical reorganization.....	35
1.6.a Immediate effects of denervation.....	35
1.6.b Reorganization.....	37
1.7 Regulation of RF size and shape in the normal raccoon.....	40
1.7.a GABAergic inhibition.....	41
1.7.b Histological identification of GABAergic synapses.....	42



1.7.c GABA within the somatosensory system of normal raccoon.....	43
1.7.d Physiological effects of GABA <sub>A</sub> antagonism.....	44
1.8 Regulation of RF size and shape in amputated animals.....	48
1.8.a Activity dependent histochemical changes in rodent.....	48
1.8.b. Activity dependent histochemical changes in primate.....	51
1.9 Role of GABA in cortical reorganization of the adult raccoon: Rationale.....	51
1.10 Hypotheses.....	53
1.10.a BMI effects on RF organization in control animals.....	53
1.10.b BMI effects on RF organization in amputated animals.....	53
<b>2 Methods.....</b>	<b>55</b>
2.1 Animals and surgery.....	55
2.2 Electrophysiological recordings.....	57
2.3 Microiontophoresis of Glutamate, GABA and Bicuculline Methiodide.....	59
2.3.a Application of the Iontophoretic Current.....	62
2.4 Quantifying the change in RF size.....	63
<b>3 Results.....</b>	<b>65</b>
3.1 Description of receptive fields and cortical responsiveness.....	65
3.1.a Receptive field mapping in the control animal.....	65
3.1.b. Receptive field mapping during reorganization.....	74
3.1. c. Changes with time after amputation.....	83
3.2 Effect of iontophoretically applied GABA, glutamate and BMI.....	87
3.2.a Drug application in control cortex.....	87
3.2.b Drug application in reorganizing cortex.....	90
3.3. RF organization before and after GABA <sub>A</sub> antagonism.....	92
3.3.a BMI effects on RF organization in the control animal.....	92

3.3.b BMI effects on RF organization in amputated animals.....	110
<b>4 Discussion.....</b>	<b>143</b>
4.1 GABA <sub>A</sub> receptor antagonism produces RF expansion that is limited to the on- focus digit in control animals.....	144
4.1.a RF expansion.....	144
4.1.b Disinhibition versus excitation.....	148
4.2 The effect of GABA <sub>A</sub> antagonism on deafferented neurons depends on time after amputation.....	148
4.2.a Reactivation of the gyrus.....	148
4.2.b RFs in the amputated animal.....	149
4.2.c BMI induced changes in RFs in the amputated animal.....	151
4.2.d The interaction of time and the role of the GABA <sub>A</sub> receptor in RF expansion.....	154
4.2.e Disinhibition versus excitation.....	155
4.2.f GABA and the reorganization process.....	156
4.3 Other Drug Effects.....	156
4.4 Progression of reorganization at cortical neurons.....	162
4.4.a The generation of new RFs.....	162
<b>5 Conclusion.....</b>	<b>166</b>
<b>6 Appendices .....</b>	<b>168</b>
<b>7 Bibliography.....</b>	<b>181</b>

## List of Figures

Figure 1	Outline of the ascending somatosensory pathway.....	7
Figure 2	The process of reorganization in the deprived cortical region..	18
Figure 3	Cortical representation of the fourth digit.....	67
Figure 4	Sampling distribution by cortical depth for control and amputated animals.....	71
Figure 5	Distributions of RF size on different parts of the forepaw in control animals.....	73
Figure 6	Average number of cells per penetration at different time intervals after amputation.....	78
Figure 7	Examples of RF types found in the deafferented region during reorganization.....	81
Figure 8	Proportion of joined, split and confined fields at different times after amputation.....	86
Figure 9	RFs showing the range of expansion produced by BMI in control animals.....	95
Figure 10	Frequency histogram of the expanded RF areas for the distal and proximal digit pad and palm.....	99
Figure 11	RF size & expansion vs depth in the control animal.....	102
Figure 12	Absolute RF expansion categorized by functional region of the forepaw.....	105
Figure 13	Relative RF expansion categorized by functional region of the forepaw.....	107
Figure 14	Variability of RF expansion shown as box plots.....	109
Figure 15	Original RF size and expanded RFs versus depth in the amputated animal.....	112
Figure 16	Example of BMI application adding subfields to a joined field.....	116
Figure 17	Example of BMI application converting a split field into a joined field.....	120
Figure 18	Example of a transition from a confined field to a split field with BMI.....	122

Figure 19	Example of a transition from a confined field into a joined field with BMI.....	125
Figure 20	Example of a single claw RF that expanded to include claws on adjacent digits with BMI.....	127
Figure 21	RF appearance before and after transition.....	131
Figure 22	Differential effects of glutamate and BMI on a RF.....	134
Figure 23	Different effects of glutamate and BMI on RFs at 8 weeks post-amputation.....	137
Figure 24	Differential effects of glutamate and BMI on RFs at 11 – 15 weeks after amputation.....	139
Figure 25	Different effects of glutamate and BMI on RFs at 19 – 37 weeks after amputation.....	142
Figure 26	Opposite effects of GABA <sub>A</sub> antagonism and reorganization of cortical neurons.....	160
Appendix		
A1	Cytochrome oxidase reactivity in control and deafferented cortex.....	175
A2	IR profiles for GAD and an example of somatosensory cortical layers.....	180

## List of Tables

Table 1	Number of penetrations and cells in the 4 <sup>th</sup> digit representation.....	75
Table 2	Number of joined, split and confined fields at different times after amputation.....	84
Table 3	Effects of drug application on neuronal excitability.....	89
Table 4	The number of neurons showing transitions of RF classification following BMI application.....	117
Table 5	Summary of the frequency of RF expansion and transition in reorganizing cortex.....	128

## **Abstract**

In the adult raccoon, neurons in somatosensory cortex acquire new receptive fields during denervation-induced reorganization. Furthermore, RF size changes considerably during reorganization. Intra-cortical inhibition has been shown to regulate the RFs of cortical neurons in the normal cat and primate. The central question of the present thesis was whether intra-cortical inhibition could account for differences between control neurons and neurons studied at different stages of reorganization. To examine this possibility, bicuculline methiodide (BMI), a specific antagonist of the GABA<sub>A</sub> receptor was applied to cortical neurons in 12 normal raccoons and 10 raccoons that had previously undergone amputation of the fourth forepaw digit 2 weeks to 37 weeks earlier. BMI application altered the receptive fields in 62/102 neurons in the control animals and 64/103 neurons in denervated cortex. In reorganized cortex, simple receptive field expansion that preserved the shape of the original receptive field was seen in 39 neurons. In 22 cells BMI produced more complex changes such as a transition from single digit to multi-digit fields after BMI application, a degree of expansion that was never produced in the normal animal. These data indicate that pre-existing anatomical connections cannot account for the appearance of new RFs after amputation and suggest that cortical inhibitory synapses shape or focus the RF in the normal cortex as well as during reorganization.

## List of Abbreviations and Symbols

ABC	avidin biotin complex
BMI	bicuculline methiodide
ChAT	Choline Acetyltransferase
CNS	central nervous system
cm	centimeter
CO	cytochrome oxidase
D	Kolmogorov Smirnov non-parametric test for independent (small) samples
DAB	diaminobenzidine (DAB)
DC-ML	dorsal column medial lemniscal system
DMSO	dimethylsulphoxide
df	degrees of freedom
EPSP	excitatory post-synaptic potential
Fig.	Figure
g	grams
GABA	gamma aminobutyric acid
GABA <sub>A</sub>	gamma aminobutyric acid receptor, subtype A
GAD	glutamic acid decarboxylase
H	Kruskal-Wallis, non-parametric analysis of variance by ranks
Hz	Hertz
i.m.	intra-muscular
I.V.	intra-venous
IR	immunoreactive
kDa	kiloDalton
KHz	kilohertz
M	molar

<b>MΩ</b>	<b>megOhm</b>
<b>mm<sup>2</sup></b>	<b>millimeter squared</b>
<b>min</b>	<b>minute</b>
<b>n</b>	<b>number</b>
<b>nA</b>	<b>nanoAmperes</b>
<b>NGS</b>	<b>normal goat serum</b>
<b>p</b>	<b>probabilty value</b>
<b>PBS</b>	<b>phosphate buffered saline</b>
<b>sec</b>	<b>second</b>
<b>kg</b>	<b>kilogram</b>
<b>mg</b>	<b>milligram</b>
<b>msec</b>	<b>millisecond</b>
<b>mm</b>	<b>millimeter</b>
<b>RF</b>	<b>receptive field</b>
<b>S1</b>	<b>primary somatosensory cortex</b>
<b>SE</b>	<b>simple expansion</b>
<b>t</b>	<b>Student's t value</b>
<b>T</b>	<b>transition</b>
<b>TBS</b>	<b>Tris buffered saline</b>
<b>Tr</b>	<b>triradiate sulcus</b>
<b>wks</b>	<b>weeks</b>
<b>χ<sup>2</sup></b>	<b>Chi square, non-parametric test for independent samples</b>
<b>°C</b>	<b>degrees Celsius</b>
<b>μm</b>	<b>micrometer</b>
<b>μl</b>	<b>microliter</b>



## **Acknowledgements**

I would like to thank my supervisor, Dr. D. Rasmusson for the opportunity to complete this project and for his help, patience and instruction throughout my graduate education. I would also like thank my thesis committee for their feedback and direction. Thank you also to Dr. Phillip Hicks who offered equipment and guidance that greatly facilitated the completion of this Ph.D. Superb technical assistance was also provided Mr. Stephen Whitefield.

Sincerest thanks to my friends and family, in particular, I would like to thank my father for his guidance and sound advice, my mother for her compassion and my sister for her enthusiasm. Heartfelt thanks to Raphael Pinaud, for his efforts, advice and support were critical to the completion of this thesis.

# ***1. Introduction***

## **1.1 Reorganization and plasticity**

Neural plasticity is a property of neurons that allows for permanent modifications in connectivity and performance. The term plasticity has been used to describe both the capacity to change the performance and structure of neural circuits as well as the process by which the underlying connectivity is changed. For the purpose of clarity, I will restrict the use of the term plasticity to describing this capacity for change and the terms development, learning and repair when describing processes or biological forces that mediate changes using plasticity. These processes are the major factors that shape the performance of the central nervous system (CNS) throughout life.

Neural development includes the generation of cells, their migration and formation into neural circuits. Developmental changes are mainly determined by the genome and proceed according to an internal and pre-determined set of instructions but some aspects can be modified by environmental factors. This circuitry supports both reflexive and instinctive behaviors and acts as a template upon which later changes are made.

Learning is a second major force that shapes the connectivity of the CNS. It has been described as the change in behavior that results from experience. One of the greatest

challenges in neuroscience has been to relate physical changes in the CNS to the process of learning. At the synaptic level, learning is hypothesized to depend upon stable alterations in synaptic strength that affect cell behavior. The cumulative effects of such changes modify the performance of neural circuits and are the physical correlates of modified behavior of the organism. One demonstration of the link between experience and altered CNS connectivity is the expansion of cortical representation areas that are activated during extensive behavioral training. For example, an expansion of the cortical digit representation occurs in owl monkeys that are rewarded for touching a spinning disc for prolonged periods (Jenkins et al. 1990).

The third process that relies on neural plasticity is CNS repair that promotes the reactivation of deafferented neurons and optimizes the survival and performance of damaged pathways. To some extent CNS repair is probably a continuous process that corrects the effects of minor injuries and age-related degradation of neural circuits. In addition, CNS repair is crucial for regaining capabilities following more severe insults such as stroke.

The reactions of the CNS to damage of sensory pathways have been studied extensively in order to understand its capacity for functional recovery following a trauma. It has been shown that parts of the CNS undergo a reordering of the highly topographic organization in response to a disruption of sensory inputs. The outcome of sensory deprivation was initially characterized in regions of cerebral cortex, and was referred to

as the process of “reorganization”. This term is now conventionally used to describe changes in a sensory pathway that follow a stable alteration in sensory input. The reorganizational process has been identified in several sensory modalities.

The majority of experimental manipulations designed to study this process have been carried out in the somatosensory system and have focused on the sense of touch. Much of the interest in this system originated from a clinical need to manage phantom limb sensations that are perceptions in the absence of the corresponding part of the body. A second practical reason for studying the somatosensory system is that the skin can be accessed and manipulated easily. Neurons in the somatosensory cortex that serve the sensation of touch have receptive fields (RFs) that are especially well defined. This feature facilitates somatotopic mapping and the assessment of reorganization after injury. In order to understand the variety of outcomes for CNS reorganization, this process has been explored with several denervation and/or recording techniques and different species including the cat (Kalaska and Pomeranz 1979), raccoon (Kelahan et al. 1981; Rasmusson 1982; Kelahan and Doetsch 1984), rat (Wall and Cusick 1984), owl monkey (Merzenich et al. 1983a; Merzenich et al. 1983b) and flying fox (Calford and Tweedale 1988).

Kalaska and Pomeranz (1979) conducted one of the landmark papers on reorganization of the somatosensory system in the somatosensory cortex of cats. These investigators crushed and ligated the superficial radial, median and ulnar nerves, which

abolished sensory input from the forepaw. After 8 weeks of recovery from the denervation, a recording electrode was placed into the region of the primary somatosensory cortex that responded to stimulation from the forearm in the normal animal. These authors found that sensory deafferentation did not result in an unresponsive region of cortex. Instead many of the neurons (52%) encountered responded to stimulation of the neighboring areas of intact skin on the forearm. However, in both the mature and immature animals the reorganized cortex was generally less responsive to evoked activity than the corresponding area of cortex in the control animals. Another important finding in this study was the appearance of abnormally large RFs, an outcome that was not seen in the kitten but was characteristic of reorganization in the adult. Similar differences in the average RF size were subsequently demonstrated in adult and immature raccoons (Carson et al. 1981; Kelahan et al. 1981; Rasmusson 1982; Kelahan and Doetsch 1984), the experimental animal used in the present study.

It has been difficult to distinguish the ways that reorganization may alter CNS connectivity from the influences of developmental or learning processes. The experiment by Carson et al. (1981) indicated that in young animals reorganization might interact with developmental processes. However, the fact that reorganization has been demonstrated in adult mammals proved that reorganization is not limited to early developmental periods. It has been equally difficult to separate reorganization, defined as neural restructuring caused by deafferentation, from changes in activation patterns resulting from behavioral

developmental processes. However, the fact that reorganization has been demonstrated in adult mammals proved that reorganization is not limited to early developmental periods. It has been equally difficult to separate reorganization, defined as neural restructuring caused by deafferentation, from changes in activation patterns resulting from behavioral changes such as postural adjustments or other learned compensatory behaviors that result from the altered use of the injured forepaw.

## **1.2 Somatosensory Pathways**

### **1.2 a. Anatomical organization**

The major pathway studied in connection with somatosensory reorganization is the dorsal column - medial lemniscal (DC-ML) system (Fig. 1). Sensory activation at each level of this pathway is initiated by mechanoreceptors in the skin that are responsive to touch. The innervation pattern of the skin is reflected within the somatotopic organization of this pathway. The prefix "somato" refers to the body and "topographic" describes the fact that neighboring areas in the CNS represent neighboring areas of the receptive sheet. This somatotopic organization is found at both of the major relay nuclei in the pathway (dorsal column nuclei and thalamus) and may be important in preserving many aspects of the spatial relationship of sensory receptors during sensory processing.

**Figure 1**

Schematic representation of the ascending somatosensory system for the body.

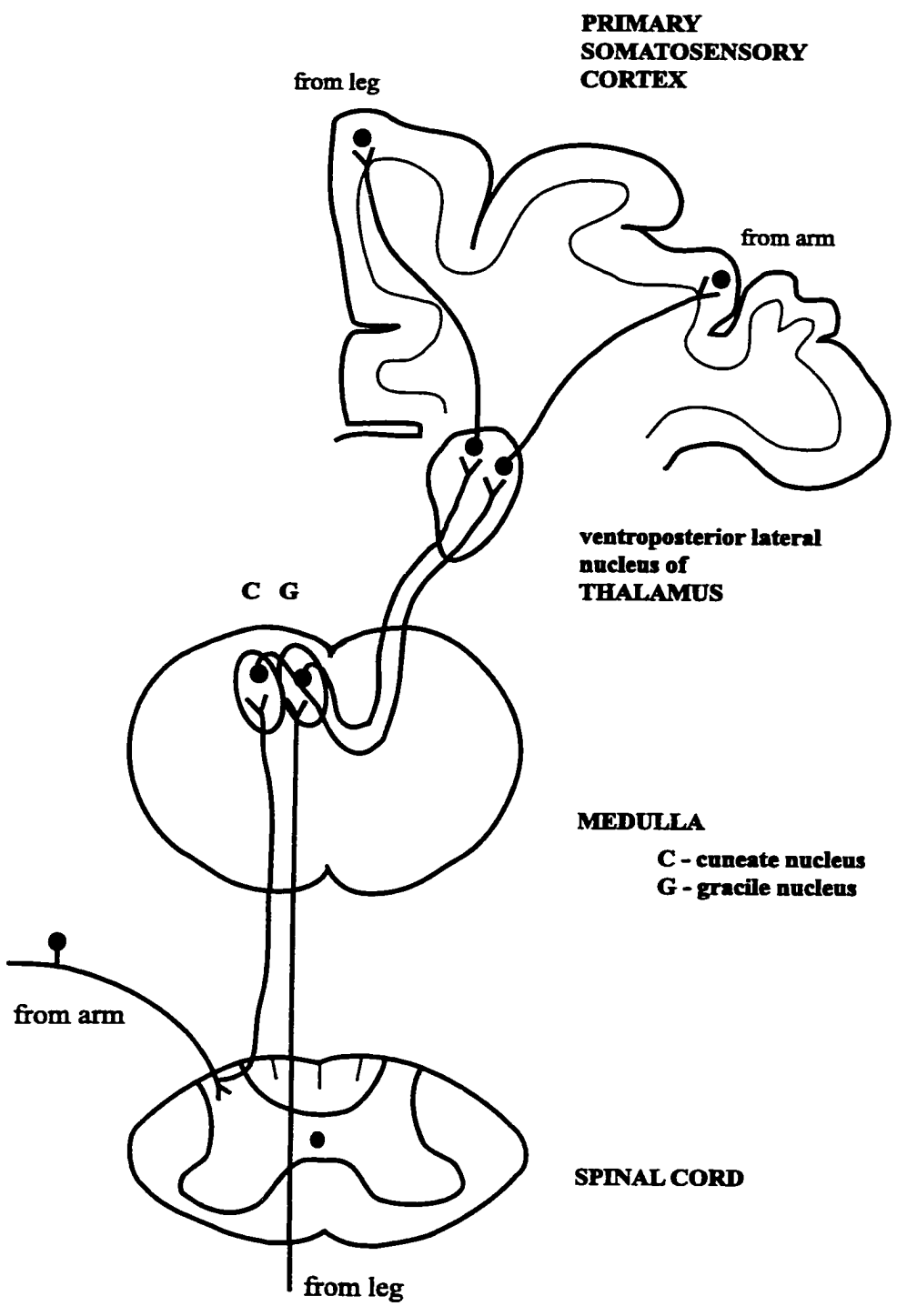


**Figure 1**



For example, physical proximity of functionally related cortical neurons might have metabolic advantages, as it should be more efficient to form and maintain connections between close neurons. Likewise, the timecourse and metabolic effort for communication between cells should be reduced according to the distance between cells.

The first order neurons of the DC-ML system are afferents with specialized nerve endings (receptors) in the skin and their cell bodies in the dorsal root ganglion (DRG). The axons from these DRG neurons send projections that ascend in one of two fasciculi within the dorsal columns. The fasciculus gracilis conveys information from the lower limbs and lower thoracic regions. Information from the upper thoracic region and the upper limbs is conveyed via the fasciculus cuneatus.

Information from the upper and lower body continues to be segregated in the brainstem. Each fasciculus terminates in a separate nucleus (the cuneate and gracile nuclei) that is found near the dorsal surface in the medulla. The cells in these brainstem nuclei send axonal projections that cross the midline and ascend contralaterally as the medial lemniscus. These second order neurons form synaptic connections with neurons in the ventroposterior lateral (VPL) nucleus of thalamus. Neurons in the thalamus send projections to primary somatosensory (S1) cortex and provide the major afferent drive on both the excitatory and inhibitory cortical neurons (Burt 1993).

The somatotopic organization of the DC-ML system may be of particular importance in the cortex where excitatory neurons and inhibitory interneurons have been

proposed to interact extensively in the dynamic regulation of RF size, threshold, latency of response and other specialized RF features such as directional sensitivity or vibration detection (Mountcastle 1957; von Békésy 1967; Costanzo and Gardner 1980; Gardner and Costanzo 1980; Dykes et al. 1984).

### **Somatosensory system of the adult raccoon**

Research on the somatosensory system in the adult raccoon provided early examples of reorganization in the adult mammal. The forepaw representation of this species is particularly well suited for studying CNS reorganization as it is exceptionally large throughout the ascending pathway of the somatosensory system. In the first detailed description of this system in raccoon, Welker and Seidenstein (1959) identified that approximately 60% of the entire primary somatosensory cortex is dedicated to the forepaw and that over 95 % of this representation is dedicated to processing information from the glabrous skin. Therefore, this representation is considerably larger than the corresponding representation area in primates (Welker and Seidenstein 1959). Amputation of a forepaw digit affects approximately 30 - 40 mm<sup>2</sup> of somatosensory cortex. In the owl monkey, the species of primate that is commonly used in reorganization studies, the affected region is considerably smaller, between 0.5 and 2 mm<sup>2</sup> (Turnbull and Rasmusson 1991).

In the raccoon, the neurons responsive to each digit have a clear somatotopic organization and are distinctly segregated by regions of white matter at each relay station.

This physical segregation of neural processing from different parts of the forepaw is more pronounced in this species than in primates or rodents. In the cortex there are distinct gyri that represent each digit; these gyri surround the triradiate sulcus. A large proportion of each gyrus is responsive to cutaneous mechanoreceptors found in the distal pad of the digit which is the most densely innervated region of the digit. (Munger and Pubols 1972; Rice and Rasmusson 2000). The palm is represented posterior to the digit representations, behind the triradiate sulcus.

### 1.2.b Activation of the somatosensory cortex from the periphery

Neurons in the DC-ML system respond best to stimuli that activate the mechanoreceptors in the skin. Under experimental conditions, cutaneous receptors and the corresponding ascending sensory pathway can be stimulated with an instrument that depresses small regions of skin. With this apparatus it is possible to probe the skin surface until a neural response can be evoked. For each neuron, the RF is defined as the region of skin that produces an optimal excitatory response that has the greatest relative magnitude (the most action potentials per stimulation) and the shortest latency. This RF is not strictly the expression of all excitatory anatomical inputs to a given neuron but is the reflection of relative excitatory and inhibitory drives on a final target neuron (for review in somatosensory cortex, Laskin et al. 1979). Supra-threshold mechanical stimuli

from neighboring regions outside the RF may also activate the neuron but with a lesser magnitude and at a longer latency (Laskin and Spencer 1979).

In somatosensory research the convention has been to define the RF using mechanical stimulation because this method of stimulation does not activate pain and temperature responsive receptors and therefore more closely resembles natural touch. Both rapidly and slowly adapting neurons have been identified within the DC-ML system. Rapidly adapting neurons have the strongest discharge at the onset of the stimulus and may also discharge at the offset, whereas slowly adapting neurons continue to fire action potentials for the duration of stimulus contact.

Many studies in CNS reorganization have used electrical stimulation to activate populations of CNS neurons. This method of stimulation allows for greater precision of the intensity and onset of the stimulation; however, this method is not selective for mechanoreceptors.

The terms "on-focus digit" and "off-focus digit" have been used to describe the location of stimulation relative to the RF. Stimulation that is applied to the digit containing the RF is called "on-focus" stimulation. For example, if a cell has a RF on the fourth digit, this fourth digit would be the "on-focus" digit and stimulation from other digits or the palm would be classified as "off-focus". The response to off-focus stimulation is characterized as having a longer latency and higher threshold. In addition,

it has been shown that off-focus stimulation can have an inhibitory effect on many somatosensory cortical neurons. This response profile reflects the fact that inhibitory RFs are usually larger than excitatory RFs (Mountcastle and Powell 1959; Laskin and Spencer 1979).

### **1.3 CNS reorganization following digit amputation in the adult raccoon**

#### **1.3.a Primary Somatosensory Cortex**

Removal of the third, fourth or fifth forepaw digit has been shown to provoke CNS reorganization in the adult raccoon (Rasmusson 1982; Kelahan and Doetsch 1984). Digit amputation permanently destroys the connection between a cortical somatosensory neuron and its RF. The result of this procedure is that cortical neurons acquire new RFs. The region of cortex that had its inputs disrupted by the amputation has been referred to as either deafferented or deprived cortex. The progression of reorganization in this region has been evaluated in terms of the size of the new RFs, their locations on the forepaw and the latency at which the reorganized cells respond to mechanical or electrical stimulation. This effect of time appears in all species studied and has been used as a framework in describing the considerable differences in cortical responsiveness immediately after denervation and during the early and late stage of reorganization

(Merzenich and Kaas 1982; Rasmusson and Turnbull 1983; Turnbull and Rasmusson 1990; Cusick 1996).

Immediately after digit amputation the responsiveness of cortical neurons in the deafferented gyrus is drastically altered (Rasmusson and Turnbull 1983; Kelahan and Doetsch 1984). The strong RA response, typically found at the majority of the neurons in this cortical region, is eliminated but a strong excitatory off – response remains (Rasmusson and Turnbull 1983). When Kelahan and Doetsch (1984) used low intensity mechanical stimulation to map the RFs of cortical neurons immediately after amputation they found that neurons in the deafferented cortex had abnormally large RFs that often included skin from at least one of the adjacent digits. This responsiveness to mechanical stimulation disappears shortly after amputation.

In the 1 – 2 weeks that follow the amputation, the deafferented pathway is characterized as lacking evoked somatosensory activity and having an elevated level of spontaneous activity. The term "functional silence" therefore refers specifically to the inability to evoke a response in these cortical neurons using mechanical stimulation in the periphery. Rasmusson et al. (1992) also found that digit removal increased the incidence of inhibition from off-focus stimulation by an average of 16%, which may have accounted for some aspects of the loss of responsivity.

The fringe area of the deprived cortex had a different response profile when compared with the functionally silenced region and tended to have response properties

that resembled cortex in the control condition (Kelahan and Doetsch 1984). One of the main differences between the transitional or fringe area and the core of deafferented cortex was that low intensity stimuli evoked responses from the fringe region almost immediately after amputation. In contrast, at least two weeks were normally required before similar activity was detected in the core region of cortex that had been completely deafferented from low-threshold, peripheral mechanoreceptors. Despite the lack of somatotopy in this fringe area, the early recovery of responsiveness in the fringe has been hypothesized to reflect the presence of pre-existing anatomical overlap, from adjacent digits that strengthen after amputation (Rasmusson 1982; Rasmusson and Turnbull 1983; Kelahan and Doetsch 1984).

By two weeks post-amputation, new receptive fields began to appear in the core area of the deprived cortex. The appearance of new RFs may have been partially enabled by a decrease in inhibition. Rasmusson and Turnbull (1991) demonstrated that by 2 weeks after the amputation the number of sites responding to off-focus stimulation with an inhibitory response decreased by half. The limited excitatory activity that appeared at two weeks post-amputation could not be considered as typical for this region of somatosensory cortex. Instead, RFs in deprived cortex had thresholds that were much higher than in control cortex and were abnormally large, often spanning more than one digit (Rasmusson 1982; Kelahan and Doetsch 1984; Rasmusson et al. 1992).

By eight weeks after the amputation, there was an increase in the responsiveness of the deprived cortex, particularly to moderate and high intensity mechanical stimulation. Additionally, a few sites could be found in the deprived region that responded to low intensity stimulation. This was the first time point at which low threshold responses could be found. There was also greater variability in the sizes of the new RFs. Some cortical neurons responded to mechanical stimulation of the entire palmar surface, some had large multi-digit fields or responded to dorsal, hairy skin stimulation while other neurons had acquired RFs that were similar in size to the control condition (Rasmusson 1982; Kelahan and Doetsch 1984).

After sixteen weeks of denervation there was nearly a complete reactivation of the deafferented area. At this timepoint 92% of the sites sampled by electrophysiological recording responded to glabrous skin on the forepaw. This high rate of responsiveness is in sharp contrast with the percentage of responsive sites found at two weeks (5%). At the later interval there was an increase in the number of sites that were responsive to low and moderate intensity inputs, as well as in the number of sites that had small RFs. It was still possible, however, to find cortical neurons that had abnormally large RFs (Rasmusson 1982).

Kelahan and Doetsch (1984) found that by 36 - 52 weeks post-amputation the deprived region was highly responsive to cutaneous inputs from the glabrous surface of the adjacent digits. By 52 weeks RF parameters such as size and threshold were



quantitatively similar to the control condition for many cortical neurons (Kelahan and Doetsch 1984). In fact there was no statistically significant difference from controls in the mean threshold pressure that successfully evoked cortical responses beyond 36 weeks post-amputation. Likewise, the overall responsiveness of the deafferented region was similar to an unamputated animal. Yet, three features remained which could be used to differentiate the deprived cortex from control cortex. First, activation of a cortical neuron from the new RFs was slow; this latency reflected the normal off-focus condition rather than control values. Second, the reorganized region was not somatotopically organized. Third, some of the neurons found in the reorganized cortex had RFs of abnormal size and shape that have never been found in the unamputated animal. Therefore, reorganization is either incomplete by 52 weeks post-amputation or certain differences between control and reorganized cortex are permanent. The schematics in Figure 2 illustrate one hypothesized pattern for reactivation of deafferented cortex.

### 1.3.b Thalamic reorganization

An important consideration in understanding reorganization is whether the changes seen at the cortical level are actually occurring in the cortex or simply reflect reorganization earlier in the DC-ML pathway. Few studies have examined subcortical reorganization. In the thalamus, the immediate effect of amputation was an increase in the inhibition produced by off-focus stimulation. This effect was specific to stimulation

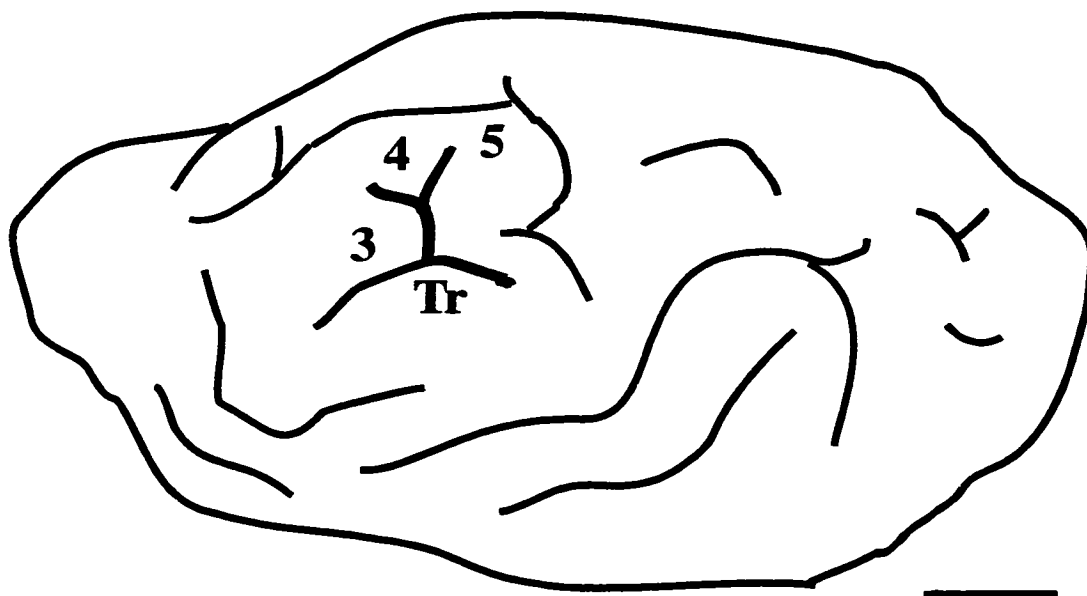
**Figure 2**

The process of reorganization in the deprived cortical region.

(A) a diagram of the left hemisphere of the raccoon brain. The cortical representations of the third, fourth and fifth digits surround the triradiate sulcus (Tr).

(B) Following amputation of the fourth digit, that cortical area begins to respond to mechanical stimulation of the skin on the third and fifth digits.

A



B

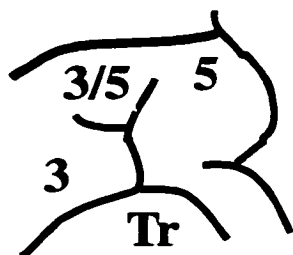


Figure 2

from the glabrous regions of the intact digits and was not seen in response to stimulation of the hairy skin (Rasmusson et al. 1993b). At longer intervals after amputation of the fourth digit there were several signs that reorganization had taken place within the representation area that had been deafferented (Rasmusson 1996). One indication was that no functionally silent area could be detected between the representational areas of the third and fifth digits. A second sign was that the neurons with RFs of abnormal shape and size and location on the forepaw (e.g. multi-digit fields) were found in the position that corresponded to the deafferented zone. A third consideration was the region between the end of the normal fifth digit representation and the beginning of the normal third digit representation was approximately equal to the size of the other digit representation areas (Rasmusson 1996).

Although the size and shape of new RFs in the deafferented region of the VPL differed remarkably from control neurons this was not the case for other response properties of reorganized cells in the thalamus when tested with electrical stimulation (Rasmusson 1996). Four months after amputation, 91% of the neurons in the deafferented region had acquired RFs on off-focus or adjacent digit versus 63% in the control animal. In addition to the appearance of new cells that were responsive to off-focus stimulation, the threshold for activation by electrical stimulation from an off-focus digit was lowered.

### 1.3.c Cuneate reorganization

Primary afferent neurons in the DC-ML system terminate on cells within the cuneate nucleus; therefore changes in the periphery should be strongly reflected at this level. The RFs of cuneate neurons observed immediately after denervation did not include the adjacent digits (Northgrave and Rasmusson 1996). This finding challenges the hypothesis that the appearance of new RFs is explained by the release of inhibition at pre-existing connections from off-focus digits. In the normal animal, many neurons in the cuneate nucleus do not have an excitatory response to the off-focus digit even when tested at relatively high (electrical) stimulation intensities. Although two-thirds of cuneate neurons did respond to off-focus stimulation they responded at longer latencies and with lower probabilities when compared with on-focus stimulation. Two to five months after amputation cuneate neurons, however, the probability of a response to off-focus stimulation of cuneate neurons increased as did the response magnitude. The cells also responded to stimulation at lower thresholds of electrical stimulation (Rasmusson and Northgrave 1997).

As in the thalamus and cortex, neurons in the deafferented region of the cuneate nucleus also had abnormally large RFs. Cuneate neurons had an increased probability for firing from off-focus stimulation and had decreased thresholds for off-focus activation. Deafferented cells in the cuneate nucleus did not have shortened latencies due to

reorganization, and therefore responded on a time scale that resembled the control off-focus response.

Reorganization identified in both cuneate and thalamus indicates that reorganization at the cortical level is not purely a cortical phenomenon. Furthermore, the failure to see the immediate appearance of new RFs in either thalamus or cuneate indicates that the changes in RF properties at longer post-amputation periods may involve more than the strengthening of pre-existing connections (Northgrave and Rasmusson 1996).

#### **1.4 Somatosensory reorganization with digit amputation: comparison across species**

CNS reorganization has been demonstrated in several species of adult mammal and within a variety of sensory systems (reviewed by Kaas et al. 1983; Kaas 1991). Experimental observations and conclusions must often be interpreted according to the species and deprivation method used because of the species specific features of the pathways (for review see Johnson 1990) and different degrees of sensory interruption.

In this thesis digit amputation in the raccoon was used to study the acquisition of new RFs as a result of somatosensory reorganization. Similar investigations following digit amputation have been conducted in adult owl monkey, flying fox, and rat. However,

there are a number of species specific features that can influence somatosensory reorganization including differences in peripheral innervation patterns and central nervous system connectivity, both of which have been postulated to reflect behavioral importance of the body part to the experimental subject. The following paragraphs review the outcomes of CNS reorganization as a result of digit amputation in the above mentioned species. Relevant examples of similarities and differences between the raccoon and each of these species will also be discussed.

#### 1.4.a Reorganization and the somatosensory cortex in primate

One of the principle differences found between primate and raccoon was that amputation of the third digit resulted in a somatotopic reorganization of the deafferented cortex in the owl monkey (*Aotus trivirgatus*) (Merzenich et al. 1984). In contrast cortical reorganization in the raccoon is not somatotopically organized (Rasmusson 1982; Kelahan and Doetsch 1984). In a second experiment Merzenich et al. (1984) tested the spatial limits of cortical reactivation by amputating two adjacent digits. This procedure produced a functionally silent region found at distances beyond 700  $\mu\text{m}$  from the intact cortex. This silent cortical area was still unresponsive to cutaneous stimulation eight months after amputation (Merzenich et al. 1984; Garraghty et al. 1994).

Johnson (1991) has reported that there are several common features of the somatosensory pathway in raccoon and anthropoid primates. Although the organization

of cortical primary and secondary somatosensory regions of raccoon cortex may be more similar to the cat rather than the primate, the otherwise high degree of anatomical agreement has been postulated to reflect similarities in the behavior of these animals with respect to use of the forepaw. Both raccoons and primates use their digits extensively in tactile exploration and this behavioral importance of cutaneous sensory information corresponds to the disproportionately large representation of the distal pad of the digit in S1. In the periphery, this behavioral importance is also indicated by the high density of innervation at the distal pad, especially the tips, features shared by both types of animal. Interestingly, the distribution patterns of the new RFs that appear during CNS reorganization (on distal digits and around the wound) are also similar between the raccoon and primate. These common attributes of the primary somatosensory pathway greatly facilitate comparisons between the reorganization process for these two species.

Despite the similarities, several important differences between the two species have been observed in cortical reorganization that followed digit amputation. Of primary importance are the discrepancies in the degree of somatotopy for the reorganized area. Reorganization in the cortex of the primate is somatotopic, whereas in the raccoon it is not. Differences in the spatial constraints of cortical reorganization have also been identified. Merzenich et al. (1983) initially reported that reorganization would not proceed more than 700  $\mu\text{m}$  from intact cortex. Subsequently, this conclusion was challenged by the findings of Pons et al. (1991), who studied reorganization after very



long post-amputation times and documented cortical reorganization of a much greater spatial extent.

#### 1.4.b Reorganization and the somatosensory cortex in bat

Somatosensory reorganization in response to digit amputation has been studied extensively in bat. Both the flying fox (*Pteropus poliocephalus*) and the little red flying fox (*Pteropus scapulatus*) have been used (Calford and Tweedale 1988; Calford and Tweedale 1991a; Calford and Tweedale 1991b; Calford and Tweedale 1991c). Removal of the single forelimb digit in either species was associated with the immediate appearance of new large RFs on adjacent regions of the wing and arm (Calford and Tweedale 1988). A similar effect was produced with a temporary block of nerve conduction in the digit (Calford and Tweedale 1991a). One week after digit amputation the RFs found in the deafferented region were small and confined to the region where the digit had been removed. These authors concluded that large fields were due to an initial unmasking of excitatory connections. With time, inhibitory mechanisms were reinstated and reduced the area of the new RF (Calford and Tweedale 1988). Later work by this group implicated C-fibers, which conduct pain related sensory signals, as mediators in the RF size of cortical neurons through inhibitory mechanisms (Calford and Tweedale 1991b). These authors concluded that a cortical neuron is connected to a RF as well as a large surrounding area of unexpressed but viable excitatory inputs. Such findings have

been used to support the hypothesis that new RFs result from the unmasking of pre-existing excitatory connections of a cortical neuron.

The acute effects of digit amputation on cortical reorganization in the bat and raccoon are different, as new excitatory RFs appear immediately after digit amputation in the bat, but not in the raccoon. However, the chronic effects of digit amputation in the bat are similar to those described for raccoon. In both species, abnormally large RFs become reduced in size with increased time after the amputation. However, one important difference between the two species is that reorganization in the raccoon resulted in the appearance of small RFs on adjacent digits and/or the amputation site. Sensory activity that is evoked from the amputation site is likely caused by direct activation of the nerve stumps and may not reflect reorganization. Since increased post-amputation time is associated with a decrease in the number of RFs around the wound and an increase in RFs found on the digits, the RFs on the digits are more likely to be the result of reorganization. In the bat, assessing reorganization is complicated because RFs at short and long post-amputation periods always overlapped the amputation site. Hence, in the flying fox it may be more difficult to separate the effects of disuse on RF size during reorganization from the acquisition of new small RFs (Calford and Tweedale 1988; Calford and Tweedale 1991a; Lundy-Ekman 1998).

### 1.4.c Reorganization and the somatosensory cortex in rat

Digit amputation in rat resulted in the expansion of intact cortical representations into the deafferented region, an effect that could be detected at 1 month post-amputation. At this time, new RFs were found on one or both adjacent digits and were somatotopically organized (McCandlish et al. 1996). Doetsch et al. (1996) also reported the immediate enhancement of the off-focus response within the cortical representation of the amputated digit. However, comparisons of the immediate effects between digit amputation in the rat and raccoon may be especially inappropriate. In a normal rat, many cortical neurons have multi-digit RFs, therefore part of the original cutaneous RF would remain after the amputation of a single digit, a situation that does not occur in raccoons (Doetsch et al. 1996).

One of the most prominent anatomical differences in the somatosensory pathway of the rat and other mammals is the massive and complex cortical representation of the vibrissae. In contrast, the raccoon has the greatest proportion of primary somatosensory cortex dedicated to the forepaw representation (Welker and Seidenstein 1959; Johnson 1990). These differences in the anatomical organization of the somatosensory systems are presumed to reflect different degrees of behavioral importance for the forepaw in either animal that may influence any use dependent aspects of the reorganization process.

## **1.5 Altered sensory input: comparison of different methods of deafferentation on cortical reorganization**

Digit amputation is only one of several experimental methods that have been used to produce altered sensory activity at the forepaw. Some other methods of denervation include transection of one or all nerves from the forepaw nerve crush, application of local anesthetics and cooling. Each method has been associated with different consequences for cortical reorganization including the size and shape of RFs, the completeness of cortical reactivation and the time course of reorganization (Brandenberg and Mann 1989; Kaas 1991; Garraghty et al. 1994). The following paragraphs provide examples of permanent and reversible deafferentation techniques that have been used to block sensory input from regions of the forepaw.

### **1.5.a Nerve cut**

Turnbull and Rasmusson (1990) reported pronounced differences in the denervation patterns that were apparent immediately after digit amputation compared to the transection of a combination of ventral and/or dorsal nerves that innervate the fourth digit in the raccoon. When the ventral nerves, which carry the vast majority of the afferents from glabrous skin, were transected but the dorsal digital nerves unaltered, the cortical neurons in the deprived region responded to abnormally large RFs that could include skin from multiple digits. Transection of a single ventral nerve produced minor

changes when compared with amputation, complete denervation or denervation of both ventral nerves. The loss of the dorsal nerves, alone or accompanying the transection of a single ventral nerve, had a minimal impact on the response properties of the corresponding cortical neurons (Turnbull and Rasmusson 1990).

Usually nerve cut experiments have involved denervation of larger regions of the body. The classic examples of nerve cut experiments were performed by denervating the forepaw by transecting one of the major nerves in the forearm (Kalaska and Pomeranz 1979; Dykes et al., 1995). There are three nerves that innervate the forepaw: the radial nerve carries cutaneous information from the hairy skin, whereas the median and ulnar nerves each innervate approximately half of the ventral surface with some overlap along the midline of the hand. The dorsal and ventral nerves also have an overlapping innervation pattern for the regions of skin near the claw (Kitchell et al. 1982).

Merzenich et al. (1983) demonstrated extensive cortical reorganization after median nerve transection and ligation in owl monkey which normally innervates almost half of the glabrous surface of the hand. Denervated cortex became functionally reactivated within two months. In area 3b, which is similar to the cortex studied in raccoon amputation experiments, most of the reorganized region responded to inputs that resembled the normal innervation of the radial nerve. The reorganized region contained an expanded representation of normal somatosensory input or new RFs that were acquired in a manner that was consistent with the somatotopic organization of the

remaining skin and provided a new somatotopic map. Reactivation of the cortex was extensive as very few, if any, functionally silent areas remained after 2 - 8 months post-amputation (Merzenich et al. 1983a).

Subsequently Garraghty and Kaas (1991) demonstrated in squirrel monkey (*Saimiri sciureus*) that transection of the median and ulnar nerves resulted in a functional void that was greater than 3 mm in diameter and therefore exceeded the predicted spatial limit of cortical reorganization, which was 0.7  $\mu\text{m}$  from normally activated regions (Merzenich et al. 1984). Nevertheless, this large deafferented region was completely reactivated within 2-5 months after amputation. To explore the reason for this discrepancy in results, Garraghty et al. (1994) tested the effects of combined transections of radial and medial nerves or radial and ulnar nerves. The hypothesis was that the removal of both the dorsal and ventral inputs to the same structure, such as a hand or digit, would replicate the findings associated with digit amputation. It was argued that a functional void would result from the loss of both dorsal and ventral innervation for the same part of the body. This hypothesis was supported as it was demonstrated that the loss of innervation to both hand surfaces produced a functional void in the cortex that does not reorganize, and therefore mimicked the effects of multiple digit amputation (Garraghty et al. 1994).

When the two ends of a cut nerve are sewn together (nerve repair) aberrant sprouting or regrowth can lead to misdirected reinnervation which results in location

errors in humans (Hallin et al. 1981; Wall and Kaas 1986). The new RFs that are mapped in the cortex of monkeys are unusual in size, number or position and appeared several months after nerve transection. Florence et al. (1994) found that some of these sensory abnormalities may have been related to the reinnervation patterns in the spinal cord and/or brainstem. Projections from one digit were found over the entire median nerve territory in either the spinal cord or the cuneate nucleus. The abnormal RFs that were encountered after median nerve repair remained for periods that exceeded the time span of cortical reorganization after digit amputation. One implication for these findings is that the CNS may be unable to correct for regeneration errors.

### 1.5.b Nerve crush

Following nerve crush injuries there can be complete functional restoration of peripheral and CNS innervation patterns. Unlike amputation, nerve ligation or nerve repair, the recovery from nerve crush has been described as indistinguishable from the pre-crush condition. Cellular cords formed by Schwann cells play a major role in guiding neuronal regrowth after nerve crush injury. These glial cells proliferate in the area of the crush and secrete trophic factors and cell surface adhesion molecules that also direct the regrowth (Fugleholm et al. 1994).

Wall et al. (1983) detailed the CNS recovery from nerve crush injury for primate and Brandenberg et al. (1989) for cat. In the primate species (owl monkeys), the entire

skin territory of the median nerve was completely reinnervated after only 142 days. However, at a shorter period of 32 days, cortical neurons in the median nerve zone had RFs with abnormal RFs that included regions of glabrous and hairy skin. This finding indicated that nerve crush resulted in a short-term reorganization as a result of temporary absence of low-threshold, cutaneous input, but that the original central organization was subsequently restored as peripheral reinnervation occurred (Wall et al. 1983).

In a subsequent report Brandenberg et al. (1989) crushed all sensory nerves from one forepaw in cat. The denervated cortical neurons had abnormally wide RFs that included skin from three or four paws. All neurons with reorganized inputs, including those with RFs that resembled controls, responded at a longer latency than normal. In addition, certain cells had higher thresholds and/or increased response magnitudes. This study provided evidence for altered neuronal responsiveness during periods of cortical reorganization. Furthermore, increased latency and threshold of new responses at 31 days to 63 days after nerve crush, and before peripheral nerve reinnervation, suggested that removal of the dominant input may have revealed pre-existing but weaker excitatory connections. Therefore, the effects of nerve crush are consistent with their hypothesis that an initial stage of reorganization is a "changed neuronal responsiveness" to pre-existing excitatory connectivity.

In a study on rats, Korodi and Toldi (1998) found an expansion of the digit representations following nerve crush to the infra-orbital nerve, which carries sensory



input from the vibrissae. This expansion of the digit representation persisted after the reinnervation of the whiskers and created an overlapping zone where stimulation of either the vibrissae or the digits evoked a response in these neurons. Similar overlapping cortical representations from whiskers and forepaw digits were uncovered with the application of picrotoxin (an antagonist to the GABA<sub>A</sub> receptor) directly onto the cortex in normal animals. This finding suggested that there was a pre-existing overlap in the anatomical connectivity for both the whiskers and digits that may normally be masked by GABA receptor activity. However, the failure to restore the discrete representation areas characteristic of the control animals, suggested that the cortex underwent a long-term reorganization as a result of the altered sensory input following the nerve crush (Korodi and Toldi 1998).

### 1.5.c Local anesthesia

Application of a local anesthetic to skin or peripheral nerves has been used to evaluate the immediate effects of denervation in the absence of nerve injury. Using this technique, Calford and Tweedale (1991) were able to demonstrate that the effects of reversible deafferentation of the thumb of the flying fox on cortical neurons strongly resembled those of amputation. In both cases, deafferentation led to an unmasking of excitatory inputs which was seen as large RFs on an adjacent part of the body. The rapidity of the initial RF expansion provided evidence that the new inputs for the large

fields were not dependent on mechanisms of plasticity, but rather the unmasking of pre-existing connections (Calford and Tweedale 1991a).

The effects of local anaesthetic and the immediate effects of digit amputation were compared in rat by Byrne and Calford (1991). The outcome of this comparison was that local anesthetic and digit amputation produced identical effects on RF size and the immediate appearance of new RFs on adjacent digits. When the amputation removed only part of a RF, there was considerable expansion of the new RF to an adjacent digit and/or onto the palm.

Calford and Tweedale (1991) reported a similar set of findings in the macaque (*Macaca fascicularis*). Denervation with injections of local anesthetic produced immediate reversible RF expansion. The expanded RFs included skin from adjacent digits. As was the case in rat, incomplete removal of the original RF resulted in expansion of the remaining field.

In the animals that received local anesthetic injections, recordings were made in the cortex that was contralateral to the injections as well as the ipsilateral cortex, with RFs on the opposite, unaffected hand. Interestingly, application of local anesthetic was associated with RF expansion for neurons that were responsive to the untreated hand as well as the anesthetized hand. It was postulated that RFs from the ipsilateral cortex were modified by commissural projections from the denervated cortical region in the opposite hemisphere (Calford and Tweedale 1991c).

### 1.5.d Crossed median nerve repair, syndactyly and transplant

In an attempt to elucidate the mechanisms of mislocation following median nerve repair in humans, Wall and Kaas (1986) cut both ventral nerves and redirected the ulnar nerve to reinnervate territory that was formerly served by the median nerve. Therefore, this experiment was a modified form of the nerve cut and repair technique reviewed earlier.

It was clear that some sensory input was restored following nerve repair. However, the performance of these owl monkeys on a behavioral task was described as misdirected and indicated errors in locating tactile stimuli from this region of skin. Electrophysiological investigation demonstrated that responses to skin normally innervated by the median nerve occurred in the area normally representing the ulnar nerve inputs. The somatotopic representation was "discontinuous", the cortex was not completely reactivated and some neurons had multiple RFs. Furthermore, many of these cells had high thresholds. In other regions, there was an expansion of the representation of hairy skin into the denervated region (Wall and Kaas 1986).

Other means of altering sensory input have also provided evidence of the relationship between the manipulation of the receptor sheet and the ensuing cortical reorganization. When two digits were sewn together in a process known as syndactyly, cortical neurons were found that responded to RFs that spanned the cutaneous surface

across two digits. Similarly, transplantation of skin grafts that still had the original vasculature and innervation onto a new site on the forepaw was also associated with a disorganization of the somatosensory map (Allard et al. 1991; Merzenich and Jenkins 1993). In another experiment where innervation of the glabrous surface of the hand was entirely removed, the deafferented cortex acquired new RFs on the hairy skin (Garraghty and Kaas 1991; Garraghty et al. 1994).

## **1.6 Time Course of Cortical Reorganization**

Changes in the RFs and cell responsiveness within the deafferented gyrus that are present immediately after peripheral denervation have been described by some authors as the earliest forms of reorganization and by some as a distinct period that precedes reorganization. Characteristic differences in the response properties of neurons in the immediately deafferented state versus neurons studied at periods greater than one day after amputation have been reported in several species. Changes reported within 24 hours following denervation will be considered first as the immediate effects of denervation, whereas changes occurring after one day will be reviewed in the subsequent section.

### **1.6.a Immediate effects of denervation**

It is extremely important to characterize the response properties of deafferented cortical neurons immediately after denervation, for this is a template upon which

reorganization would proceed. Following denervation in rat, flying fox and monkey, the deafferented gyrus was immediately responsive to the remaining, adjacent areas of skin. In contrast, transection of the median nerve in the cat produced an area that was unresponsive to peripheral stimulation (Li et al. 1994). There is conflicting evidence for the situation in the raccoon immediately after digit amputation. Kelahan and Doetsch (1984) described the immediate effects of digit amputation in the raccoon as an unmasking of responses to off-focus digits. Their findings were not supported by an investigation made by Rasmusson and Turnbull (1983), who identified only inhibitory off-responses in connection with off-focus digit stimulation.

In rat, flying fox and macaque monkeys the RFs that appeared immediately after denervation and activated neurons in the deprived cortical region were abnormally large with low thresholds (Byrne and Calford 1991; Calford and Tweedale 1991a; Calford and Tweedale 1991c). These large RFs are attributed to the unmasking of weaker responses to stimulation outside the low threshold field that are normally present but overwhelmed by the dominant, low threshold RF. Another consequence of unmasking may be reduced drive onto inhibitory neurons that have been postulated to shape the spatial limits of the excitatory field in the control animal.

The choice of anesthetic can greatly influence the outcome of cortical mapping studies, an effect that may be greatest during the immediate phase of reorganization. The major methodological concern is that there may be a masking effect of the anesthetic and

therefore the extent of the pre-existing anatomical connectivity is underestimated. However, anesthetic effects do not account for the discrepancies found in these species. Ketamine along with zylazine (in the rat, flying fox and primate) and ketamine alone (in the cat) have been shown to increase spontaneous and evoked activity in the cortex and therefore it is unlikely that they suppressed weak sensory signals (Harding et al. 1979). Likewise the anesthetic  $\alpha$  - chloralose, used in the later studies on raccoon, does not suppress activity in somatosensory pathways and may also have a facilitatory effect on the cortex (Patel and Chapin 1990). Therefore, the differences are more likely to have been related to species differences rather than to an anesthetic effect.

### 1.6.b Reorganization

The interaction of time and the reorganizational process has been identified by several researchers (Rasmusson 1982; Kaas et al. 1983; Merzenich et al. 1983b). These changes have usually been evaluated as changes in the number or proportion of recording sites where cutaneous activity could evoke a response, increases in the proportion of sites that were responsive to low threshold mechanical stimulation or decreases in the size of the RF.

#### **1.6.b.1 Early stages of reorganization following digit amputation**

During the early stage of reorganization in the raccoon (approximately 1 day to 4 months) the rapid onset, excitatory responses to cutaneous, mechanical stimulation which

have been lost are reinstated. Kelahan and Doetsch (1984) reported an increase in the percentage of responsive sites beginning at day 1 after the amputation but qualified that the increase in reappearance of low-threshold RFs did not occur until approximately 3 weeks after amputation. Rasmusson (1982) also reported a few responsive sites at 2 weeks after amputation, but the greatest increase occurred around 8 weeks after amputation. By 16 weeks post-amputation, many sites responded to cutaneous input and 14% of these locations responded to low-threshold stimulation. In summary, the proportion of the deafferented cortex that responded increased one day after amputation but the reintroduction of low threshold fields was more strongly associated with the end of the early phase.

During the early stage of cortical reorganization in raccoon, new RFs had high thresholds and poorly defined RF boundaries. Some cortical neurons were responsive to more than one subfield on either adjacent digit; these subfields are discrete patches of skin that, when stimulated independently, evoke a response at a common cortical neuron. (Rasmusson 1982; Kelahan and Doetsch 1984; Merzenich et al. 1984).

In primate, the shortest post-amputation time studied was 2 months (Merzenich et al. 1984). At this post-amputation time many cortical locations responded to low threshold mechanical stimulation which indicated that the early stage of reorganization may be shorter in this species. Alternatively that the early stage of reorganization identified in raccoons does not occur in these primates. Interestingly, in both raccoons

and primates the distribution of the RFs found at 16 weeks was biased towards the tips of either digit and/or around the wound (Rasmusson 1982; Merzenich et al. 1984).

### **1.6.b.2 Late Stages of Reorganization**

Cortical reactivation during late stages of reorganization in primate is associated with the appearance of a somatotopic expansion of the pre-existing map (Merzenich et al. 1984). In the raccoon, neurons with RFs were found throughout the deafferented region, but neighboring cortical neurons often had RFs that responded to discrete, non-adjacent regions of skin. Therefore, the reorganized gyrus did not appear to be somatotopically organized (Kelahan and Doetsch, 1984).

A wide variety of RF types have usually been detected in the deafferented zone in late stages of reorganization. Abnormally large fields were detected throughout this period in cat, monkey and raccoon (Kalaska and Pomeranz 1979; Rasmusson 1982; Merzenich et al. 1983b; Kelahan and Doetsch 1984; Merzenich et al. 1984). However, there is also a prominent increase in the number of low threshold RFs and small RFs reported for both raccoon and primate following amputation. A similar trend towards smaller RFs was also identified with increased time after nerve transection in primate (Merzenich et al. 1983a). In a review of the primate literature, it was proposed that during the late reorganizational stage the inputs to behaviorally relevant subfields are strengthened and less behaviorally meaningful inputs are eliminated resulting in small RFs that appear similar to controls (Churchill et al. 1998).



## **1.7 Regulation of RF size and shape in the normal raccoon**

There is considerable indirect evidence that inhibitory mechanisms play a major role in regulating RF size. It has been hypothesized that capsaicin, which selectively destroys C-fibers, releases inhibitory mechanisms in the somatosensory pathway. This effect has been proposed to account for the large RFs produced in cortical neurons (Calford and Tweedale 1991b) and thalamic neurons (Rasmusson et al. 1993a; Katz et al. 1999) after application of this drug onto a peripheral nerve. Likewise, blocking the inputs from the corpus callosum produced disinhibitory effects associated with RF expansion (Calford and Tweedale 1990b). The latter two methods provide compelling evidence that RF size in cortical and thalamic neurons is regulated by inhibitory mechanisms (Clarey et al. 1996).

The most direct evidence for inhibitory regulation of RF size comes from the studies on the phenomenon of lateral inhibition. Lateral inhibition is a pattern of neuronal interaction that enhances the sharpness of the border of the RF for sensory neurons. It has been hypothesized to occur as a result of the co-activation of principle, or relay neurons and inhibitory interneurons that shape the RF through the precise timing and strength of their interaction. In the cortex, the source of this afferent input is the glutamatergic innervation from thalamocortical neurons. The appearance of RFs in a

deafferented cortical region immediately after denervation is heavily influenced by the degree of thalamocortical overlap. The smaller RFs that are characteristic of deafferented neurons studied at later post-amputation times have been postulated to reflect the reinstatement of inhibitory processes, mainly lateral inhibition.

### 1.7.a GABAergic inhibition

The predominant inhibitory neurotransmitter of the mammalian brain is gamma-aminobutyric acid (GABA). In the cortex, approximately 30 % of the neuronal population is GABAergic (Jones 1993). The discovery of GABA in the brain was made by two separate research groups, Awapara et al. and Roberts and Frankel, in 1950; over the next two decades this amino acid was confirmed to be an inhibitory neurotransmitter (Florey 1961; Kravitz et al. 1963; Otsuka et al. 1967). In early theories on GABAergic function in the neocortex, this neurotransmitter was postulated to act globally in the form of a tonic suppression of cerebral cortical excitability. However, it is now generally recognized that the anatomy of inhibitory and disinhibitory neurocircuitry is complex and the physiological roles for these systems are quite sophisticated (Freund and Meskenaite 1992; Jones 1993).

The most prevalent GABA receptor is the GABA<sub>A</sub> subtype. This receptor belongs to a superfamily of ligand gated channels. The GABA<sub>A</sub> receptor has a pentameric structure with over 850 possible combinations of subunits ( $\alpha$ ,  $\beta$ ,  $\gamma$ ,  $\delta$ ,  $\rho$ ) and a

molecular weight of 275 kDa (Macdonald and Olsen 1994). A wide range of subunit combinations has been detected, which cause different receptor populations to respond to different drug categories such as benzodiazepines, barbiturates, ethanol and corticosteroids. The action of GABA on this structure is to induce the influx of chloride, which drives the membrane potential towards the equilibrium potential for this anion, approximately -75 mV (Connors et al. 1988). Activation of the GABA<sub>A</sub> receptor can block action potentials or reduce excitability by "shunt" inhibition that coincides with excitation, or shorten or shape an on-going excitatory response. The GABA<sub>A</sub> receptor is the principle source of fast-acting and powerful inhibition in the cortex and can therefore significantly influence cell signaling at this level.

### 1.7.b Histological identification of GABAergic synapses

There are a number of histological markers for GABAergic cells and synapses. Antibodies have been used against the amino acid itself, subunits of the GABA<sub>A</sub> receptor or the rate-limiting enzyme in GABA formation, glutamic acid decarboxylase (GAD). Antibodies raised against GAD are the most commonly used markers for GABAergic neurons. GAD cleaves one carboxylic acid terminus from glutamate to yield GABA. Characteristically this reaction occurs in presynaptic terminals of GABAergic neurons, but can also take place in the cell body. Correspondingly, labeling with this antibody tends to be weak at the cell body but robust at terminals. There are two forms of GAD

that are distinguished by their molecular weight, 65 or 67 kDa. However, both enzymes are specific to GABAergic neurons and the antibodies to either enzyme are considered to be an accurate marker of GABAergic neurons and terminals.

### 1.7.c GABA within the somatosensory system of normal raccoon

A role for GABA in somatosensory processing in the cortex and thalamus of the raccoon was strongly indicated in a study by Doetsch et al. (1993). In this report, robust immunoreactivity (IR) of terminals was detected at all cortical depths. None of the pyramidal cells in the cortex were GABAergic and those neurons that were GABAergic were concentrated in the cortical layers 2 and 4. The most prevalent cell types that were identified by the GAD antibody were small and medium sized cells that were presumed to be interneurons. The densest band of terminal labeling was found at a cortical depth that corresponded to cortical layer 3 with the faintest labeling seen in cortical layer 5. In the thalamus most regions had some GAD IR, however, the cells of the reticular nucleus were most strongly labeled. In the ventroposterior lateral thalamus, GAD IR cells were found in groups that corresponded to the lamellae that represent separate forepaw digits. Characterization of the effects of deafferentation and reorganization on GAD IR in raccoon has not yet been reported.

#### 1.7.d Physiological effects of GABA<sub>A</sub> receptor antagonism

The effects of pharmacological antagonism of the GABA<sub>A</sub> receptor on cutaneous RF properties have been explored using two selective GABA<sub>A</sub> receptor antagonists, picrotoxin or bicuculline methiodide (BMI). BMI has been identified as the GABA<sub>A</sub> receptor antagonist with the highest specificity for this receptor (Feldman et al. 1997). Sillito was one of the first authors to demonstrate that iontophoretic application of BMI, can alter the RF properties of neurons in the visual cortex in cat (Sillito 1975a; Sillito 1975b). Batuev et al. (1982) provided some of the first evidence that cutaneous RFs could be altered with iontophoretic application of a GABA<sub>A</sub> receptor antagonist (picrotoxin) in the primary somatosensory cortex of cats. In the same year, intravenous injection of picrotoxin was reported to result in enhanced on and off-focus responses to cutaneous stimulation in the adult raccoon, although the data were not presented in this paper (Doetsch et al. 1984).

More recently, the effects of this drug were tested in cat S1 cortex (Hicks and Dykes 1983; Dykes et al. 1984; Alloway and Burton 1986; Alloway et al. 1989), cat thalamus (Hicks et al. 1986) and monkey cortex (Alloway and Burton 1991). In these experiments drug application was performed by local application onto cortical neurons using microiontophoresis.

The two classic papers in this field, Hicks and Dykes (1983) and Dykes et al. (1984), demonstrated that antagonism of the GABA<sub>A</sub> receptor in the S1 cortex of cats increased RF area and lowered the threshold for mechanical activation. A second important finding in these studies was that BMI application simultaneously expanded RFs or exposed a RF while removing post-stimulus inhibition. Therefore, one hypothesis that resulted from this work is that the appearance of RF expansion may be associated with the regulation of temporal summation on a cortical neuron. In addition GABA<sub>A</sub> antagonism did not influence the sub-modality of the affected neuron; however, in addition to RF expansion, a separate RF was occasionally revealed. These studies strongly implicated activation of the GABA<sub>A</sub> receptor as a crucial mechanism in the shaping of RFs at cortical neurons.

Dykes et al. (1984) provided a detailed comparison and description of the effects of GABA, BMI and glutamate. One central finding of this work was that BMI altered the RF organization at 85% of the rapidly adapting (RA) neurons tested. In contrast, BMI only altered the RF size of 13% of the slowly adapting (SA) neurons tested and often these SA cells required stronger iontophoretic currents (> 100 nA) in order to alter neuronal activity. At RA neurons, glutamate and BMI had similar effects of lowering the threshold to cutaneous stimulation for some neurons and exposing RFs of other neurons that had previously been unresponsive to cutaneous inputs. However, glutamate did not

cause RF expansion in any of these cells (n=104). An additional difference between BMI and glutamate was that there was an almost linear relationship in the dose-dependent increase in cell activity with glutamate that contrasted sharply with the altered bursting pattern seen with BMI application.

These authors also reported a large range in sensitivity to iontophoretically applied GABA, with deeper neurons (below 1500  $\mu\text{m}$ ) being the most sensitive to GABA administered with very low currents. If there were GABAergic effects on RF size, they occurred too quickly to detect. GABA application that depressed spontaneous activity was not sufficient to prevent the evoked response from within the RF and when it blocked responses to cutaneous stimulation, GABA suppressed all neuronal activity. (Hicks and Dykes 1983; Dykes et al. 1984).

Neuronal response properties were also explored, in the VPL of thalamus with BMI (Hicks et al. 1986). The proportion of cells modified by BMI in the thalamus was considerably smaller than in cortex; only 4 of 21 neurons (19%) in a RA background and 2 of 20 slowly-adapting neurons (10%) displayed RF expansion during GABA<sub>A</sub> antagonism. In 2 neurons the RF was actually reduced in size with BMI application. In contrast, these authors had previously demonstrated that 85% of neurons in a RA background in the cortex demonstrated RF expansion with BMI. The findings of this

study indicated that the predominant role of rapid inhibition in thalamic neurons was to alter the response pattern and not to modulate RF size (Hicks et al. 1986).

In order to quantify the magnitude of expansion produced with BMI, Alloway et al. (1989) measured the RF size of 111 cortical neurons in the cat. These authors determined that the mean expansion of 141% in RF size for cortical neurons that responded to the forepaw.

In their study in primate, Alloway and Burton used a mechanical stimulus of constant intensity to generate a response profile across regions of skin that contained the RF for a given cortical neuron (Alloway and Burton 1991). Of the 34 neurons studied, 26 were RA. The maximum RF expansion produced by BMI was a RF that was 4 times the size of the original RF. As previously reported in cat, the response latencies to stimulation of the initial field were unaffected by BMI application. However, the average response latency from the region that was exposed by GABA<sub>A</sub> antagonism was reported to be longer, although no mean value was presented. These investigators were able to show that BMI expanded the RF such that one spike per stimulus could be elicited from skin indentations on digits that were adjacent to the on-focus digit that contained the original field. Three examples of this expansion were illustrated in the paper and the authors reported that expansion of this magnitude was a common effect of BMI application. One implication of this finding was that the new RFs found following digit



amputation could be explained by pre-existing excitatory connectivity that is not expressed in the control condition due to GABA<sub>A</sub> block.

## **1.8 Regulation of RF size and shape in amputated animals**

### **1.8.a Activity dependent histochemical changes in rodent**

There is considerable histological evidence that GABA levels are reduced after deafferentation and are accompanied by changes in the expression of the GABA<sub>A</sub> receptor. In the somatosensory system, these studies have used histological techniques and have mainly focused on activity dependent changes in GAD expression. Altered somatosensory input, usually vibrissal ablation or amputation results in a reduction in GAD and GABA<sub>A</sub> expression in rodent (Land and Akhtar 1987; Warren et al. 1989; Welker et al. 1989a; Akhtar and Land 1991; Land et al. 1995).

Vibrissal or cutaneous sensory deprivation was also associated with a decrease in overall activity, as assessed by cytochrome oxidase (CO) label. The enzyme cytochrome oxidase is considered to be an endogenous marker of neuronal activity (Wong-Riley 1989). It is an integral transmembrane protein found in the mitochondria of all eukaryotic cells and plays a vital role in energy metabolism based on aerobic cell respiration. In neurons, energy metabolism and neuronal activity are highly correlated. Likewise, mean mitochondrial size and CO staining also reflects levels of activity. This

information, along with the minimal contribution of glia to CO levels, allows one to identify regions of relatively active neurons versus inactive cells by CO histochemistry (Wong-Riley 1989).

Wong-Riley and Welt (1980) demonstrated that sensory deprivation by whisker removal produced a decrease in CO staining of the corresponding barrels within the vibrissal representation of neonatal and adult mice, an effect that was still present 2 months after the whisker follicle had been removed. Subsequently, Land and Akhtar (1987) demonstrated an activity dependent decrease in GAD IR. Whisker trimming for 63 days also reduced GAD label in the corresponding vibrissal barrels in the mouse. The first study to explore the relationship between decreased CO levels and GAD IR in the somatosensory system of the rodent was conducted by Warren et al. (1989). These authors were able to demonstrate a decrease in CO activity in the hindpaw representation cortex that was evident two weeks after transection of the sciatic nerve. To the contrary, only a small decrease in GAD (16% reduction in the number of cell bodies labeled for GAD) was produced in cortical layer 4, with the other cortical layers having GAD IR levels that were equal to controls.

The time course for changes in GAD IR due to altered somatosensory inputs in the adult mouse was documented by Welker et al. In one study (Welker et al. 1989b), they related a decrease in GAD IR to the removal of a row of vibrissal follicles. These authors showed that sensory deprivation was associated with decreased intensity of GAD

IR at both puncta and cell bodies, and that this decrease was greatest between 2 and 4 weeks following removal of the whisker follicles. GAD IR returned to control levels by 6 weeks and remained at control values when tested 7 months following denervation. In this study it was postulated that GAD IR was a more accurate marker of neuronal activity than CO activity, which reflects overall metabolic activity. These authors argued that the rapid decrease (three days) and reinstatement (6 weeks) of GAD IR at puncta and cell bodies was a more accurate indicator of neuronal activity, whereas depression in CO levels persisted for at least 2 months following a similar procedure. A subsequent report located a transient increase in GAD IR within the cortical barrels that represented hyperstimulated follicles, a biochemical effect that outlasted the stimulation period by 32 days (Welker et al. 1989a). Therefore, activity dependent modulation of GAD IR reflects increased, as well as decreased, activity within the somatosensory system of adult rodents.

In 1991 Akhtar and Land demonstrated that sensory deprivation, achieved by whisker trimming, depleted GAD IR in the adult but not in the developing rat. It was postulated that sensory disruption during development led to a loss in the ability to regulate GAD in adulthood. Subsequently Land et al. (1995) compared the IR profiles of the GABA<sub>A</sub> receptor with CO staining and GAD IR in the vibrissae representation in rat. These comparisons were made in control rats, rats that experienced sensory deprivation

during development and animals that experienced chronic deprivation as adults. This study revealed a correlation of CO activity and GABA<sub>A</sub> IR in control cortex. Whisker trimming did not decrease the labeling of the GABA<sub>A</sub> receptor. On the contrary, ablation of the whisker follicle decreased IR for this receptor, a finding that suggested altered GABA<sub>A</sub> IR may not strictly reflect changes in activity but require damage or removal of the follicle itself (Land et al. 1995).

### 1.8.b. Activity dependent histochemical changes in primate

Although several investigations had shown activity dependent decreases in GAD IR in the visual system of primates (for review see Jones 1993), Garraghty and Kaas (1991) have provided the only investigation in the somatosensory system of a primate following nerve transection. These researchers documented an initial decline in GAD IR as well as the return to control levels over the course of 5 months. Altered GAD IR was not attributed strictly to changes in activity level because there was no corresponding decrease in cytochrome oxidase (CO).

## **1.9 Role of GABA in cortical reorganization of the adult raccoon:**

### **Rationale of the present thesis**

Although there is a great deal of evidence relating GABAergic mechanisms to the shaping of normal cortical RFs in a variety of species, only two relevant studies have

been carried out in the raccoon. First, Doetsch et al. (1983) mentioned that intravenous injections of picrotoxin enhanced on and off-focus responses of cortical neurons in the control animal. In addition, Rasmusson and Turnbull. (1983) demonstrated that 70% of the novel responses seen in the deafferented region could be explained by rebound excitation following the release of inhibition versus direct excitation from the periphery.

Since RF expansion can be produced in cats and primates (previous section), we decided to explore the extent of expansion in the raccoon, using the microiontophoretic application of the specific GABA<sub>A</sub> receptor antagonist BMI. Of the utmost importance was to learn if GABA<sub>A</sub> antagonism would reveal pre-existing excitatory connectivity from skin beyond the on-focus digit, since such connections could explain the appearance of new RFs found with cortical reorganization.

The results showing histochemical changes in the GABA system after denervation, discussed in the previous section, suggest that the role of GABA might change during reorganization and perhaps account for some of the characteristic responses seen in reorganizing cortex. Therefore, the second goal of this thesis will be to repeat the iontophoresis experiments at different intervals after amputation. If GABAergic function is changing during reorganization or even contributing to the process, the effects of BMI should vary at different intervals after amputation.

## ***1.10 Hypotheses***

### **1.10.a BMI effects on RF organization in control animals**

- 1** Antagonism of the GABA<sub>A</sub> receptor at a single cortical neuron will result in the expansion of the neuron's RF.
- 2** GABA<sub>A</sub> antagonism with BMI will reveal large RFs that extend onto other digits.
- 3** GABA<sub>A</sub> antagonism will produce the same amount of expansion on all cells within a given functional zone (distal digit, proximal digit and palm).
- 4** The magnitude of RF expansion induced by GABA<sub>A</sub> antagonism will vary depending on the laminar location of the neuron.
- 5** The effects of GABA<sub>A</sub> antagonism on RF size and/or organization will differ from the effects of direct excitation by glutamate.

In order to test these hypotheses, the effects of GABA<sub>A</sub> receptor antagonism on RF organization will be explored using microiontophoresis of BMI onto neurons in the primary somatosensory cortex. RFs will be mapped before, during and after BMI application and changes in RF size will be calculated. These will be compared to the effects of iontophoretically applied glutamate on the same neurons.

### **1.10.b BMI effects on RF organization in amputated animals**

- 6** GABA<sub>A</sub> receptor antagonism will also cause RF expansion for neurons in reorganized cortex.

- 7** Greater RF expansion will be seen for small RFs than for large RFs in deprived cortex. This would indicate that intracortical inhibition is responsible for producing small RFs during reorganization.
- 8** BMI effects will have more pronounced effects with increased time after amputation.
- 9** The magnitude of RF expansion induced by GABA<sub>A</sub> antagonism will differ depending on the laminar location of the neuron.
- 10** The effects of GABA<sub>A</sub> antagonism on RF size and/or organization will differ from the effects of direct excitation by glutamate.

RFs found in the deafferented cortical region will be classified before and after BMI application in animals that have undergone digit amputation 2 - 37 weeks prior to recording.

## **2. Methods**

### **2.1 Animals and surgery**

Electrophysiological recordings were made in thirty-two adult raccoons (*Procyon lotor*) of either sex that weighed between 3 and 11 kg. Animals were obtained from a professional trapper and housed communally with free access to food and water, in accordance with animal care regulations at Dalhousie University.

In twelve animals the fourth digit on the left forepaw was amputated. Animals were sedated by an intramuscular injection of ketamine hydrochloride (10 - 20 mg/kg, Ketalean: MTC Pharmaceuticals) and then placed under halothane anesthesia (2-3% in oxygen). The removal of the digit was carried out under sterile, surgical conditions in accordance with the animal care protocols at Dalhousie University. To perform the amputation, the skin was cut and retracted at the base of the digit. The four main ventral and dorsal nerves were ligated with 3-0 suture and then cut distal to the ligation. The digit was removed at the metacarpophalangeal joint. The remaining glabrous skin was pulled up over the joint and sutured to the dorsal hairy skin. During the animal's initial recovery from the surgery, it was injected with buprenorphin (0.3 mg/kg, i.m. Buprenex, Reckitt – Coleman) and antibiotic (15 mg/kg, i.m. cesazolin sodium, Lilly) The entire forepaw was wrapped in several layers of bandage. No animal experienced an infection



of the forepaw as a result of this procedure. The animals were allowed to recover overnight in an isolated cage, then returned to the communal housing facility.

For recording experiments, animals were initially sedated with ketamine at the dose stated above. Halothane was then supplied so that an intravenous catheter could be inserted into the radial vein of the right forearm. The animal was maintained in an areflexic state with the i.v. administration of  $\alpha$ - chloralose (5% in propylene glycol). Approximately 1 hour prior to opening the skull, animals received one of two 0.5 ml injections of hydrocortisone (50 mg I.V. Solu-Delta Cortef: Upjohn) to reduce cerebral edema during the experiment. The second injection was given several hours later. In order to monitor and regulate body temperature at 37.5° C a negative feedback system comprised of a rectal thermometer and heating pad was used. The actual body temperature of the animals used ranged between 35.5 and 37.5° C. In some cases, animals were ventilated at 17 strokes/minute at 50 ml/stroke.

Animals were positioned in a Kopf stereotaxic frame. To expose the skull, the skin was cut down the midline and the muscles were retracted. A trephine (1.5 cm diameter) was used to create a hole in the skull over S1 cortex, contralateral to the forepaw with the amputation. This hole was sufficient to expose the entire primary cortical representation of the fourth digit as well as parts of the palm, third and fifth digit representations. Impression Compound (Kerr, Romulus, MI) was used to build a dam

around the hole in the skull. The dura mater was cut and reflected to expose the brain. The well was filled with warmed Elliott's solution (Abbott Laboratories, Montreal) which helped to preserve the biological viability of the exposed pia and cortical surface.

## **2.2 Electrophysiological recordings**

In the present experiment multibarrel pipettes attached to a recording electrode. Three different multibarreled-electrode assemblies were used to record neural activity as described in 2.3. In all cases the impedance of the recording electrode ranged between 0.5 and 4 M $\Omega$  (measured at 1KHz with an OMEGA Tip Z; Ohm-meter World Precision Instruments, Sarasota, FL). The output signal was amplified by 10,000 to 50,000X, filtered (0.2 - 500 kHz) and sent to a noise eliminator (Humbug, Quest Scientific, North Vancouver, BC). This equipment identifies periodic waves in a 50 - 80 Hz range within the input signal, and subtracts these repeating waveforms from its output. The resulting signal was monitored through an audio speaker and displayed on a storage oscilloscope (Tektronix 5111, Beaverton, OR).

In order to create a cortical map, recordings were made in each exposed gyrus. Penetrations were made perpendicular to the pial surface. To avoid vascular damage, the electrode was positioned while viewing the brain through an operating microscope.

Once the electrode was lowered to a position that was appropriate for recording, attempts were made to evoke neural activity by activating mechanoreceptors in the skin of the forepaw. In order to define the area of the cell's RF a series of hand held probes and von Frey hair monofilaments (Stoelting, Wood Dale, IL) was used. Von Frey hairs are a series of graded monofilaments that are pliable so that each fiber bends at a different force. This feature standardizes the mechanical force used to stimulate the skin, as only one level of maximal pressure is possible for a particular filament. By using an ascending series of monofilaments, it was possible to determine the threshold and boundaries for the RF with the lowest supra-threshold monofilament. Subfields with higher thresholds for cell activation were also characterized in this manner.

To make a record of the RF, a sketch was made on standardized drawings of the raccoon forepaw to represent the area of skin from which a response could be evoked with the lowest grade of von Frey hair. Separate sketches were made for a cell's RFs with at least two grades of von Frey hair and/or a hand held glass probe. The area of skin that evoked the strongest neural response was marked directly on the skin with a felt tip pen and the length and width of this field were measured with callipers.

By making multiple penetrations in all exposed cortical regions, it was possible to approximate the borders and different functional zones of each digit representation and demarcate the deafferented zone in amputated animals. Within the deafferented zone, multiple penetrations were made that were spaced approximately 2 mm from each other.

Once the electrode had penetrated the brain it was advanced in 10  $\mu\text{m}$  steps using either an Inchworm microdrive (Burleigh, Fishers, NY) or a manual micromanipulator (Narishige, Japan). A cell was selected for further study when activity could be evoked by gentle indentation of the glabrous skin. An additional criterion was that the amplitude of the action potential be at least three times greater than the height of the background activity. In most cases, the activity for a given cell was recorded for at least five minutes prior to performing any drug manipulations to assess the stability of the recording.

## **2.3 Microiontophoresis of Glutamate, GABA and Bicuculline**

### **Methiodide**

Commercially available multibarrel pipettes were used that had assemblies of five or seven glass tubes (A&M Systems Inc., Carlsborg, WA.). The pipette was placed in a vertical microelectrode puller (Narishige) which uses a combination of heat and force to "pull" the pipette. The tapered end of the pipette was then broken off resulting in a total tip diameter of approximately 5 $\mu\text{m}$ .

Microiontophoresis was carried out using one of three types of electrode-multibarrel pipette assembly. The type of electrode used in the earliest experiments was designed by Dr. H. Swadlow (University of Connecticut). These electrodes are constructed by gluing a 0.001 inch (25  $\mu\text{m}$ ) diameter platinum-iridium wire to the tip of

multibarrel micropipette with Insl-x, a commercial lacquer which also has electrical insulation properties (Insl-x Products Corporation, Yonkers, NY). In order to decrease the impedance of the recording wire, it was flattened at one end. Consequently, the insulation was also removed at this same end of the wire. The final product was an electrode with a low impedance recording tip positioned adjacent to the open ends of the micropipette. The total diameter of the electrode tip was approximately 50  $\mu\text{m}$ . The recording electrode was connected to a stainless steel post with Silver paint (Epoxy Technology, Billerica, MA). This post had a gold pin connector at the opposite end, which allowed the recording electrode to be connected to the amplifiers and other signal processors.

The second type of electrode assembly used was a 0.005 inch (tip diameter, 125  $\mu\text{m}$ ) Parylene C-coated tungsten electrode (A&M Systems Inc., Carlsborg, WA) glued to a five-barrel micropipette. The recording electrode was aligned with the tapered end of the micropipette. Light-sensitive glue for dental adhesion that is cured under UV light was used to bind the recording electrode to the multi-barrel pipette. The diameter of the tip of this electrode was also approximately 50  $\mu\text{m}$ .

In the third type of electrode, the recording component of the electrode-multibarrel assembly was an insulated carbon fiber monofilament. This fiber, 7  $\mu\text{m}$  in diameter, was inserted into one of the five-barrels of the micropipette before it was pulled on the vertical puller. After pulling, the carbon fiber protruded about 2 mm from the tip

of the glass. The carbon fiber was then chemically etched by passing a current through 5 % chromic acid. This protocol (Armstrong et al. 1980) creates a fine point at the end of the carbon fiber. The final tip diameter of this electrode assembly was approximately 20  $\mu\text{m}$ . In order to strengthen the delicate glass and the tip end of the electrode, nail polish was painted along the taper up to approximately 1.5 mm from the end. In order to connect the recording fiber to the signal processing equipment, saline was injected into the micropipette barrel that contained the recording tip and a 0.125 mm diameter chlorided silver wire (WPI, Sarasota, Florida) was placed into the saline, protruding from the blunt end of the pipette. This silver wire was soldered to a gold-pin connector which was then connected by a cable going to the pre-amplifier.

The preparation of ionized glutamate, GABA or BMI has been described in detail (Dykes et al.1984). GABA (Sigma, St. Louis, MO) was diluted to 0.5M in distilled water. The pH of this solution was adjusted to 3.5, which allows GABA to carry a positive charge. L-glutamate (Sigma, St. Louis, MO) was prepared at a concentration of 0.5M with a pH of 8.0 at which it is negatively charged. BMI (Sigma, St. Louis, MO) was used at a concentration of 5 mM in 0.9% saline. The pH for BMI was adjusted to 3.3. The drugs were stored in 500  $\mu\text{l}$  aliquots and frozen at  $-20^{\circ}\text{C}$  until use. Each solution was injected into a barrel of the microelectrode using a syringe and flexible

plastic (Microfil) needle (World Precision Instruments) immediately before the use of the electrode.

### 2.3.a Application of the Iontophoretic Current

Drugs were administered by the process of microiontophoresis. A Neurophore apparatus (Medical Systems Corporation, Greenvale, NY) was used to generate the appropriate ejecting and retaining currents for GABA, glutamate and BMI. This piece of equipment has a cable that connects separate current generating units with discrete insulated silver wires. Gold-pin connectors were attached to the end of each wire. The complementary half of this type of connector was soldered to a 0.125 mm diameter chlorided silver wire (WPI, Sarasota, Florida). These wires were inserted into individual pipettes of the electrode assembly.

Retaining currents or ejection currents could be applied to each barrel independently or in combination. This caused ionized drug to be held in the pipette or repelled into the brain. A retaining current (ranging from 9 - 20 nA) was applied to each barrel in order to prevent hydrostatic efflux of drugs into the recording site. In some experiments, one barrel was filled with 0.9% saline so that a current balancing technique could be employed in which an equal and opposite charge is applied to a barrel filled with saline so that the net charge is zero. In the present experiments there was no

apparent difference in spontaneous or evoked activity of cortical neurons for conditions where current balance was used.

The effects of drug administration were monitored by observing changes in spontaneous activity. This was used to determine appropriate ejection times and recovery periods for each drug. Preliminary experiments were carried out in rats. In the later experiments with raccoons, similar testing of drug and/or microelectrode effectiveness was performed between trials of BMI application and RF mapping.

## **2.4 Quantifying the change in RF Size**

Prior to the drug administration phase of the experiment, one Von Frey monofilament was selected from an ascending range of these calibrated monofilaments, that was suitable to map the peri-threshold RF. A felt tip marker was used on the skin to indicate the size of this original field. A schematic drawing was made that represented the position and size of the field on the forepaw. The RF was remapped several times throughout the drug administration period and the time relative to drug ejection was recorded. After the ejection current was turned off, the field was remapped and the results sketched on the same schematic as the original field. A calliper was used to measure the maximum length and width of the field in the original state and following



drug administration and these values were recorded. Notes were also made on the shape of the field.

In the present experiment, the RF has been defined as the area from which an action potential can be evoked in response to punctate indentations. Therefore expansion was defined as an increase in the area of skin from which a response could be evoked. A field was considered to have been expanded when there was an increase in the length or width of the field that was greater than 2 mm.

The area was calculated from the formula for an ellipse and compared to the original RF area (area =  $\pi ab$ , where  $2b$  is the major axis of the ellipse and  $2a$  is the minor axis). To measure the expansion of the RF, the area of the RF was calculated before and after drug application. The relative change in area was calculated as (expanded – original) / original RF area.

Descriptive data of cell activity were recorded during all parts of an experiment. However, in order to quantify the effects of a particular drug on the spontaneous firing rate of a neuron in some experiments, the spikes/second were counted before and during drug administration. A window discriminator was used to detect spikes that passed over minimum threshold (BAK Electronics Inc., Clarksburg, MD). These spikes were counted over 1 second time periods with an interval of 20 seconds between collection periods. This timing was controlled by a Master – 8 stimulator (AMPI, Jerusalem). The number of spikes/sec was displayed on a screen and was manually recorded.

### **3.0 Results**

#### **3.1 Description of receptive fields and cortical responsiveness**

##### **3.1.a Receptive field mapping in the control animal**

Electrophysiological recordings were made in the primary somatosensory cortical regions representing the glabrous skin from the third, fourth and fifth forepaw digits as well as the subjacent palm, pads C and D. Figure 3A is an illustration of the left hemisphere of raccoon cortex. The shaded circle indicates the area of cortex that was normally exposed during an experiment. In 17/20 control animals, the triradiate sulcus (Tr, dotted lines) was used as the major landmark to locate the cortical representations of the digits. In the remaining three animals, the opening in the skull was rostral to the triradiate sulcus; however, the gyri representing the third, fourth and fifth digits were still accessible.

Cortical mapping revealed an organization of the forepaw representation that was consistent with the first description in Welker and Seidenstein (1959). The present findings also agreed with the more detailed description of each cortical forepaw digit representation (Rasmusson et al. 1991). The representation of the proximal digit was found adjacent to the triradiate sulcus with the distal parts of the digits found closer to the anterior end of its gyrus. The ulnar region of each digit was represented on the medial edge of the corresponding gyrus and radial inputs were sent to the lateral edge of the

**Figure 3**

Cortical representation of the fourth digit. A) A drawing of the left hemisphere of the raccoon brain. The grey circle indicates the region of somatosensory cortex normally exposed by the craniotomy. The major surface landmark of the forepaw representation is the triradiate sulcus (**Tr**). B) Drawing of the exposed cortex in one experiment showing the triradiate sulcus and the location of nine penetrations. In this region, somatosensory information from each digit is sent to a separate gyrus and information from the palm is represented caudal to the triradiate sulcus. C) RFs of neurons obtained from the penetrations shown in B. RFs associated with the proximal digit pad (e.g. RF # 6) were generally large and round, whereas those on the distal portion of the distal digit were usually small, with the smallest fields found near the midline (e.g. #1).

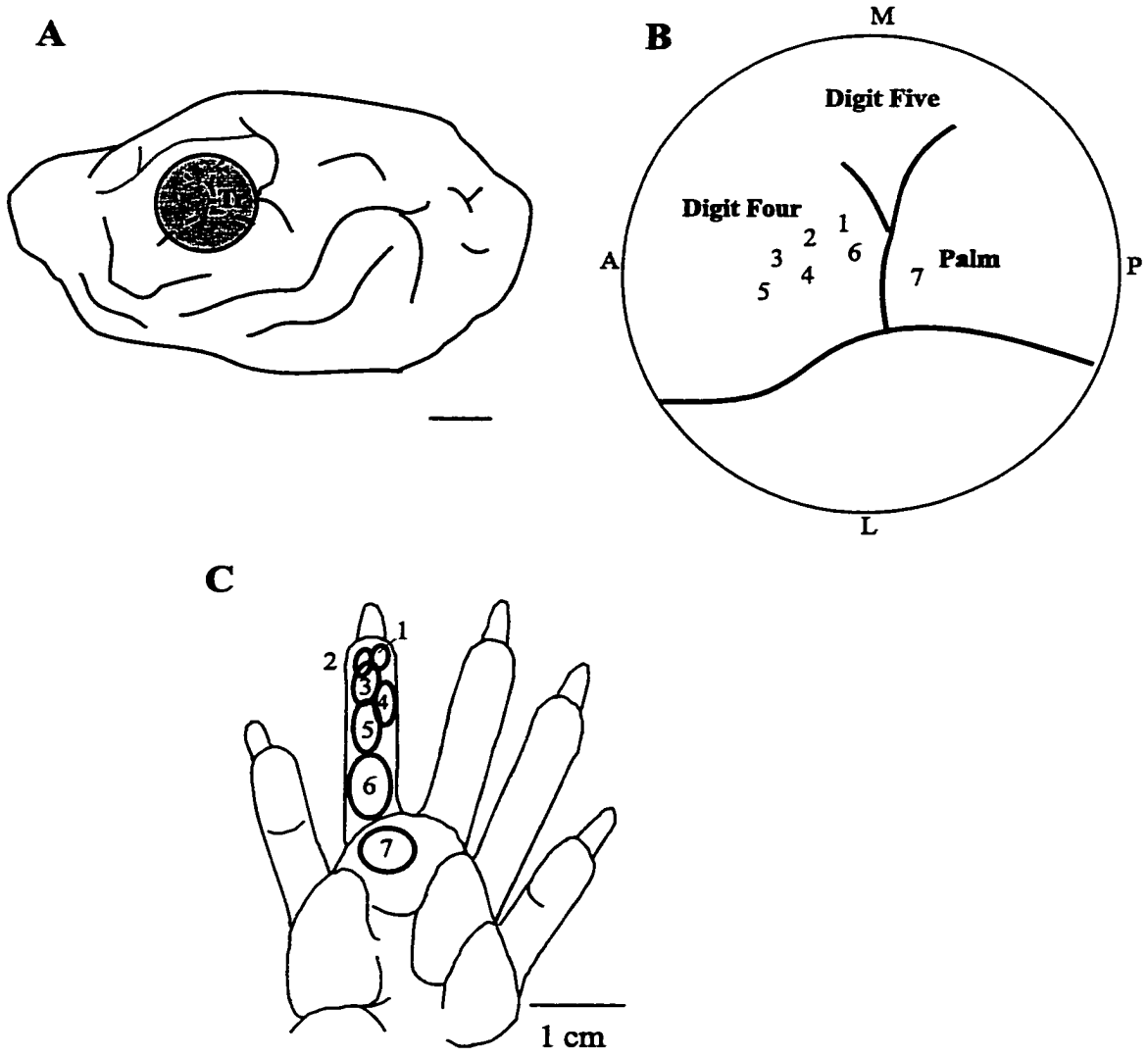


**Figure 3**

gyrus. Figure 3B shows the locations of nine penetrations made with the recording electrode in a representative animal. The numbers on this figure correspond with the numbers for RFs shown in Figure 3C.

In the cortex, each digit representation had a large portion with RFs on the distal pad. When recordings were made from neurons that responded to the midline of the distal pad the RF tended to be small in comparison with RFs found on either the proximal pad or palm. In the cortical representation of the proximal digit the RFs tended to be large and round. The progression of small to large fields between the distal and proximal pads is illustrated in the example shown in Fig. 3C. RFs of neurons that responded to the lateral edges of the digit, at the border of the glabrous and hairy skin, were longer than RFs found at the midline, but were often narrow.

Fifty-two penetrations were made in the forepaw cortical representation area in control animals and neuronal activity was monitored from 144 cells. In control cortex, the average number of cells encountered per penetration was 2.8. In the region corresponding to the fourth digit, the average number of cells per penetration was 1.7. Almost all of these cells (136) were rapidly adapting (RA) and responded to stimulation of cutaneous mechanoreceptors. A few observations were made for SA neurons in control raccoon cortex. Only 2 cells had RFs on hairy, dorsal skin and 1 responded to movement of the claw. Due to these small numbers, only data from cutaneous RA

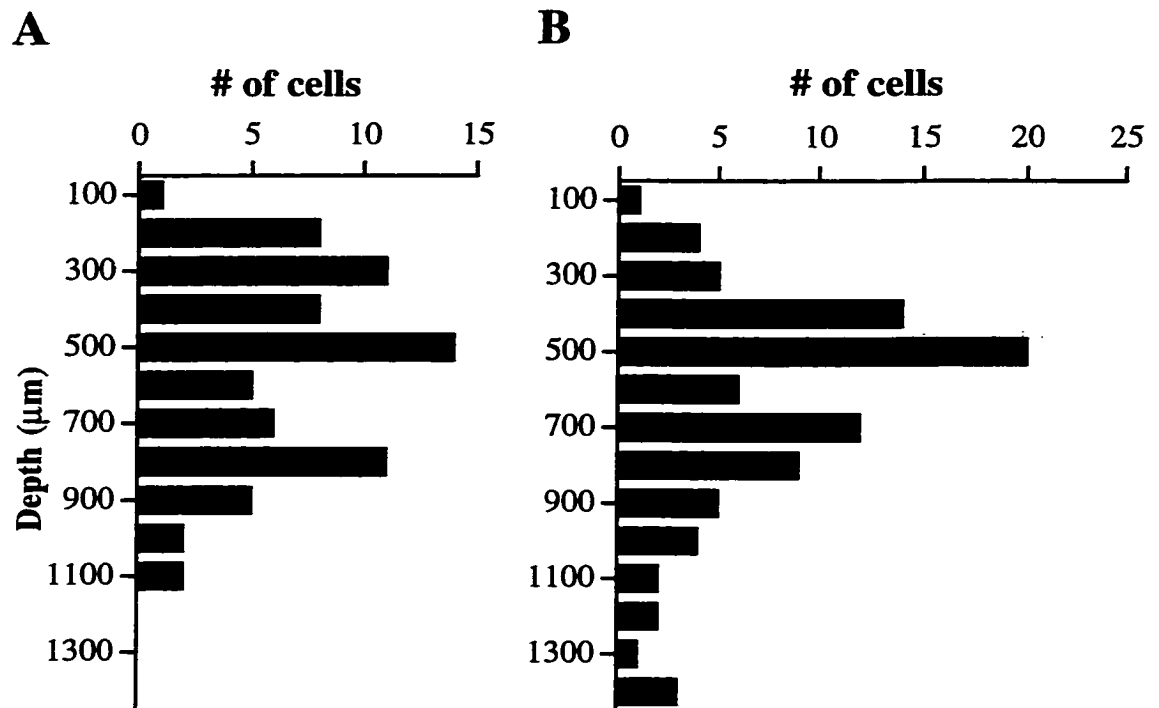
neurons with RFs on the glabrous skin will be presented. One hundred and nineteen of these cells had RFs on a digit, whereas 17 cells responded to stimulation of the skin on the palm. In no case did a RF for a RA cortical neuron extend beyond a single digit or off the palm.

Figure 4A shows the cortical depth for each cell studied in control animals. Few cells were recorded above 100  $\mu\text{m}$  and the greatest number were studied at a cortical depth of approximately 500  $\mu\text{m}$ . Sketches of the RF position and size were made for 82 cells. The RF area was calculated for 39 cells. The mean and median RF sizes for these cells were 21.8  $\text{mm}^2$  and 18.9  $\text{mm}^2$ , respectively. The histograms in Figure 5 show the frequency with which RFs of different sizes were found on different parts of the forepaw. RFs found on the distal digit (Fig. 5A) were most often approximately 10  $\text{mm}^2$  but RFs between 18 and 22  $\text{mm}^2$  were also common. One neuron had an exceptionally large RF for this region of the digit; it was an ovoid field that incorporated the entire distal pad on the glabrous surface of the digit. On the proximal pad (Fig. 5B), the RFs were frequently around 20  $\text{mm}^2$  while RFs on the distal palm (Fig. 5C) ranged from 12 to 75  $\text{mm}^2$ .

These data show that there is an overlapping range of RF sizes found on the distal and proximal pad, as well as the palm. However, there was a strong tendency for small RFs to be found on the distal pad of the digit. The probability that RFs on the distal pad, proximal pad and palm belonged to different statistically defined populations was tested

**Figure 4**

Sampling distribution by cortical depth for control and amputated animals. In the control animal (A), n=73 cells were tested with BMI. In the amputated animals (B), n=88 cells were tested with BMI.

**Figure 4**



**Figure 5**

Distributions of RF size on different parts of the forepaw in control animals. A) RFs on the distal digit pad (n=23), B) on the proximal pad (n=9) and C) on the palm ( n=7).

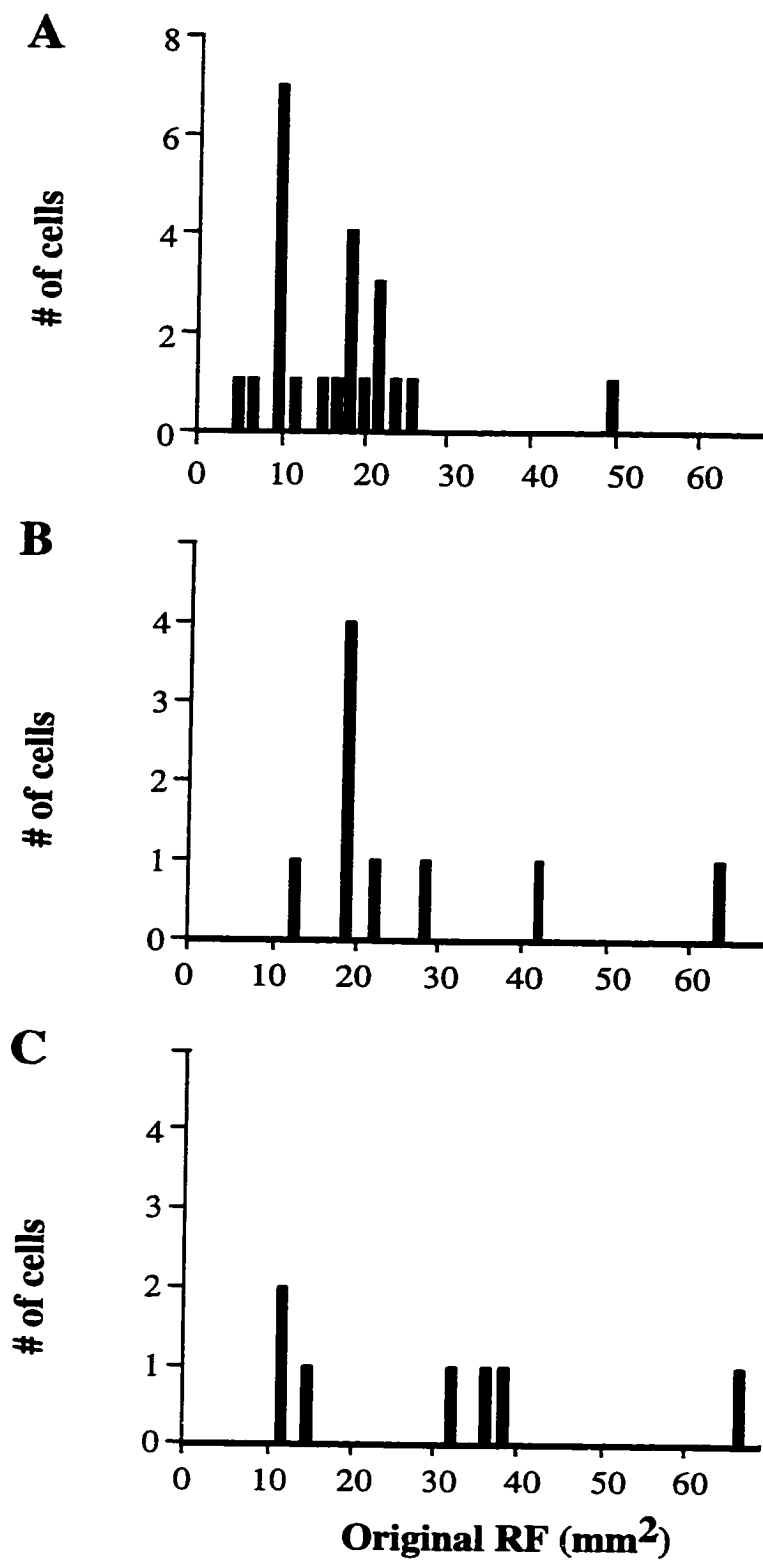


Figure 5

using a non-parametric analysis of variance, the Kruskal-Wallis one – way measure by ranks. This comparison revealed that the differences between distal, proximal and palm RFs were statistically significant ( $H=6.3$ ,  $p < 0.05$ ) indicating that each functional region was associated with a distinct range or population of RFs.

### 3.1.b. Receptive field mapping during reorganization

RF data were collected from 12 animals that had undergone amputation of the fourth forepaw digit. Electrode penetrations were made at 156 sites in the forepaw representation and a total of 154 cells were studied. Almost all ( $n=149$ ) were RA neurons that responded to cutaneous input. Within the deafferented region of cortex that normally represents the fourth digit, it was possible to map RFs of 110 RA cells in 117 penetrations. It was somewhat more difficult to find cells that responded to mechanoreceptor activation in deafferented versus control cortex. The average number of cells encountered per penetration was 0.73 in the deafferented cortex compared to 1.7 in normal animals. Table 1A presents the number of penetrations and cells in each control animal that were found to respond to stimulation of the fourth digit. Table 1B shows the number of penetrations and cells found in deafferented cortex of each amputation animal as well as the time interval between amputation and recording.

**Table 1 Number of penetrations and cells sampled in the 4<sup>th</sup> digit representation**

**A. Control animals**

Raccoon	Penetrations	Cells	Range Of Depths ( $\mu\text{m}$ )
405	2	2	300 – 640
408	3	3	650 – 1030
409	3	6	500 – 710
415	1	1	658
432	2	6	55 – 315
433	1	8	92 – 804
441	1	3	66 – 497
444	2	5	88 – 717
446	6	9	181 – 804
448	3	4	246 – 471
453	1	1	165
455	4	5	150 – 600
457	6	7	150 – 750
<b>Total</b>	<b>35</b>	<b>60</b>	<b>55 – 1030</b>

**B. Amputated animals**

Raccoon	Time after amputation (wk)	Penetrations	Cells	Range of Depths ( $\mu\text{m}$ )
437	2	10	4	73 – 623
422	8	3	5	40 – 560
460	11	30	20	350 - 850
413	12	4	5	149 – 489
425	15	10	3	350 - 529
426	19	27	5	300 - 916
461	24	23	21	500 - 1270
462	24	20	17	500 - 1200
442	34	18	19	100 - 1400
440	37	12	12	216 - 750
<b>Total</b>	<b>2 - 37</b>	<b>157</b>	<b>111</b>	<b>40 – 1400</b>

Shortly after amputation of the digit, the probability of finding a cell that was responsive to cutaneous input was low. With an increase in time following amputation the likelihood of finding a cell that was responsive to cutaneous input was improved. This change in cortical responsiveness is illustrated in Figure 6 which shows the average number of cells found per penetration plotted against the time following the amputation.

In animals that had amputations 2-8 weeks prior to recording only 9 cells were found in 13 penetrations (0.69). When recordings were made in deafferented cortex more than 30 weeks after amputation, 31 cells were found in 30 penetrations (1.03 cells/penetration). The exception to this trend was the animal recorded 8 weeks after amputation (1.7 cells/penetration) but this was from a small number of neurons (n=5).

In amputated animals, cortical neurons were studied across a wider range of cortical depths than in control animals (Fig. 4B). However, a comparison between the samples in the control and amputated animals, did not reveal a statistically significance (Komologrov-Smirnov test,  $\chi^2 = 4.10$ ,  $D=0.16$ ,  $p > 0.05$ ).

The RF was mapped for 108 cells in the fourth digit representation cortex that had RFs entirely on glabrous skin. The other 2 RFs were also responsive to stimulation of a claw or joint. The RF of neurons in the deafferented fourth digit region could be divided into 3 groups based on size and spatial organization.

**Figure 6**

Average number of cells per penetration at different time intervals after amputation.

Each dot is the average from one animal.

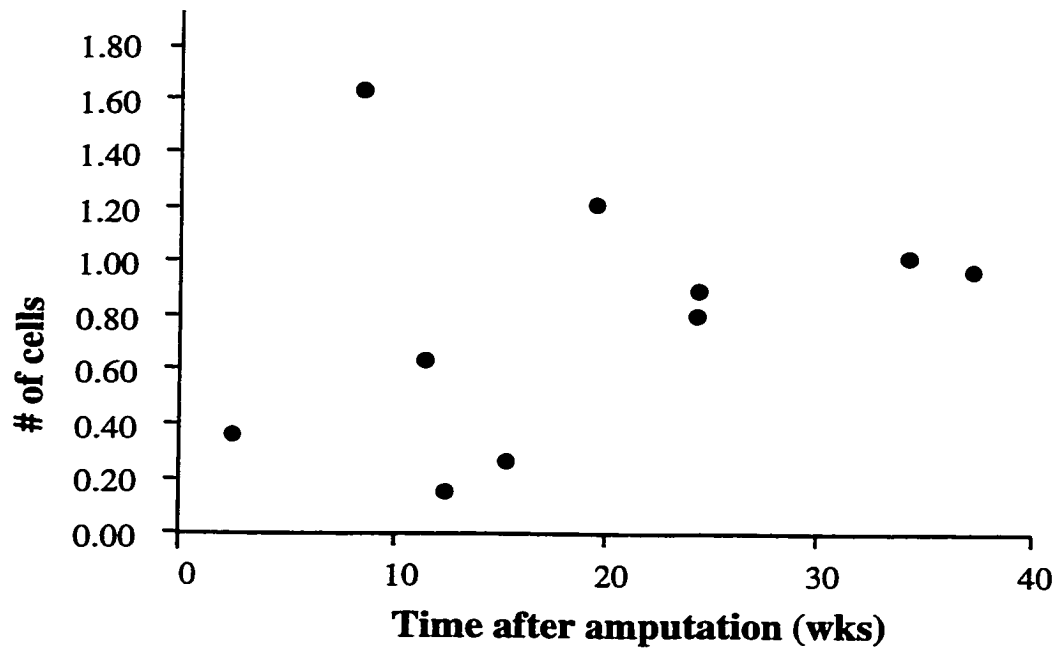


**Figure 6**

One type of RF seen at neurons undergoing reorganization was a RF that included part of the cutaneous surface beyond the boundary of a single digit; these were called “joined” RFs. The defining feature of these fields was that a portion of the RF on one digit joined with part of the RF over the wound. Often these RFs formed a large U shape and included the skin on the both digits that were adjacent to the wound (Fig. 7A). A second type was a “split” field (Fig. 7B) that had more than one spatially discrete subfield. Mechanical stimulation at any of these separate areas evoked activity in the cortical neuron but stimulation in the area between the subfields did not. The third or “confined” RF was the most frequently encountered RF type in reorganizing cortical neurons (Fig. 7C). These RFs were confined to a single digit and had an area that was similar in size to RFs found in somatosensory cortical neurons in the control animal. However, “confined” RFs in amputated animals often lacked the sharp boundary that was characteristically found in the control animal.

### **Joined fields**

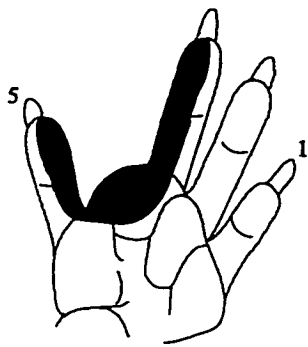
The distinguishing feature of a “joined” field was that the RF included a continuous region of skin on at least one digit and the skin over the amputation site. This RF type was found for 25/108 (23%) neurons. In 8/25 cells with joined fields the RF was only on one digit and the wound area. In the other 17 cells the RF was on the third and fifth digits as well as the wound. Joined RFs often did not have a uniform threshold, but had regions that yielded a stronger response to stimulation. These regions with lower



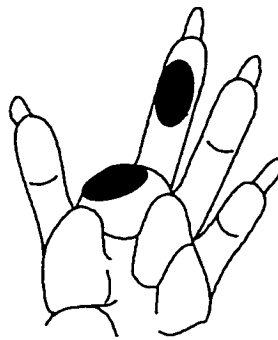
**Figure 7**

Examples of RF types found in the deafferented region during reorganization. A) The largest fields were called “joined” and were defined as fields that extended across the boundary between the wound and either (or both) adjacent digit(s). B) The “split” RF included discrete patches of skin where mechanical stimulation at any “subfields” of the RF activated the neuron but there was a nonresponsive region between the subfields. C) The “confined” field closely resembled the typical RF found on digits in normal cortex in terms of size and uniformity of threshold throughout the RF.

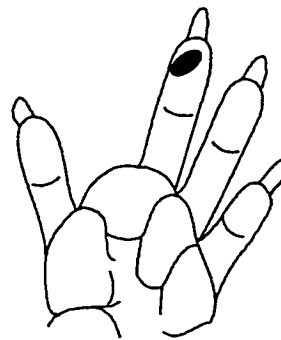
**A Joined**



**B Split**



**C Confined**



1 cm

**Figure 7**

threshold or stronger responses will be called “subfields”. For example, five RFs had only one subfield, two had two subfields and one had three subfields. No subfields were detected in the remaining 17 cells.

### **Split fields**

Split RFs were spatially separate regions of the cutaneous surface that when stimulated mechanically caused a neuronal response. A total of 24 split fields were identified (22% of all RFs). In 18 of 24 cells the subfields were found only on digits 3 and 5, and there was no response to stimulation of skin over the wound. In four cases there were subfields on both digits 3 and 5 as well as over the wound. In two cases the subfields were found on a single digit and the wound. In 6/24 cells there was a clear difference in the threshold for mechanical stimulation at the different sub-divisions of the RF while in the other 16 this threshold was approximately the same in all subfields.

### **Confined fields**

Fifty-nine neurons (55% of all RFs) had confined fields with a uniform threshold to mechanical activation throughout the RF. The area of the RFs was calculated for 16 cells that had confined RFs. The mean area of these RFs was 13 mm<sup>2</sup> and the median was 9.4 mm<sup>2</sup>. One of these RFs was over the wound, four were on the proximal pad and 11 were on the distal pad of a digit. Data for RFs on the distal pad agreed with the RF data from control animals for size and distribution.

### 3.1. c. Changes with time after amputation

Combining all the cutaneous RFs mapped in reorganizing cortex, 25 RFs were categorized as "joined", 24 as "split" and 59 as "confined". Table 2 provides a summary of the number of RF types found at different intervals after amputation. The proportion of neurons that fell into each group are plotted in Figure 8. With increasing time after amputation, the proportion of confined fields found in deafferented cortex increased. At early time points split RFs were common while at late time points, confined fields predominated. This difference in the distribution of RF types at the four time intervals was statistically significant ( $\chi^2 = 16.65$ ,  $df=6$ ,  $p < .05$ ). This statistical difference was entirely due to differences between the first two intervals ( $\chi^2 = 7.87$ ,  $df=2$ ,  $p < .05$ ) with no statistically significant difference between the last three intervals.

The data presented in this section support two hypotheses from earlier reports. First, many RFs in deafferented cortex are abnormal because they are unusually large and can include skin regions that extend beyond a single digit (joined plus split RFs). Second, the greater proportion of confined fields that appeared with time after amputation suggested that the appearance of smaller RFs is part of the reorganization process.

**Table 2 Number of joined, split and confined fields at different times after amputation**

	joined	split	confined	total
2 – 8 weeks	3	10	5	18
11 – 15 weeks	6	5	18	29
19 – 24 weeks	12	4	18	34
34 – 37 weeks	4	5	18	27
total	25	24	59	108

**Figure 8**

Proportion of joined, split and confined fields at different times after amputation.

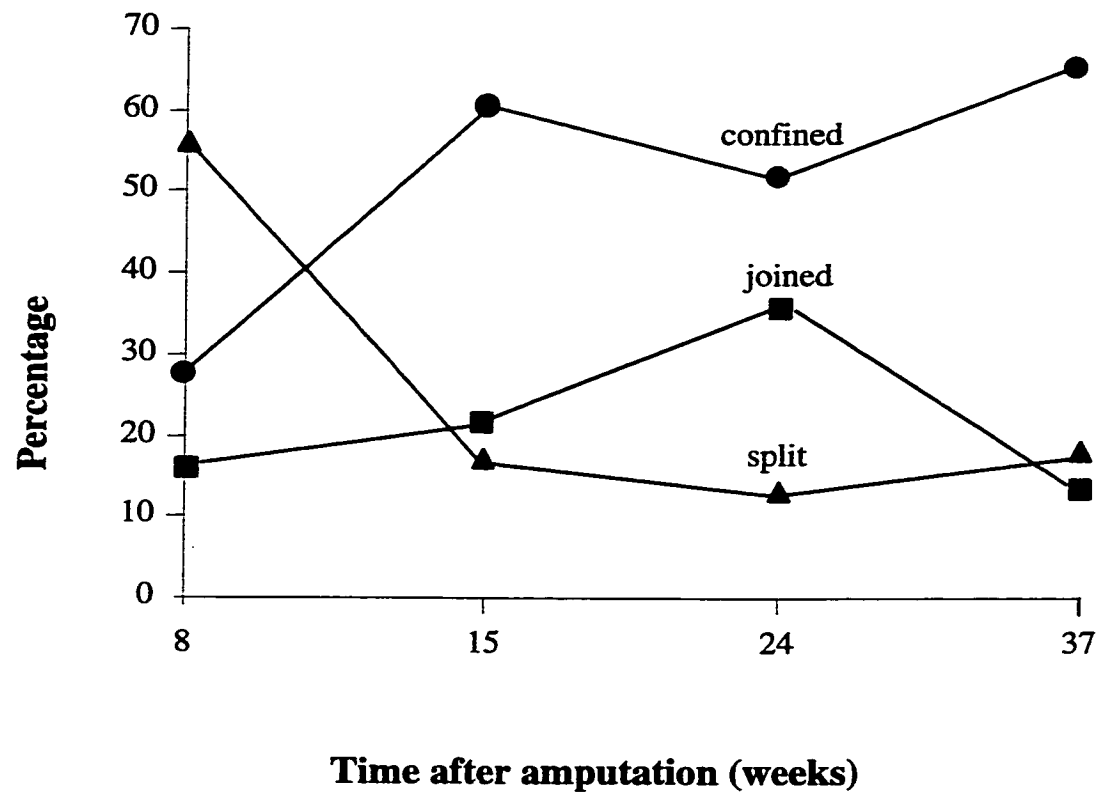


Figure 8

### **3.2 Effect of iontophoretically applied GABA, glutamate and BMI**

#### **3.2.a Drug application in control cortex**

Microiontophoresis was performed in 20 control raccoons. Detailed assessment was made during the application of GABA, glutamate or BMI. The minimum current that successfully influenced cell behavior was  $\pm 11$  nA whereas the maximum current used was  $\pm 90$  nA. The cells that were tested were located between 100 and 1300  $\mu\text{m}$  below the pial surface. A change in cell activity was identified as early as 10 sec after the current was applied to the pipette. The longest application of a drug in this experiment was 600 sec. The application condition was considered to have “no effect” if it met three criteria: the drug must have been successfully applied from the same pipette onto at another cell, at least two levels of ejection current must have been tested and the application period must have exceeded two min. The number of cells that had changes in firing rate and/or a change in the threshold as a result of drug application are summarized in Table 3A.

#### **Glutamate**

In total, glutamate was applied to 47 cells. The application of glutamate increased the excitability of 35 cells. This was evident as an increase in activity in 27 and a decrease in threshold to tactile stimuli 12 cells. Glutamate applied within the time and



current stated in the preceding paragraph failed to alter neuronal activity in 12 neurons. The increased firing rate produced with glutamate application was quantified in three neurons. The maximum effect was a 95% increase in the firing rate for one cell, and the average increase was 63%.

### **GABA**

GABA was applied to 37 cells. It resulted in a decrease in spontaneous activity in 9 cells and an increased threshold in 13, with two cells having both responses to GABA. In 10 cells it did not noticeably change the activity of the recorded neurons. Interestingly, there was an increase in spontaneous activity at 7 cells.

To quantify the effects of drug application the spontaneous firing rate was calculated for 13 cells. The average firing rate was decreased by 63.2% in 10 cells. GABA did not alter firing at one cell, perhaps due to its low spontaneous firing rate of 2.2 spikes/sec. In two cells, GABA application was associated with an increase in firing (average value = 26%).

### **BMI**

BMI was applied to 58 cells. The effects of BMI included increased spontaneous activity (n=24) and decreased threshold (n=12). This effect was especially noticeable in cells located between 200  $\mu\text{m}$  and 700  $\mu\text{m}$  below the cortical surface. No change in neuronal excitability was seen in 26 neurons. BMI application often resulted in an

**Table 3 Effects of drug application on neuronal excitability****A. Control Animals**

	<u>Glutamate</u>	<u>BMI</u>
↑ Spontaneous activity	27	24
↓ Threshold	12	12
Both	4	4
No effect	12	26
<hr/>		
Total	47	58

**B. Amputated Animals**

	<u>Glutamate</u>	<u>BMI</u>
↑ Spontaneous activity	33	18
↓ Threshold	37	37
Both	12	9
No effect	20	42
<hr/>		
Total	78	88

increase in the size of the spikes (n=7). In one situation, a cell that was excited when the skin was stimulated by stroking in one direction lost all directional preference when BMI was applied. The changes in spontaneous firing rate were not quantified for two reasons: the drug effects had a long and variable time course and they often produced an inconsistent bursting pattern of neuronal discharge.

### 3.2.b Drug application in reorganizing cortex

Drugs were applied to 116 cells in deafferented cortex. The cells that were tested were found between 40 and 1910  $\mu\text{m}$  below the cortical surface. The strength of current used to eject drug was  $\pm 10 - 85$  nA. The shortest length of time used to alter cell activity with one of the drugs was 20 sec and the longest was 360 seconds. While the main purpose of this part of the study was to investigate how GABA<sub>A</sub> receptor antagonism alters the spatial qualities of the RF, an important consideration was whether any RF changes were due to a decrease in threshold or an increase in spontaneous activity.

#### **Glutamate**

The effects of glutamate in the deafferented gyrus were similar to those reported in the control condition. It was applied to 78 cells; in 37 cells glutamate resulted in a decreased threshold, in 12 cells of which spontaneous activity was also increased. In total, 33 cells had an increase in spontaneous activity with glutamate. In 20 cases

glutamate application failed to change the activity of the cell and in two other cells it raised the threshold.

### **GABA**

GABA was applied to 31 cortical neurons in reorganizing cortex. There was no effect of GABA on 5 of these cells. The most common effects of this inhibitory neurotransmitter were to raise the threshold to mechanical stimulation (n=14) and to decrease spontaneous activity (n=14) with both effects seen at 4 cells. In 2 cells GABA increased the spontaneous activity. In one case GABA removed the directional preference for stroke stimulation across the RF.

### **BMI**

In deafferented cortex, BMI increased spontaneous activity in 18/88 cells and decreased the threshold in 37, with both effects occurring in 9 neurons. There was no effect of BMI in 42 neurons.

A chi-squared analysis was performed in order to compare the relative efficacies of glutamate and BMI. An additional analysis was performed to determine if the same drug was more effective in either control or amputated animals. When the effects of glutamate and BMI were compared, it was found that glutamate increased neuronal responsiveness at a greater number of cells than BMI, an effect that was statistically significant in control ( $\chi^2=4.19$ ,  $p <.05$ ) and amputated animals ( $\chi^2=8.62$ ,  $p <.05$ ). However no statistically significant differences were found when effectiveness for either drug was compared

between control and deafferented cortex (glutamate:  $\chi^2=0$ ,  $p >.05$ ; BMI:  $\chi^2=0.12$ ,  $p >.05$ ).

In summary, both glutamate and BMI had excitatory effects on spontaneous activity; however, the excitatory effect of BMI was less common than that of glutamate. In contrast, GABA frequently produced inhibitory responses, such as decreased spontaneous activity or increased threshold, yet may also have excitatory effects on a few cells. There was no significant difference between control and amputated animals in terms of the effectiveness of these drugs

### **3.3. RF organization before and after GABA<sub>A</sub> antagonism**

#### **3.3.a BMI effects on RF organization in the control animal**

The effects of BMI were studied during 102 drug application trials. Application of BMI resulted in RF expansion in 65 of the 102 cells. Of primary importance, in all 65 cases where BMI application resulted in RF expansion, the unmasked RF was confined to the same part of the forepaw as the original RF. For example, low threshold RFs on a digit never expanded onto the palm and those found on the palm never expanded onto the skin of a digit.

The area of expansion was quantified for 36 cells. The majority of these cells (32/36) were found below 200  $\mu\text{m}$  and above 800  $\mu\text{m}$ , although the full range of depths

was 100 - 1300  $\mu\text{m}$ . In 29/32 neurons found in the supragranular layers the RFs were ovoid while 3 fields that were very close to the tip were triangular. RF expansion produced with BMI was usually evenly distributed around the original boundary of the RF. The one exception was a cell where BMI revealed two "wings" which increased the width of the field, but not its length. The average expansion of the RF was 38.8  $\text{mm}^2$ , an average increase of 224%.

Figure 9 shows examples to illustrate the range of RF expansion when measured as absolute area (A and B) or relative expansion (C and D). Figure 9A shows the greatest expansion in absolute size that was observed in this study. This example was obtained from a cell located 150  $\mu\text{m}$  below the pial surface. The original field (black) was oval and measured 18.5  $\text{mm}^2$ . BMI was applied using a current of 35 nA for 5 min. When the field area was later mapped using the same von Frey hair (0.23 g) the cell could be activated from a considerably larger area (total = 123  $\text{mm}^2$ ; expansion = 104.5  $\text{mm}^2$  grey). The expanded field was approximately rectangular and reached the border of the hairy and glabrous skin on both sides of this digit. Application of BMI increased the spontaneous firing rate of this cell. GABA was also applied to this cell using a current of 20 nA for 1 min, and weakened the cell's responsiveness to mechanical stimulation from within the original field. GABA also decreased the spontaneous activity for this cell. In contrast, glutamate applied at -14 nA for 30 sec increased the spontaneous activity of the

**Figure 9**

RFs showing the range of expansion produced by BMI in control animals. A) RF from the neuron that showed the greatest absolute expansion. The original field (black) was oval and measured  $18.5 \text{ mm}^2$ . After BMI application the field measured  $123 \text{ mm}^2$  (grey)

B) Smallest RF expansion in absolute size. The original field was  $12.6 \text{ mm}^2$  and was expanded to  $18.9 \text{ mm}^2$ . C) The greatest relative expansion. In this example, the RF area was increased from  $18.5 \text{ mm}^2$  to  $141.4 \text{ mm}^2$ , an expansion of 685 %.

D) The smallest relative expansion produced by BMI (25%). E) An example of expansion produced by BMI for a field that was found in the palm representation of cortex. The original field expanded 117% from  $38 \text{ mm}^2$  to  $70 \text{ mm}^2$  following the application of BMI.

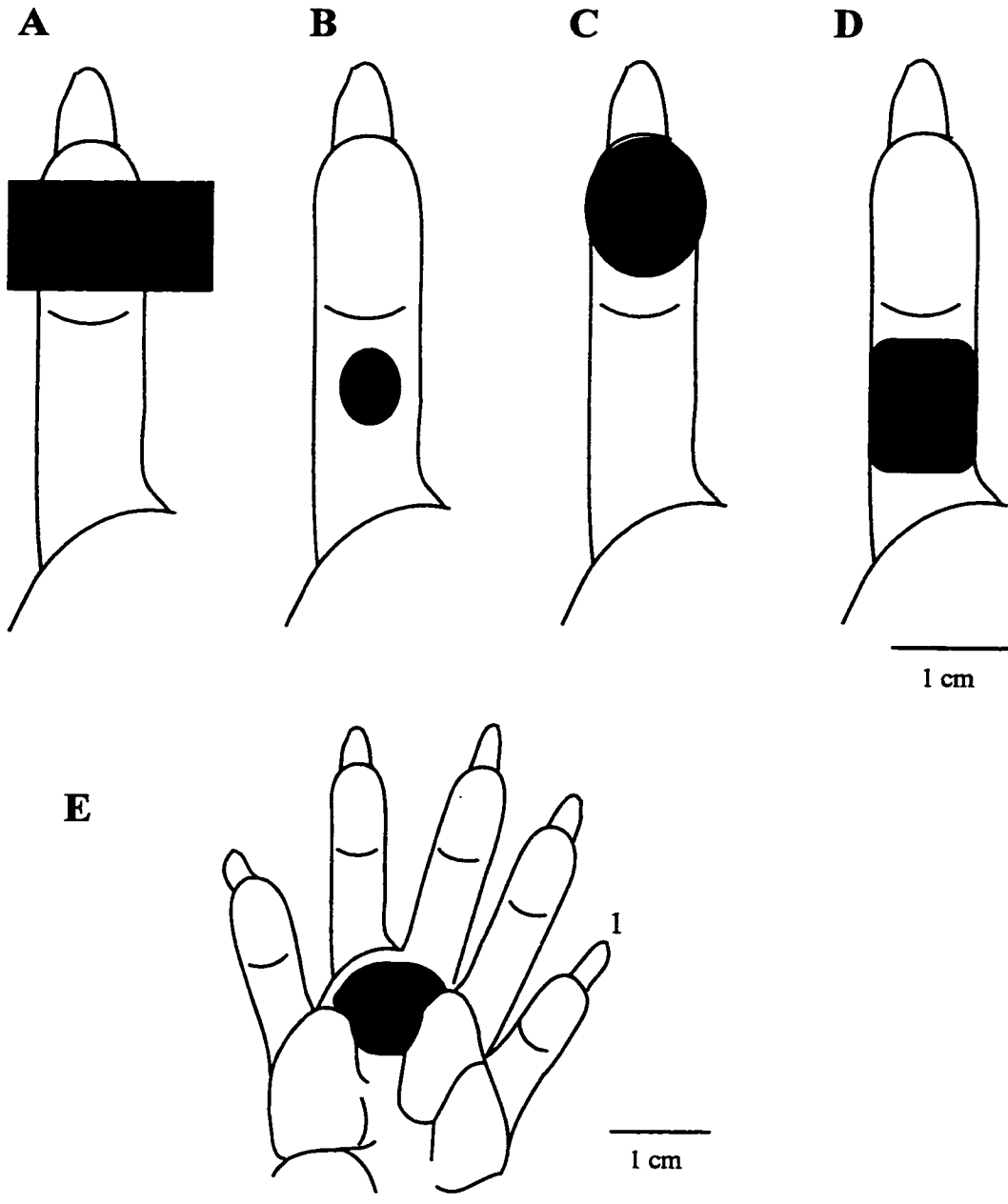


Figure 9



cell and strengthened the response to mechanical stimulation from within the original RF. These excitatory effects of glutamate on this neuron were not accompanied by RF expansion.

A second example (Fig. 9B) illustrates the smallest RF expansion in absolute size that was observed. This cell was found 500  $\mu\text{m}$  below the pial surface. The RF for this cell was mapped with a von Frey hair that exerted 0.11 g of force. BMI was applied for 5 min at 52 nA; subsequently, using the same von Frey hair, the RF area had expanded by 6.3  $\text{mm}^2$  to 18.9  $\text{mm}^2$ . Both the original and expanded fields were oval.

The extremes in terms of relative RF expansion by BMI for a digit RF are shown in Figures 9C and D. The cell with the greatest percentage expansion of its RF (Fig. 9C) was recorded at 425  $\mu\text{m}$  below the pial surface. BMI was applied with a 45 nA current for 5 min. The drug caused RF expansion and an increase in the spontaneous firing rate. In this neuron, the RF area was increased from 18.5  $\text{mm}^2$  to 141.4  $\text{mm}^2$ , an expansion of 685%. Both the original and expanded fields were oval. GABA was applied to the cell while the RF was still in the expanded state. A strong ejection current of 83 nA was used but did not reverse the RF expansion, indicating successful block of GABA<sub>A</sub> channels by BMI.

The cell with the smallest proportional expansion (Fig. 9D) was recorded at a cortical depth of 952  $\mu\text{m}$ . The threshold for this cell was 0.45 g. BMI was applied to this

cell for 10 min and resulted in only 25% expansion. In this example, the area of the original RF was 64 mm<sup>2</sup> and the expanded field was 80 mm<sup>2</sup>. Both the original and expanded fields were approximately square. The effects of GABA were not tested on this cell. The application of glutamate resulted in an increase in spontaneous activity, but did not produce RF expansion.

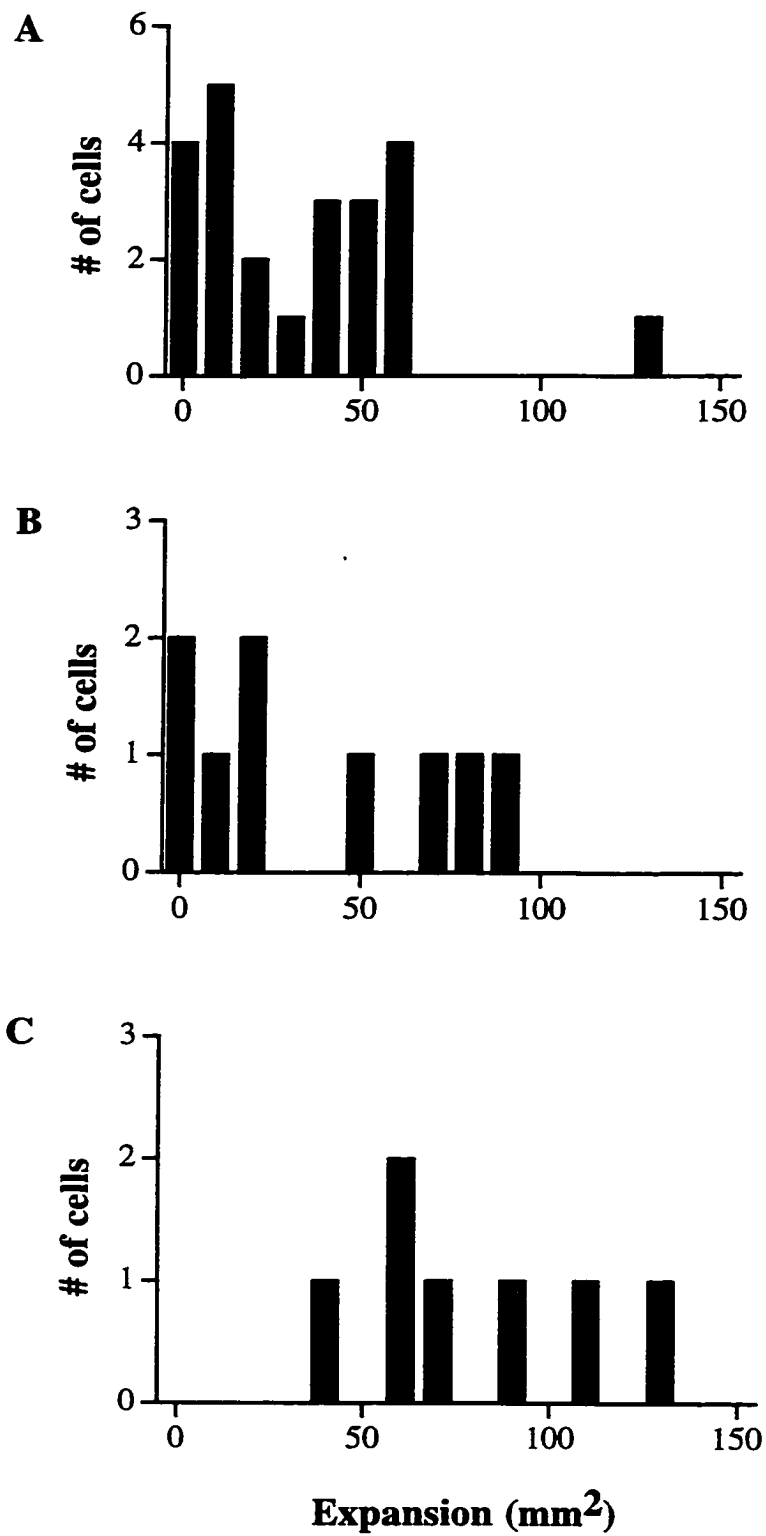
An example of expansion produced by BMI for a neuron in the palm representation of cortex is illustrated in Figure 9E. It can be more difficult to determine the exact boundaries for RFs on the palm because deep folds in the skin separate the pads on the palm and the skin in the middle of the forepaw is loose and wrinkled. In this example, the original field expanded 86% from 37.7 mm<sup>2</sup> to 70 mm<sup>2</sup> following the application of BMI.

The range of expansion of RF area following BMI application was assessed for the distal (Fig. 10A) and proximal digit (Fig. 10B) and palm (Fig. 10C). Each histogram displays the total expanded RF area. RFs on the distal digit had a mean RF expansion of 29 mm<sup>2</sup>; the median value for these data was 25 mm<sup>2</sup>. For cells on the proximal digit, the mean value was 34 mm<sup>2</sup> and for cells on the palm expansion was 76 mm<sup>2</sup>. Thus the smallest absolute and relative RF expansion was seen at RFs on the distal pad.

The difference between the digit and the palm RFs was confirmed by a Kruskal-Wallis analysis of variance which showed a statistically significant difference ( $H=9.5$ ,  $p < 0.05$ ).

**Figure 10**

Frequency histogram of the expanded RF areas for the distal(A) and proximal digit pad(B) and palm(C).

**Figure 10**

### **3.3.a.1 Relationship between recording depth and RF expansion**

RF area was plotted by cortical depth before and after the application of BMI (Fig. 11). The original field sizes of 39 cortical neurons are indicated according to depth in Figure 11A. These RFs, which included those located on the distal, proximal pad or palm ranged in size from 5.5 to 66 mm<sup>2</sup>. In Fig. 11B the area of expansion is plotted by depth. These data showed a wide range in expansion that was added to the original RF at different cortical neurons. While some neurons appeared not to have expanded, others showed considerable expansion of approximately 123 mm<sup>2</sup>. Likewise, there was a large range of percentage expansion from 0 – 898% (Fig. 11C).

It has previously been reported that BMI does not have a strong effect on neurons in sub-granular layers (Kyriazi et al. 1998) In the raccoon, the lower border of cortical layer 4 is approximately 800 μm below the pial surface. Therefore, a comparison was made for the amount of RF expansion above and below 800 μm. There was no statistically significant difference in the RF sizes of the original fields above and below 800 μm ( $t = 1.73$ ,  $df = 37$ ,  $p > 0.05$ ). Comparisons for the extent of expansion however, revealed that BMI has a strong effect on RFs of supragranular and granular layer neurons but not sub-granular cells. The differences in the effect of BMI were statistically significant whether the measure of RF expansion was absolute or percentage expansion

**Figure 11**

RF size and expansion versus depth in cortical animals. (A) the original RF size in measured in  $\text{mm}^2$  and plotted by depth. (B) shows the range of absolute expansion produced by BMI in these same neurons. The expanded area was measured as  $\text{mm}^2$ . (C) the relative expansion, expressed as percentage versus depth.

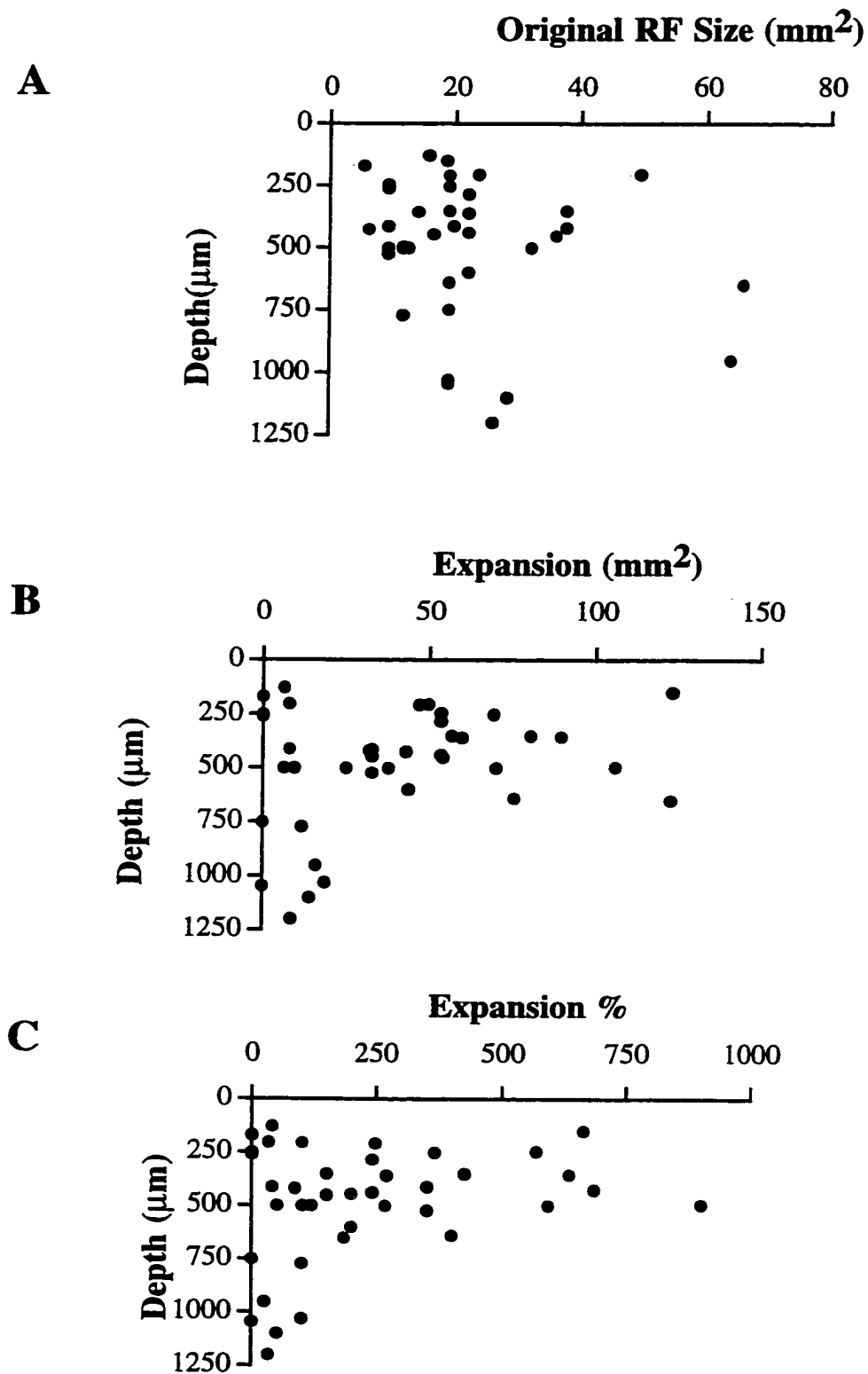


Figure 11

(absolute area:  $t = 2.08$ ,  $df = 37$ ,  $p < 0.05$ ; percentage:  $t = 2.04$ ,  $df = 37$ ,  $p < 0.05$ ).

In Figure 12 the absolute amount of expansion for cells with RFs on the distal pad (A), proximal pad (B) or palm (C) by cortical depth were plotted on separate graphs. With this arrangement of the data it was possible to see that the greatest range of expansion occurred in neurons with RFs on the distal digit.

In Figure 13 the percentage expansion for the RFs in each of the three functional subdivisions were calculated and plotted separately. Figure 13A shows the percentage expansion for RFs found on the distal pad. Figure 13B shows the percentage expansion for RFs on the proximal pad and RFs on the palm are plotted on Figure 13C. In general, neurons that represented RFs on palm and the distal digit had a greater percentage RF expansion than those cells that represented the proximal pad. All neurons that responded to the palm, in this sample, showed RF expansion with BMI and the greatest expansion was seen for a cell that responded to the palm (Fig. 13C). Of the five cells showed no RF expansion, 3 were found on the distal digit pad and 2 on the proximal digit pad.

The large range in variability seen in the plot for the amount of expansion (Fig. 14A) shows that a wide range of expansion can be produced with BMI at different RFs. The box plots in Figure 14B illustrate the variability of RF size before and after drug application. The variability is shown to be greater in the post-drug RFs. If variability in the pre-drug RF was caused by different levels of intracortical inhibition, then one might



**Figure 12**

Absolute RF expansion categorized by functional region of the forepaw. (A) distal digit; (B) proximal digit; (C) palm

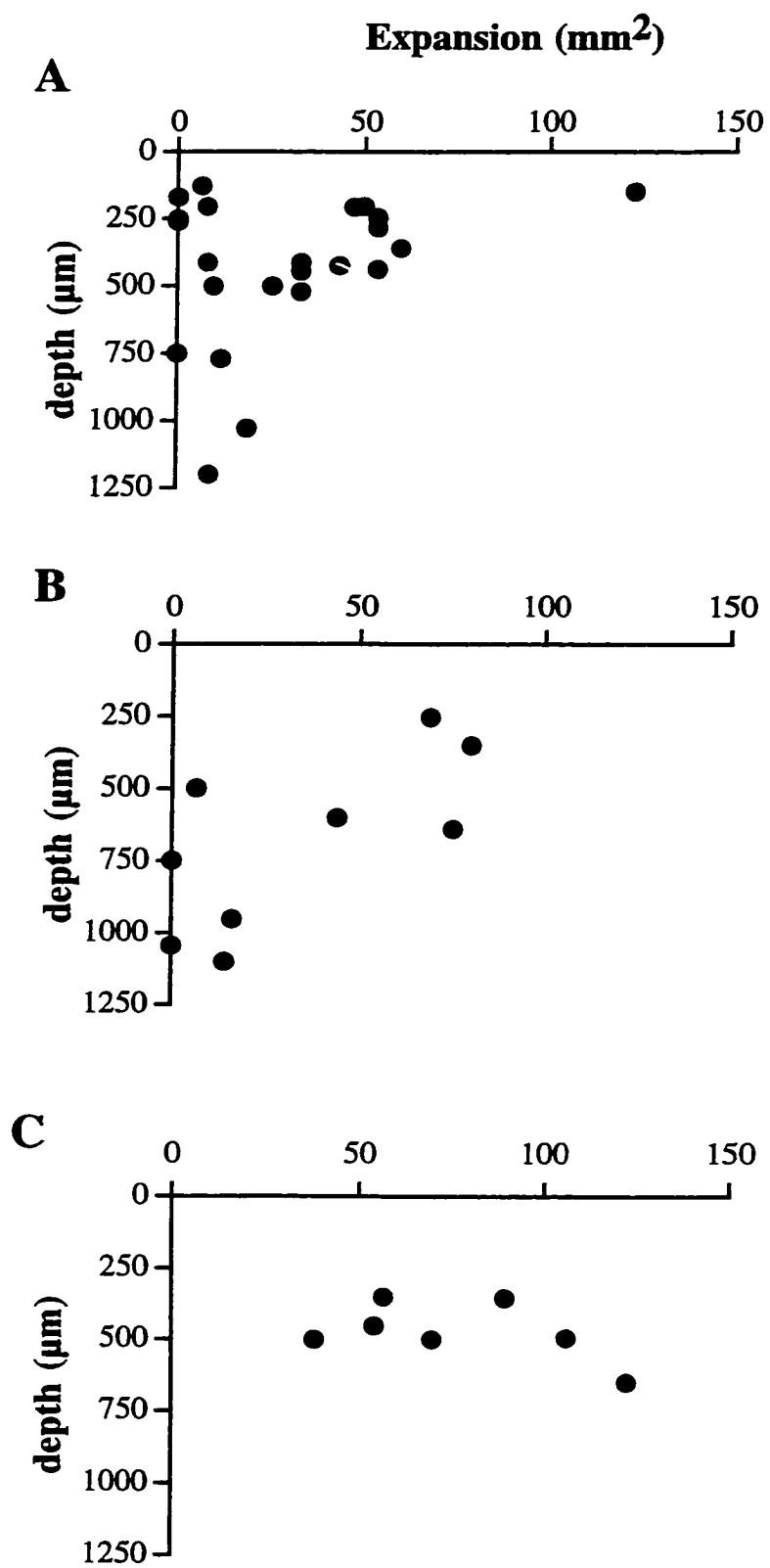
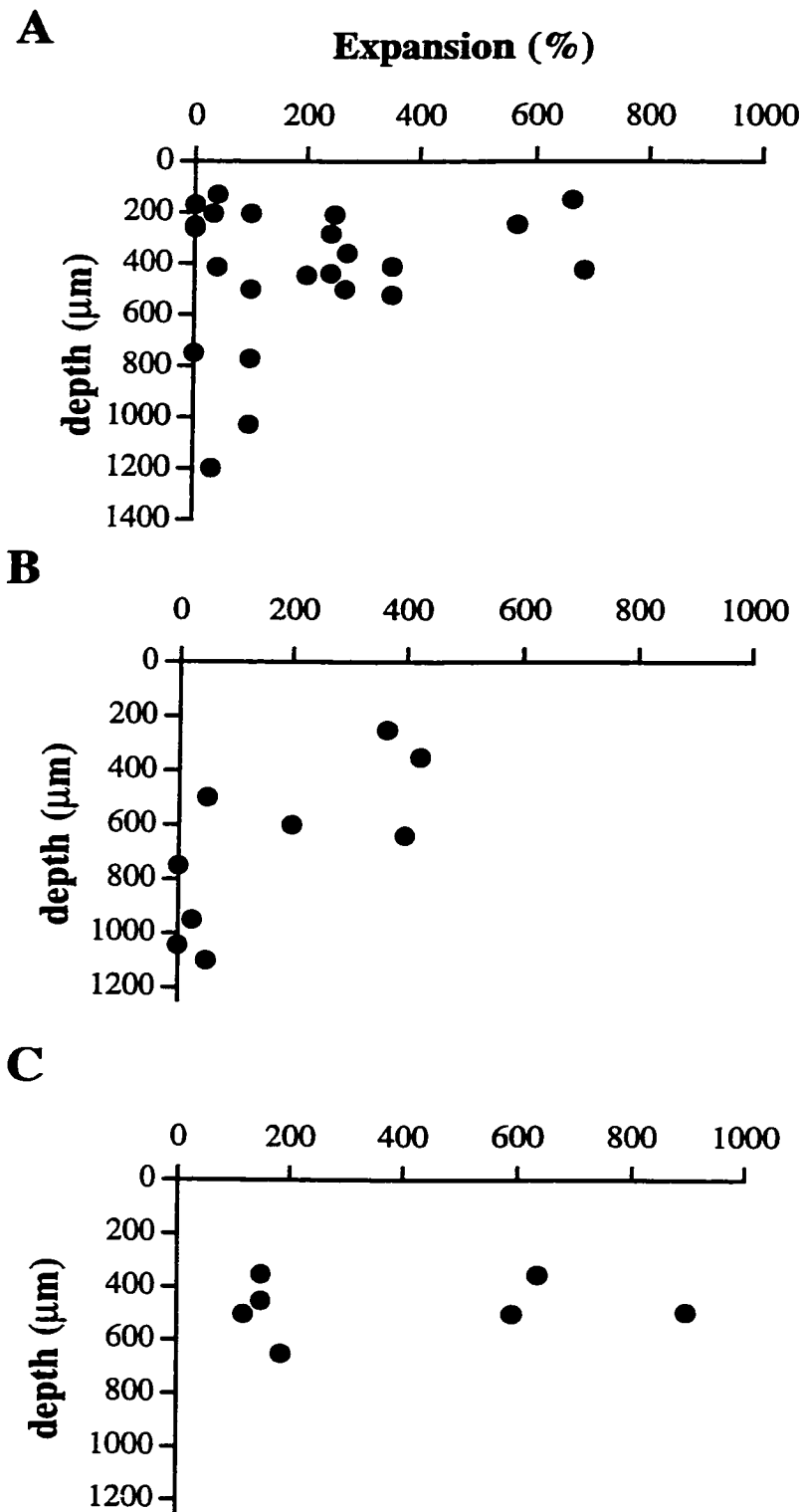


Figure 12

**Figure 13**

Relative RF expansion categorized by functional region of the forepaw. (A) distal digit; (B) proximal digit; (C) palm.



**Figure 14**

Variability of RF expansion shown as box plots for the 10th, 25th, 50th, 75th and 90th percentiles of RF size or expanded area. Horizontal line in the center of the box represents the median and outliers are represented as circles.

A) The variability in the expanded RF area (post-drug RF - pre-drug RF)

B) Figure 14B shows the variability of RF size before and after drug application.

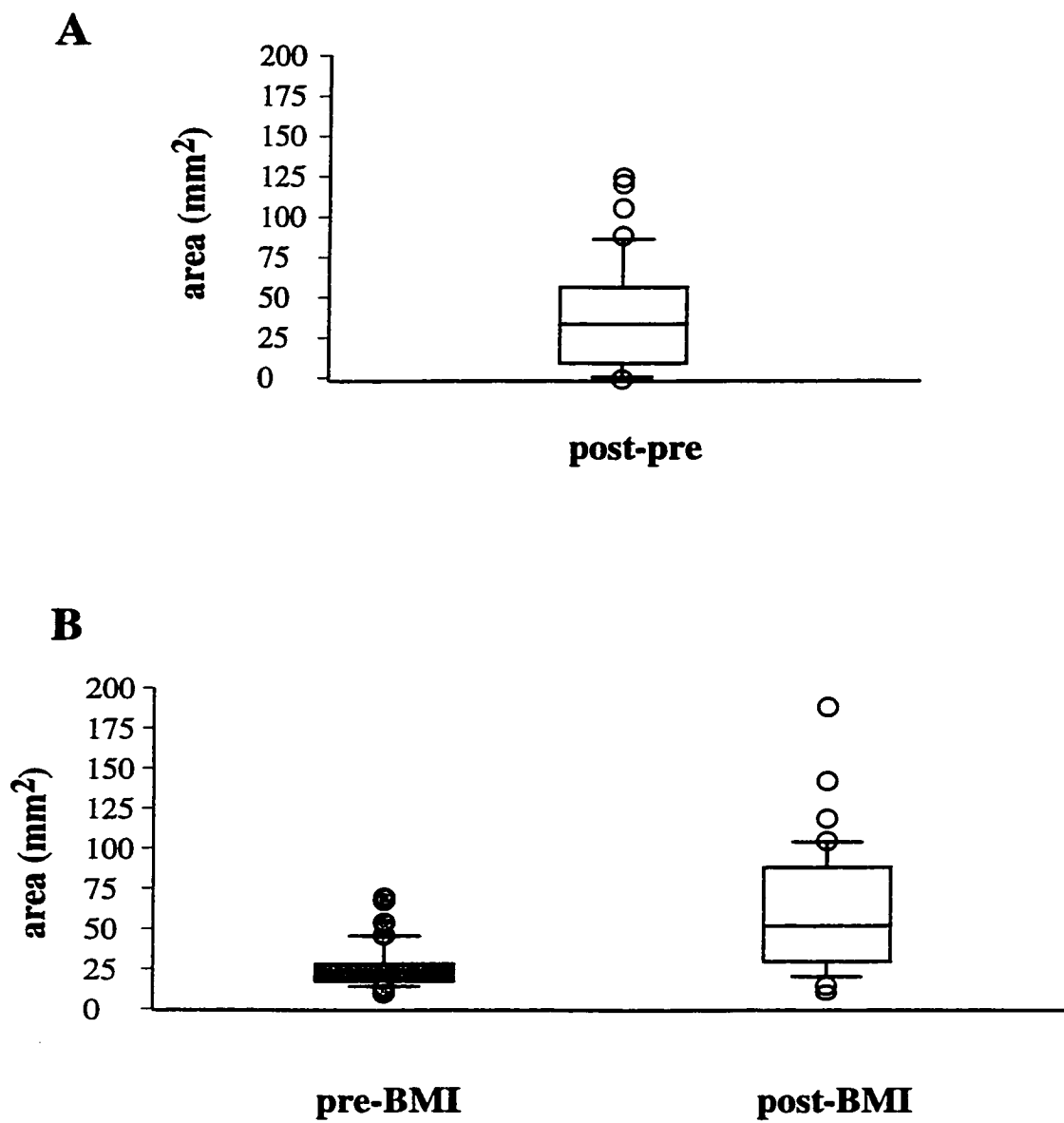


Figure 14

expect decreased, rather than increased, variability with BMI application.

### **3.3.b BMI effects on RF organization in amputated animals**

There were two types of changes produced by BMI application at cortical neurons undergoing reorganization. The first type of change was a simple expansion of the field originally encountered during the recording session. The term simple expansion was used to emphasize the preservation of the original RF shape despite an expansion of the RF. The second type of expansion drastically altered the RF shape and often involved the inclusion of a new functional region of the forepaw, such as a subfield on an adjacent digit.

#### **3.3.b.1 RF expansion with BMI in amputated animals**

BMI application led to expansion of the RF in 64/103 cortical neurons. Of the RFs that could be measured, the average expansion for this population of cells was 26.7 mm<sup>2</sup> which was an average increase of 400% in the original field sizes. It was possible to quantify the changes in area for these 15 neurons that had a confined RF prior to BMI application. The distribution of the original RF sizes is illustrated in Figure 15A. In Figures 15B and C these changes were plotted versus depth for absolute increases and percentage expansion, respectively. RF expansion for neurons that were undergoing reorganization could be as great as 100 mm<sup>2</sup>. This maximum expansion did not differ

**Figure 15**

Original RF size and expanded RFs versus depth in amputated animals.



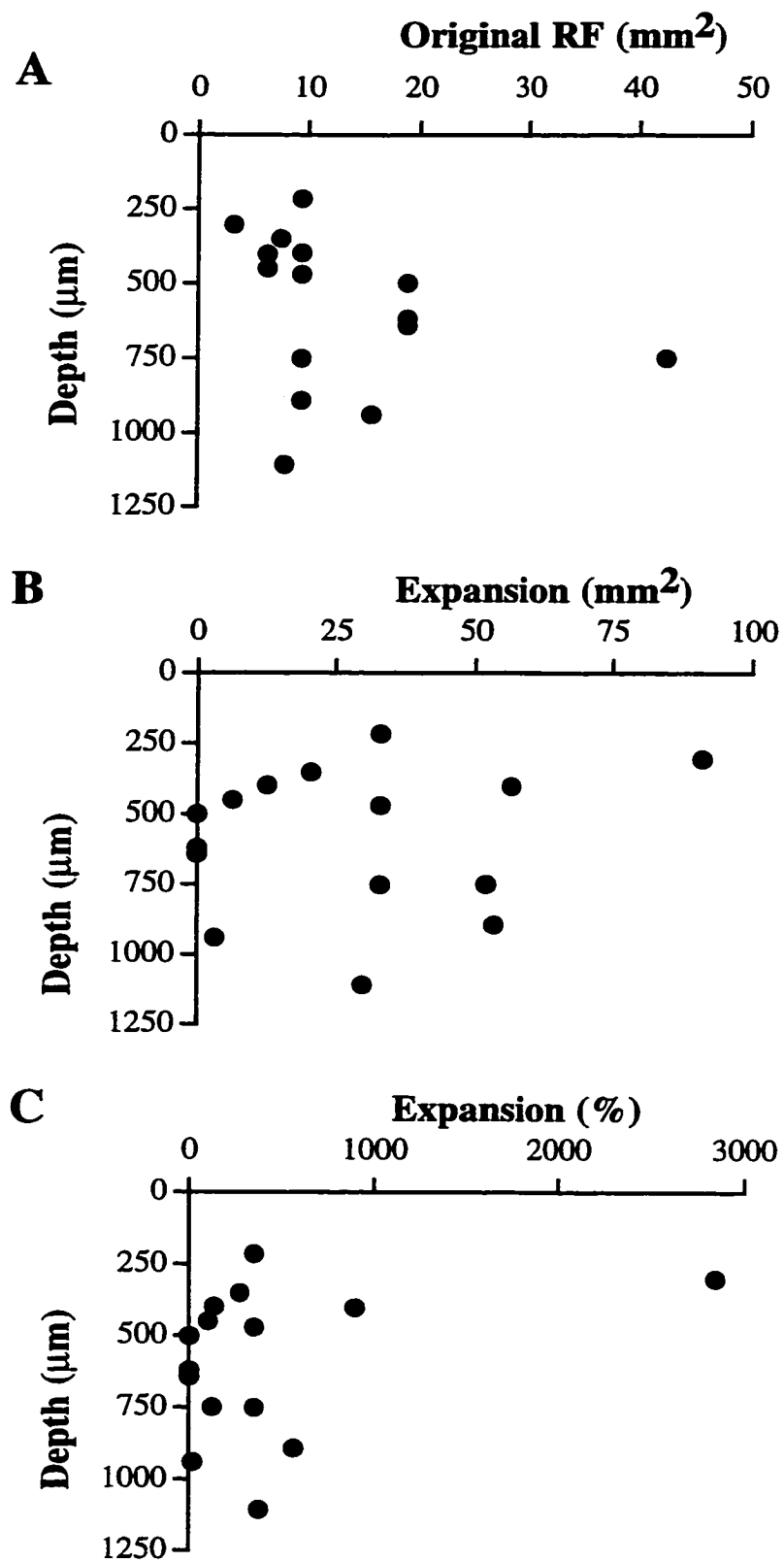


Figure 15

considerably from the expansion described in control animals (125 mm<sup>2</sup>). In control cortex the maximum RF expansion was 1000% but in amputated animals, one cell showed a percentage of expansion of 2800%. However, all of the remaining cells where the expanded RF could be quantified at a reorganizing neuron, the percentage expansion was less than 1000%.

RF expansion data was examined separately for control and reorganized neurons that had similar original positions on the digit (distal pad). None of the pre-drug RFs in the amputated animals were exceptionally large and all were confined to the distal pad (mean RF size in control animals =16.9, in reorganized animals = 13.0). In these samples the mean RF expansion for the control population (n=25) was 32 mm<sup>2</sup> with a percentage expansion of 344% (n=9). A statistical comparison of mean expansion for both absolute and percentage based calculations revealed no significant differences in the expanded area for control and reorganized neurons (absolute measure  $t=0.532$ ,  $df= 28$ ,  $p >0.05$ ; percentage measure  $t=1.06$ ,  $df=28$ ,  $p>0.05$ ).

These data indicate that the small RFs found in reorganized neurons are not abnormally large RFs that are functionally constricted by intra-cortical inhibition, instead, they are more similar to control neurons.

#### **Simple Expansion with BMI in amputated animals**

Simple expansion, where the shape of the expanded RF resembled the pre-drug RF and the expansion did not extend beyond the boundary of the on-focus digit, occurred

in 39 reorganized neurons. In 29/39 neurons that showed simple expansion the original RF was confined. Simple expansion also occurred at 3 joined RFs and 7 split RFs. Table 4A categorizes the appearance of simple expansion at the three types of reorganized RF type by time. Simple expansion of the joined RFs was only seen after 19 weeks. In contrast simple expansion of split and confined fields appeared at all post-amputation times.

### **RF Transitions produced by BMI in amputated animals**

BMI led to a transition or re-classification of the RF type in 22/103 cortical neurons. Each of these cortical neurons had RFs on the glabrous surface of the forepaw prior to the application of BMI. All but two RFs remained totally on glabrous skin after BMI application. The two exceptions were cases where BMI application caused the cell to respond to stimulation of multiple claws in addition to the confined field that was initially encountered in the pre-drug condition. Examples of the various types of transition produced by BMI are presented in Figures 16 – 20. One example of each type of transition is illustrated. Fig. 16 provides an example of a joined field that acquired distinct subfields (grey) after BMI application. Subfields were easily distinguished within the joined RF because they had a considerably lower threshold and produced a greater response when stimulated with the same von Frey monofilament. This was seen in eight cells, and in all cases the appearance of the subfields occurred within the boundaries of the pre-drug RF.

**Figure 16**

Example of BMI application adding subfields to a joined field. In these neurons new subfields appeared within a joined field in response to glutamate or BMI application.

The original RF (left), indicated by heavy line, covered all of the 3<sup>rd</sup> and 5<sup>th</sup> digits and a large part of the palm. Glutamate yielded much stronger responses from the 5<sup>th</sup> digit (black). BMI revealed two subfields (grey) on the 5<sup>th</sup> digit with decreased thresholds.

**Joined with subfields**

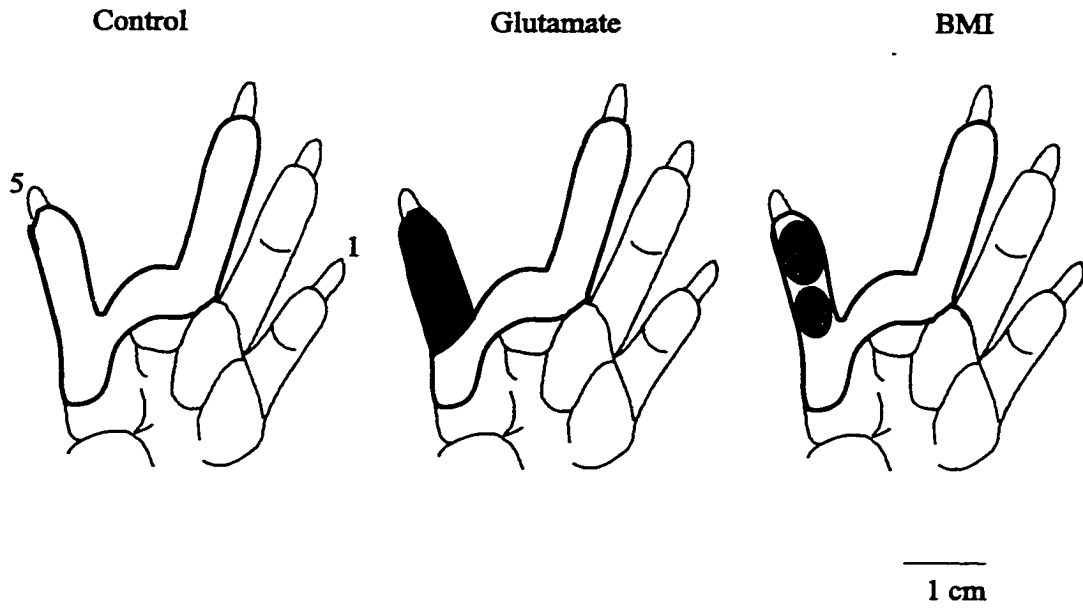


**Figure 16**

**Table 4 The number of neurons showing transitions of RF classification following BMI application**

**A. Summary of Simple Expansion across time**

time (weeks)	joined	split	confined	total simple expansion	total cells
2- 8	0	2	3	5	18
11- 15	0	2	12	14	29
19-24	2	2	8	12	34
34-37	1	1	6	8	27
	3	7	29	39	108

**B. Summary of RF Transitions across time**

time (weeks)	joined with subfields	split to joined	confined to split	confined to joined	confined to multiclaw	total cells
2 – 8	1	2	0	0	0	18
11 – 15	1	2	0	0	0	29
19 – 24	3	0	0	1	0	34
34 – 37	3	3	2	2	2	27

Another type of transition was from the split RF to a joined RF. This occurred in 7 neurons. The RF illustrated in Figure 17 is an example of a “split” RF. This cell was found at a cortical depth of 301  $\mu\text{m}$  and had an original RF that covered the surface of the third digit. There was a weak response to tapping of the claw which was strengthened with the application of BMI or glutamate. After BMI was applied, at 31 nA for 2 min, the cutaneous RF of this neuron became “joined”. The threshold for the skin near the wound was lowered across the palm, which joined the two subfields on the adjacent digits.

Fig. 18 shows one of two cases where a confined field was converted to a split field by BMI. This cell was found at a cortical depth of 242  $\mu\text{m}$ . The original field was on the distal pad of the third digit; however, following BMI application at 25 nA another subfield appeared on the distal pad of the fifth digit and the original RF was greatly expanded. A less common type of RF transition was from a confined field to a joined field ( $n = 3$ ), an example of which is provided in Fig. 19. This cell was found at a cortical depth of 1400  $\mu\text{m}$  in an animal that was tested 34 weeks post-amputation. The original RF was small and located on the distal pad of the third digit. BMI application produced an enormous expansion of the RF to include skin from the wound and fifth digit. Glutamate applied to this cell at 41 nA produced a large expansion that was restricted to the distal digit and a decreased threshold in the original RF. When GABA

**Figure 17**

Example in which of BMI application converted a split field into a joined field. The RF revealed after BMI application (grey) included skin from around the wound and joined the two RFs on the adjacent digits. Glutamate application lowered the thresholds at the original fields but did not cause expansion.



**Split to joined**

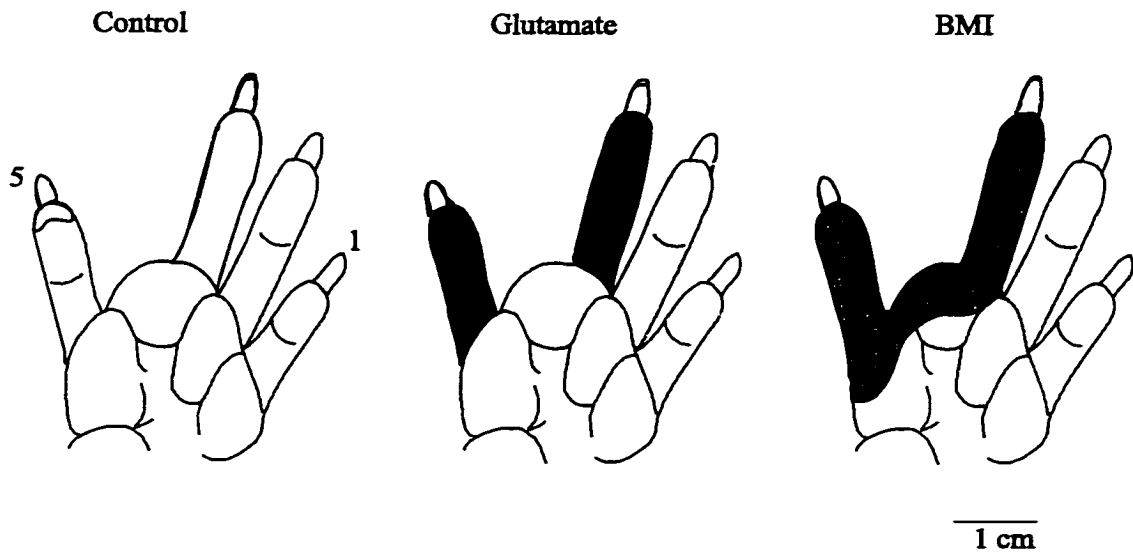


**Figure 17**

**Figure 18**

Example of a transition from a confined field to a split field with BMI. The original RF was located in the distal pad of the third digit. Glutamate (black) and BMI (grey) produced a simple expansion of the original RF. With BMI application, however, a subfield also appeared on the distal pad of the fifth digit.

**Confined to split field**

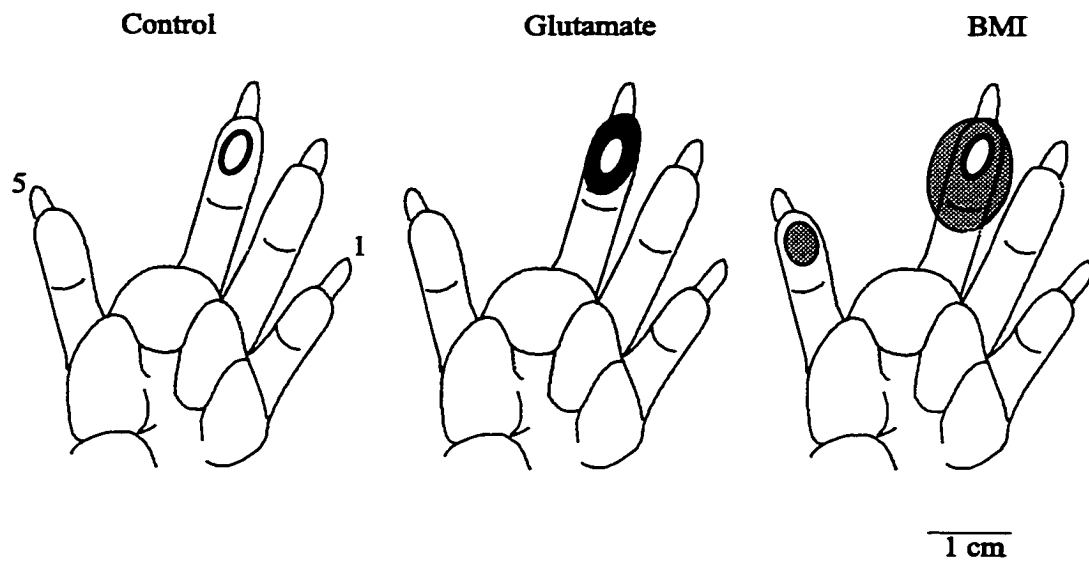


**Figure 18**

was applied to this cell, following BMI application, the RF was reduced to a size that was close to the original RF.

Figure 20 illustrates one of two examples where a confined field acquired responsiveness to stimulation of multiple claws following BMI administration. This example is derived from a cell that was found at a cortical depth of 500  $\mu\text{m}$ . Glutamate application at 60 nA for 2 min. resulted in a lowered threshold to claw stimulation at the original RF on the third digit. BMI application caused the cortical neuron to respond to claw tap of the second, third and fifth claws and lowered the threshold for the skin around the third claw (BMI application at 40 nA for 5 min).

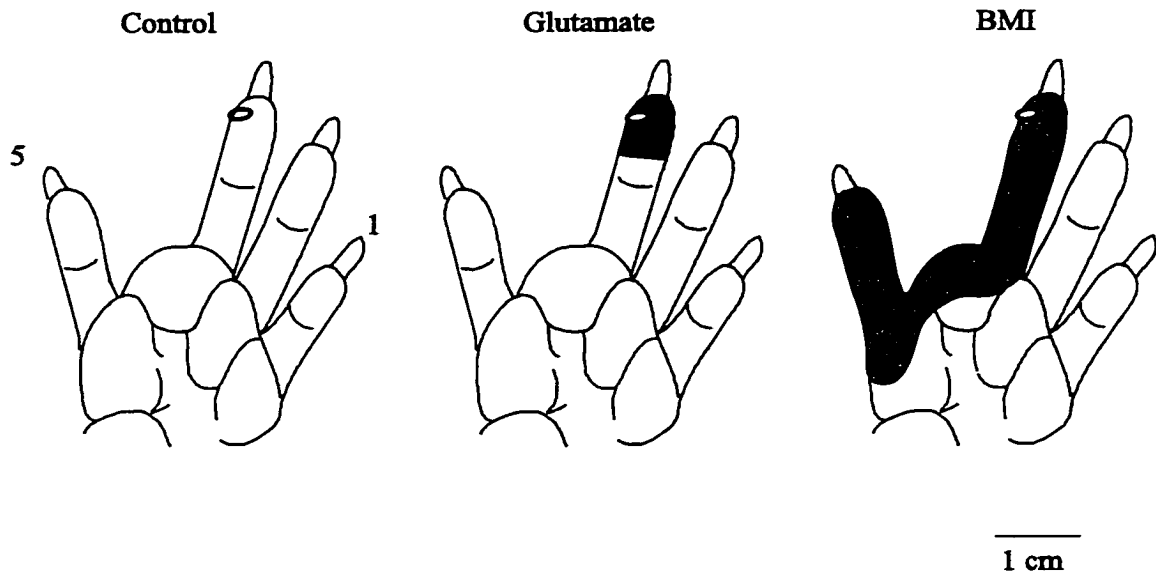
Table 5 summarizes the number of RFs that had major alterations in the size and/or shape of the RF following the application of BMI. This table shows that of the 12 large, joined RFs that were altered by BMI, 4 had RF expansion and 8 remained the same size but acquired regions of lowered thresholds. Likewise, of the 15 split fields that were altered by BMI, SE was seen at 8 RFs and at 7 cells the subfields merged into one large "joined" RF. At neurons with confined RFs ( $n=35$ ), BMI resulted in SE at 29 neurons. In 6 cells, BMI produced transitions of the RF into another classification at 6 of these cortical neurons.

Figure 21 schematically illustrates the changes typically seen in the transition of a RF at a reorganized neuron from one category of RF to another. This diagram clearly

**Figure 19**

Example of a transition from a confined field into a joined field with BMI. The confined RF initially mapped for this cell expanded to such a degree with BMI application that it was reclassified as a “joined” field (grey). Glutamate lowered the threshold at the original field and produced a RF expansion that incorporated approximately half of the distal pad (black). GABA abolished all responsiveness of the cell, both spontaneous and evoked activity.

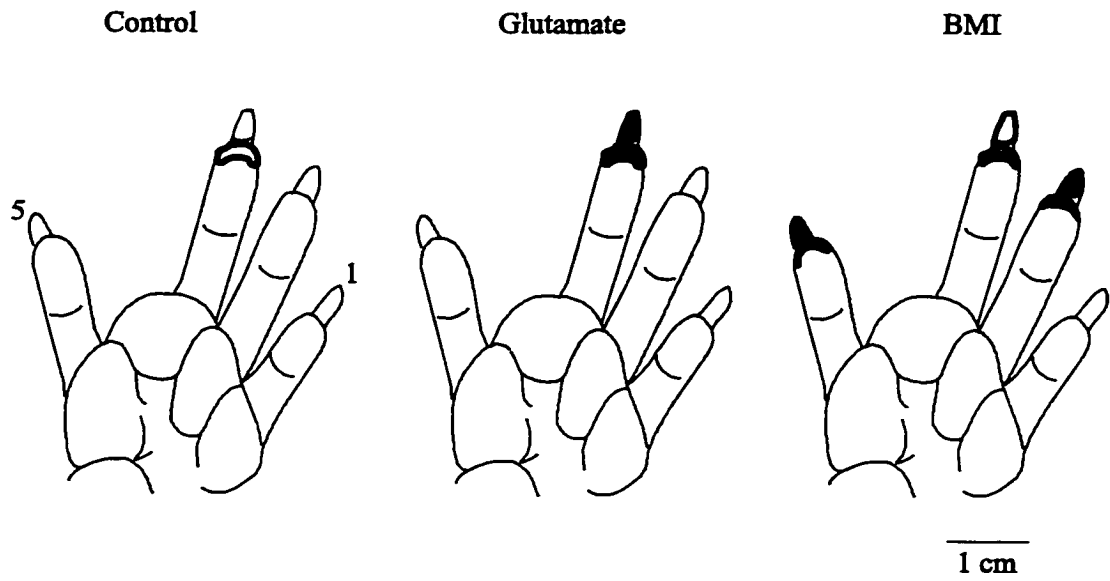
**Confined to joined**



**Figure 19**

**Figure 20**

Example of a transition from a single digit RF to a multidigit RF. The original RF included the claw of the third digit and glabrous skin around the claw. Under BMI (40 nA, 5 minutes) the cell responded to tapping of digits 5 and 2. In addition, a response of the cell could be evoked from a wider area on the skin around the claws. Glutamate (60 nA) only facilitated the response to tapping the claw of the third digit. This cell was found 500  $\mu\text{m}$  below the pial surface.

**Single to multiclaw RF****Figure 20**



**Table 5 Summary of the frequency of RF expansion and transition in reorganizing cortex**

pre- drug \ post- drug	no effect	confined	split	joined	joined new subfields	multiclaw
joined	13			4SE	<b>8T</b>	
split	9		8SE	<b>7T</b>	0	
confined	18	29SE	<b>2T</b>	<b>3T</b>	0	<b>2T</b>

T, Transitions (n=22)

SE, Simple Expansion (n=41)

Total neurons (n=103)

illustrates that transitions produced by GABAA antagonism occurred from smaller to larger, more complex fields, but never resulted in a decrease RF size.

### **3.3.b.2 RF expansion with glutamate in amputated animals**

In contrast to control animals, glutamate application caused alterations in the RF organization in some neurons in the amputated animals. In 4 neurons the RF expanded with glutamate application. Three of these cells that showed expansion had RFs on glabrous skin; one had a “joined”, one a “split”, and one a “confined” RF. In Figure 18, glutamate produced a simple expansion with the post-drug RF still confined to the original digit. Likewise, glutamate produced SE of the RF for the neuronal RF illustrated in Figure 19. In contrast, in one cell glutamate application resulted in the shrinkage of the RF and an increase in spontaneous activity.

### **3.4 BMI and Glutamate alter different regions of the RF**

It was possible to compare the effects of BMI and glutamate on 68 cortical neurons. In the majority of cases when both drugs caused alterations of RF organization these changes appeared at the same RF or subfield (43/68). Glutamate often altered the region of the RF or subfield that was close to the wound (n=12), whereas BMI did not.

These findings indicate that facilitation with glutamate may lower the threshold for direct stimulation on the nerves within the amputation site, whereas disinhibition with

**Figure 21**

RF appearance before and after transition. The three types of RF found in deafferented cortex (joined, split and confined) are illustrated in the top row.

(A) Arrows progressing from right to left show the increase in RF size associated with RF transition. The numbers over each arrow indicate the number of neurons that showed transitions of this type in the present study.

(B) Arrows progressing from left to right show a hypothetical reduction of RF. There were no examples of transitions that reduced RF size.

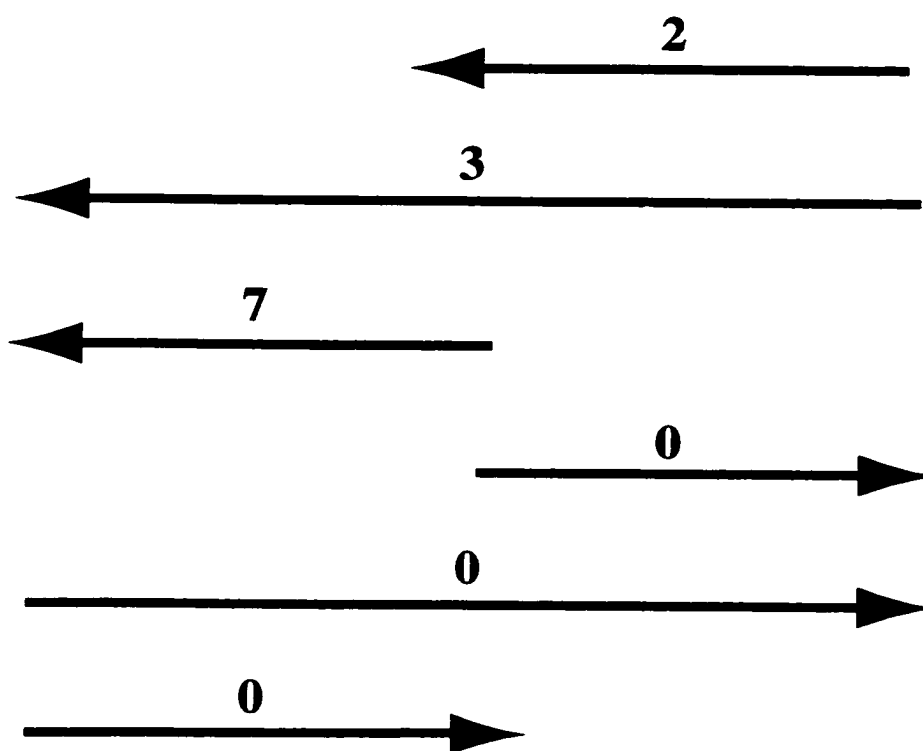
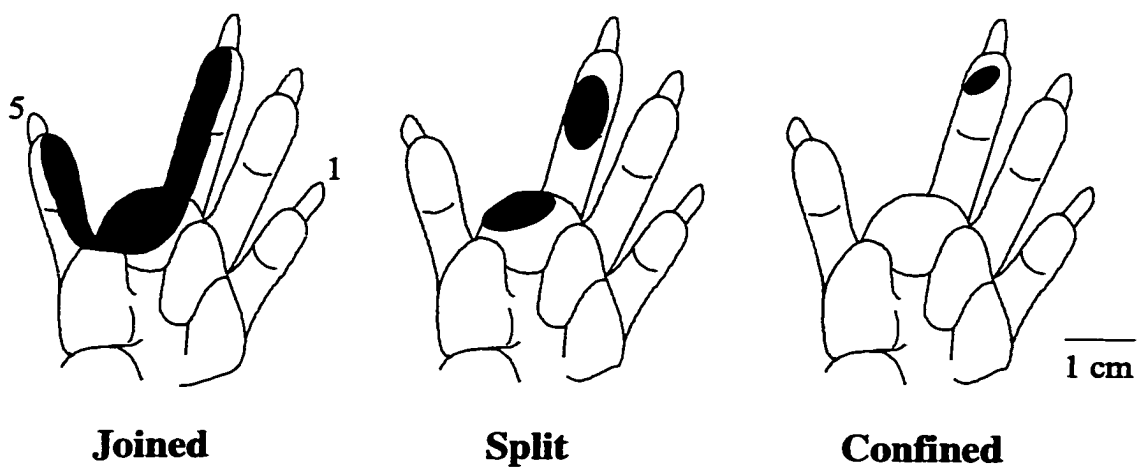


**Figure 21**

BMI may facilitate the alternative excitatory inputs to the cortical neuron, thought to underlie the generation of a new RF.

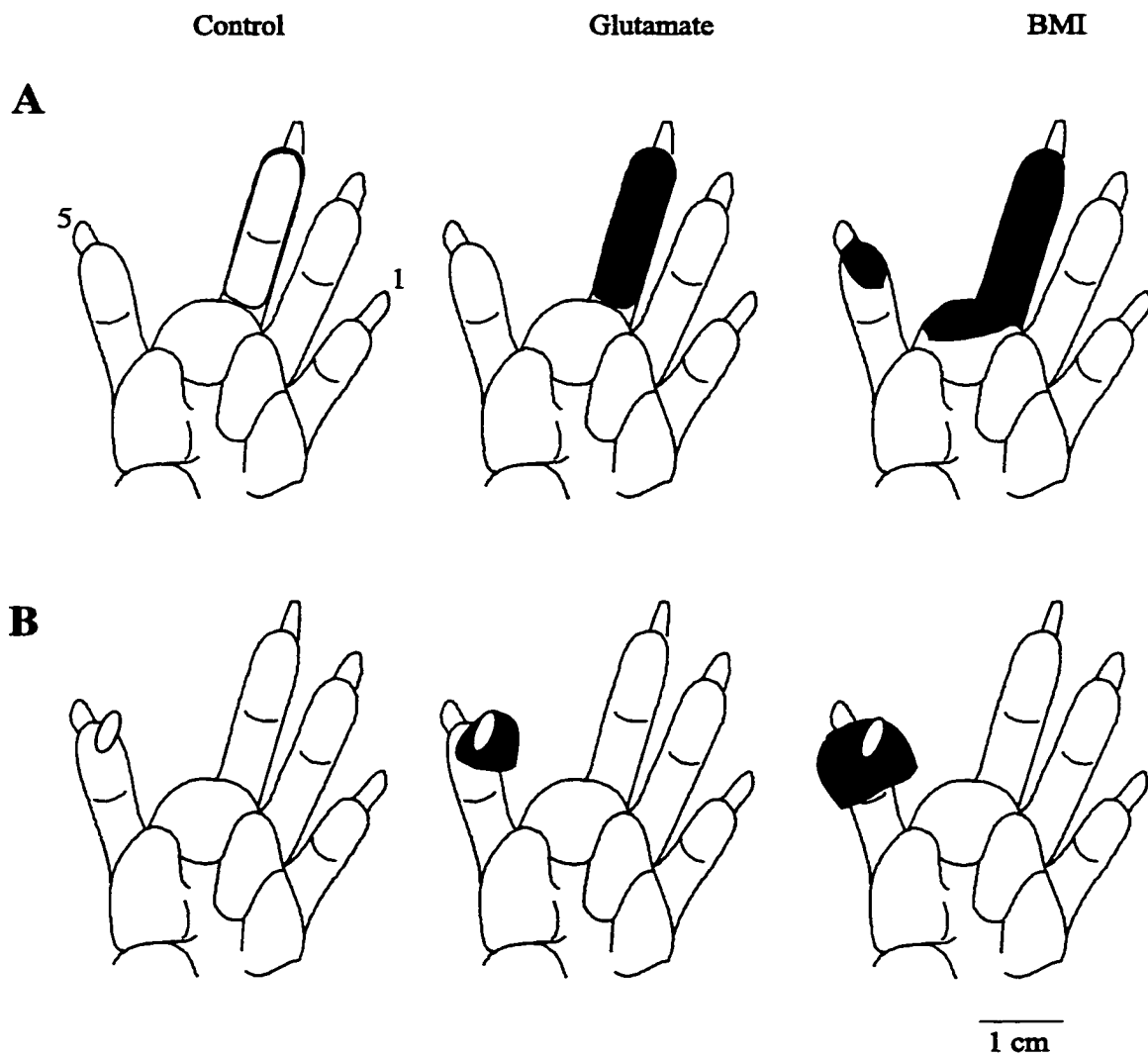
Figure 22 provides two examples where the same RF was altered with BMI and glutamate. The first cell, shown in Fig. 22A, was studied at 37 weeks post-amputation and was located at 400  $\mu\text{m}$  below the pial surface. This example shows that following glutamate application for 1 min at 30 nA, the original RF that covered the third digit had a decreased threshold to mechanical stimulation (black). BMI, applied for 5 mins at 20 nA, produced a split RF with a subfield on the fifth digit and an enlargement of the original RF (grey). At this cortical neuron, expansion of the original RF also incorporated the dorsal surface of that digit. The second example (Fig. 22B) is from a cell found at a cortical depth of 1108  $\mu\text{m}$  in a sulcus. This animal had a post-amputation period of 34 weeks prior to recording. Glutamate application, for 3 min at 30 nA, (black) and BMI, (grey) for 12 mins at 25 nA, produced RF expansion that included most of the distal pad. The extent of the RF expansion produced by BMI was, however, greater than RF expansion produced with glutamate. In 9/68 cells drug application altered spatially separated subfields. Since such a wide variety of effects on RF organization were observed, a number of specific cases will be illustrated (Fig. 23-25). Figure 23 is the schematic of a RF found in deafferented cortex 8 weeks after amputation. In this neuron, glutamate (black), applied for 5 minutes at 35 nA, lowered the threshold over the wound

**Figure 22**

Differential effects of glutamate and BMI on the same RF.

(A) The original RF, indicated in the left column, incorporated the entire glabrous surface of the third digit. Glutamate lowered the threshold to the original RF (black) as well as the on the dorsal, hairy surface. After BMI application the original expanded to include skin over the wound and a subfield appeared on the distal pad of the fifth digit (grey).

(B) A small RF was located on the distal pad of the fifth digit (left column). Glutamate application resulted in RF expansion (black). This RF area was further expanded after BMI application, the maximum expansion produced included skin from the entire distal pad (grey)

**Figure 22**

creating a third subfield from which the cortical neuron could be activated. BMI which was applied at 35 nA for 14 minutes had no apparent effect on the RF.

The RFs illustrated in Figure 24 are from cells that were studied between 11 and 15 weeks after amputation. In all four examples, the effects of glutamate were seen at the subfield over the wound. The original RF illustrated in Fig. 24A had three subfields, one over the wound and one on the pad of the third and fifth digits. The effects of glutamate on the cell illustrated in Fig. 24A were restricted to the wound area and resulted in a modest RF expansion. BMI caused expansion of the subfields on the distal pad of both the third and fifth digits, but had no effect on the RF near the wound. The cell illustrated in Fig. 23B had its original RF over the entire glabrous surface of the third digit. Glutamate application exposed a subfield around the wound. BMI application did not alter responsiveness near the wound but revealed a new subfield on the proximal pad of the third digit. In the example in Figure 24C, BMI had no effect on the RF but glutamate lowered the threshold to the original RF which was over the wound. In the fourth example, (Fig. 24D), a large joined RF was reduced to the region around the wound by glutamate, and the response to stimulation of either digit was lost. When BMI was applied at this cell (6 min. at 70 nA), a subfield with a lower threshold was revealed on the distal pad of the fifth digit.

Three cells that were studied 19 – 37 weeks after amputation are shown in Figure 25. In Figure 25A, the original field was found on the distal pads of the third and fifth



**Figure 23**

Example of different effects of BMI and glutamate at 8 weeks post-amputation. The original field was “split” with two subfields. Glutamate lowered the threshold over the wound area, (black), creating a third subfield from which the cortical neuron could be activated. There was no effect of BMI on RF shape or threshold.

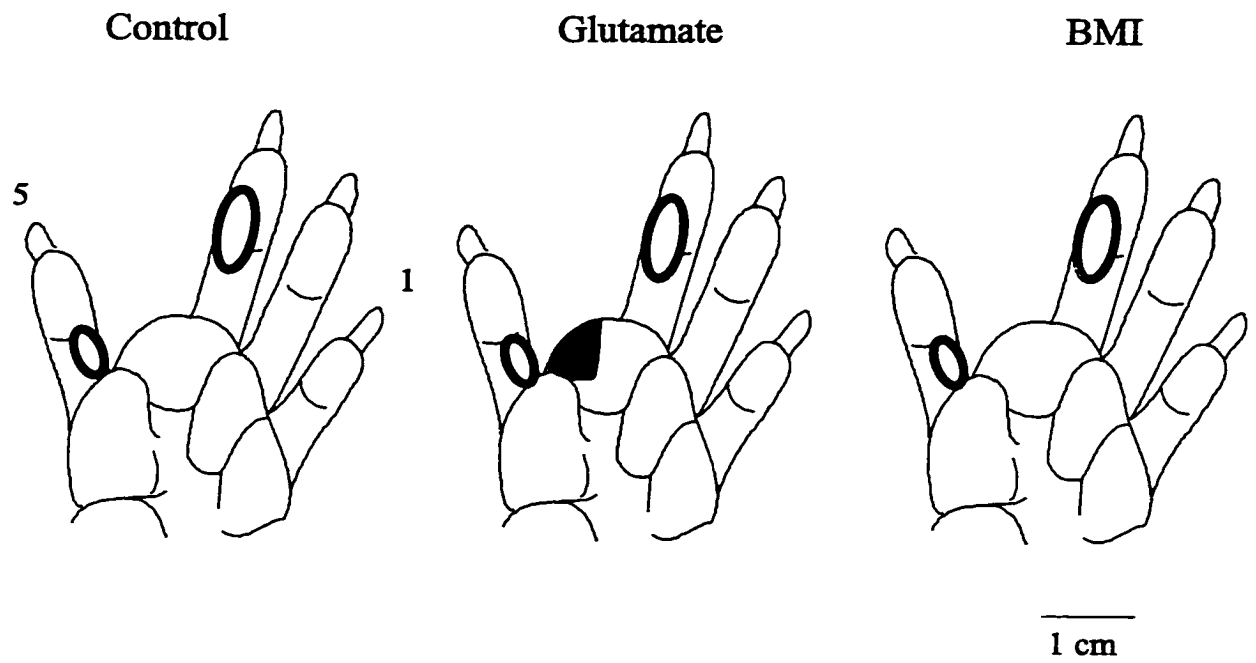


**Figure 23**

**Figure 24**

Differential effects of glutamate and BMI on cells studied 11 – 15 weeks after amputation

(A) Split RF with subfields on distal 3, distal 5 and palm. Glutamate produced an expansion of the subfield around the wound and onto the proximal fifth digit. BMI produced expansion of both the digit subfields (grey) without any change around the wound.

(B) A confined RF that included the full length of the third digit. Glutamate (black) exposed a subfield over the wound. BMI (grey) produced a subfield with a lowered threshold within the original RF, on the proximal pad of digit three.

(C) A small, confined RF around the wound. Glutamate lowered the threshold to mechanical stimulation from the original RF (black). BMI had no effect.

(D) A large joined RF that included skin from the entire length of digits three and five, as well as a large part of the palm . Glutamate (black) shrunk the RF to the area around the wound. BMI lowered the threshold to a subfield within the original RF, on the distal pad of the fifth digit (grey).

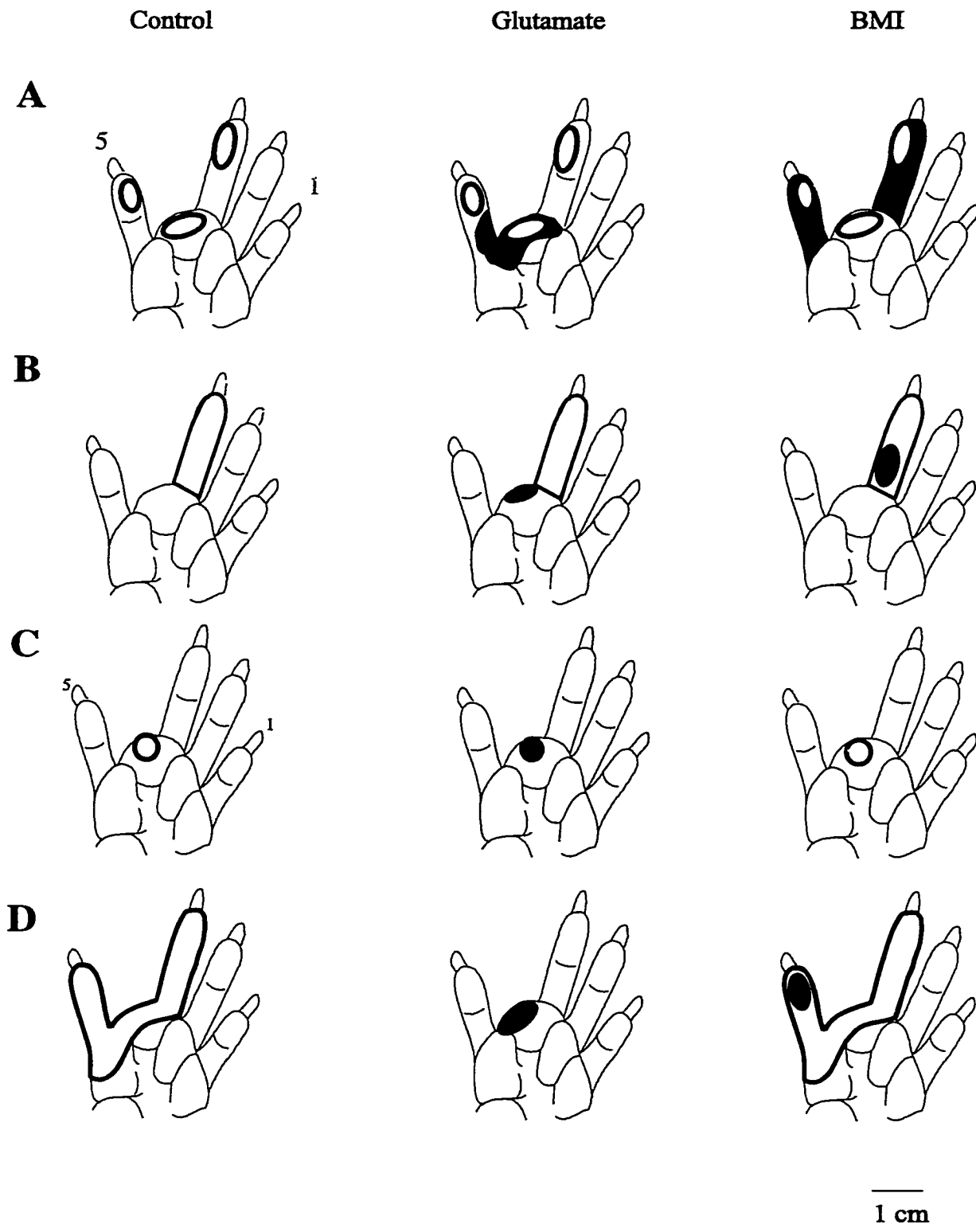


**Figure 24**

digits. Glutamate reduced the threshold at both subfields whereas, BMI produced RF expansion at both subfields. In the second example (Fig. 25B), the original RF had two subfields, with distinct responses and clear boundaries. One subfield was around the wound and another on the proximal pad of the third digit. Glutamate lowered the threshold around the wound (black) but not the subfield on the proximal pad. In contrast, BMI application removed the border between the subfields, creating the appearance of one enlarged RF. The example shown in Fig. 25C had a high threshold joined RF with portions over the entire third and fifth digits as well as the skin around the wound. In the original condition this RF had two subfields on the third digit. Glutamate application at 53 nA for 2 minutes lowered the threshold at the field on the proximal pad whereas, BMI application (5 min. at 53 nA) lowered the threshold for the subfield on the distal pad and glutamate (black) lowered the threshold at the subfield on the proximal pad.

**Figure 25**

Different effects of glutamate and BMI on RF subfields in cells studied 19 – 37 weeks after amputation.

(A) The original field for this neuron was “split” with subfields in the middle both the third and fifth digits. BMI expanded both subfields (grey), whereas glutamate lowered the threshold but did not expand the RF (black).

(B) A neuron’s RF that included skin over the wound and the proximal pad of one digit. Since the region on the palm had a slightly lower threshold than the digit, these two regions were interpreted as subfields of the RF. BMI (grey) raised the threshold on the digit, so that it was equal to the palm, and expanded the subfields, thereby merging two subfields into what appeared as a single RF. The only effect of glutamate was to decrease the RF over the wound (black).

(C) A large “joined” field with two subfields, one on the distal pad of the third digit and a second on the proximal pad. BMI (grey) lowered the threshold at the subfield

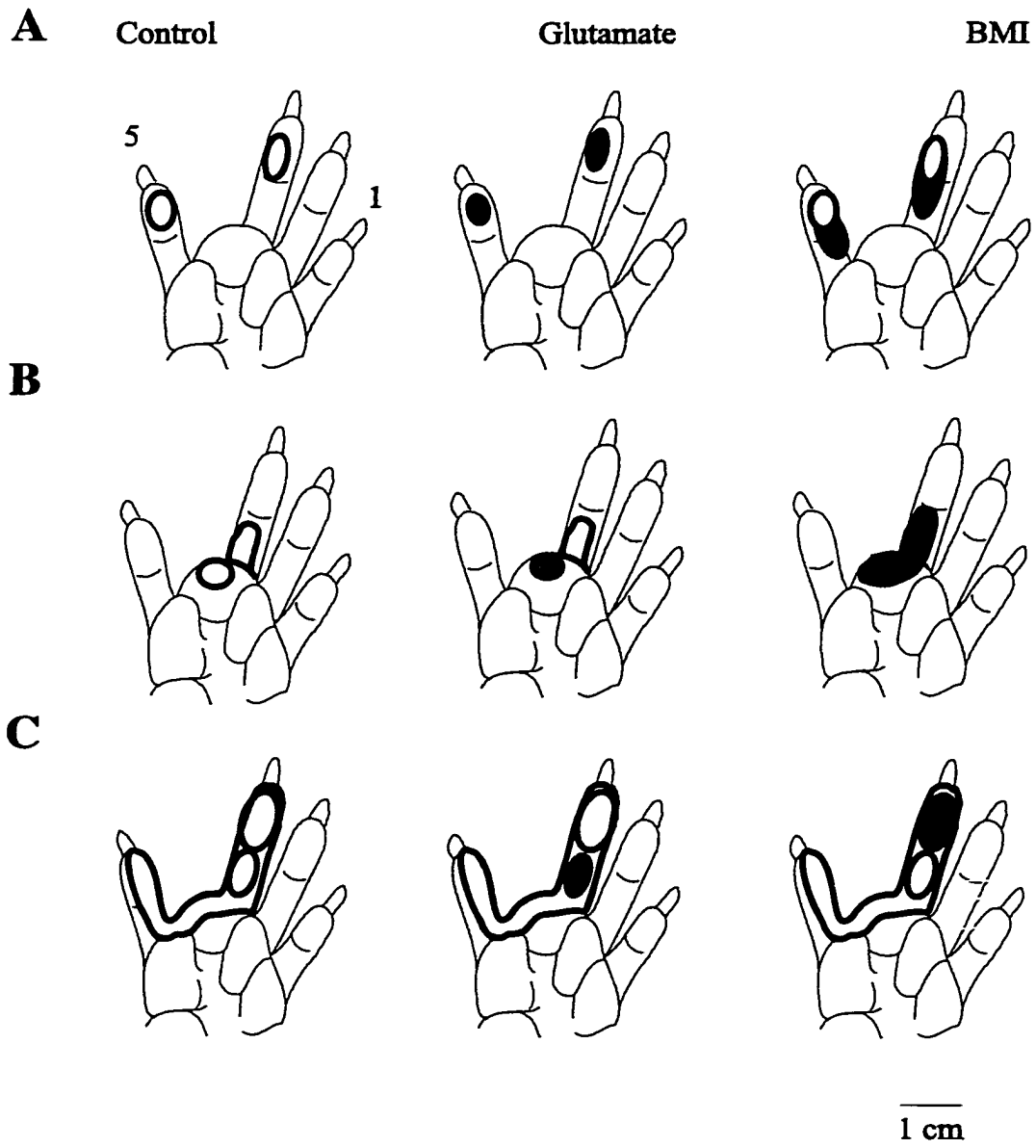


**Figure 25**

## ***4.0 Discussion***

GABA is the predominant inhibitory neurotransmitter in the brain and the most prevalent receptor for GABA is the GABA<sub>A</sub> subtype. Therefore, pharmacological antagonism of the GABA<sub>A</sub> receptor with BMI can be expected to interfere with many aspects of cortical inhibition. In this thesis, BMI was applied during RF mapping with the aim of exposing excitatory inputs that are normally suppressed in the pre-drug state. Based on the results from the control animal it is concluded that blockade at GABA<sub>A</sub> receptors does increase RF area, but RF expansion is limited to the on-focus or original digit. Therefore, the hypothesis that RFs would expand during GABA<sub>A</sub> antagonism was confirmed, but a second hypothesis, that this expansion would incorporate skin from adjacent digits, was not. Furthermore, there was considerable variability in RF expansion such that the neurons within the different functional zones did not undergo the same percentage RF expansion or expand to a constant final RF size after GABA<sub>A</sub> antagonism. The magnitude of RF expansion was, however, greater for cortical neurons in superficial layers when compared with neurons studied below the granular layer, cortical layer 4. GABA<sub>A</sub> receptor activity also modified RF shape in the deafferented cortex at all post-amputation times. However, the role of the GABA<sub>A</sub> receptor in regulating the spatial organization of the RF is more complex in deafferented cortex and varies as



reorganization proceeds. In the following sections, evidence from the present experiments will be presented to support these conclusions. In addition, the results from the experiments performed in the raccoon will be compared with the existing literature concerning RF expansion caused by GABA<sub>A</sub> receptor antagonism.

#### **4.1 GABA<sub>A</sub> receptor antagonism produces RF expansion that is limited to the on-focus digit in control animals.**

##### **4.1.a RF expansion**

The central finding of the experiments on control animals was that BMI application never produced RF expansion beyond a single digit. In addition, RFs on the palm did not expand onto digits in control animals. Even BMI ejection at higher volumes or over longer periods failed to produce RF expansion outside of these functionally distinct zones and on one occasion, BMI produced seizure like activity without additional RF expansion. This finding suggests that there is an organization within the cortical somatosensory representation that cannot be overcome by short-term alterations of the existing balance between inhibitory and excitatory inputs.

This finding differs from a similar experiment performed in primate (Alloway and Burton 1991) in which BMI applied to neurons produced RF expansion that included skin from one or two additional digits. To some extent, the different results may be due to the differences in the spatial and temporal patterns of stimulation used, as well as differences in the definition of the RF. In the primate study, the initial location of the RF was identified with a series of von Frey monofilaments, as was employed in the present study, and was used to demarcate the threshold RF. However, the quantified effects of RF expansion reported in primate were calculated with a second stimulation method that used a wider probe and a suprathreshold stimulus which produced a suprathreshold RF map. Another possible explanation for the differences in RF expansion is that these two species differ in the amount of convergence and divergence in the ascending pathway (for review see Johnson 1990).

In the present study, RF expansion was shown to be unrelated to the original RF size (Fig. 13), which is consistent with studies in cat somatosensory cortex (Alloway et al. 1989). The apparent excitatory RF results from an interaction of the inhibitory and excitatory fields at the same neuron. Therefore, it is possible that variability in the percentage of RF expansion could be explained by differences in the strength and size of the inhibitory RF. This possibility was investigated by comparing the maximum RF size following BMI application. However, removal of the influence of the GABA<sub>A</sub> receptor

did not expose excitatory RFs of equal size, even when comparisons were restricted to RFs within the same functional zone on the forepaw (Fig. 14). The wide ranges of absolute and percentage expansion that were produced with BMI (Fig. 9) likely reflect anatomical differences in both excitatory and inhibitory RFs onto individual cortical neurons.

In the cat (Alloway et al., 1989), RF expansion was shown to be unrelated to its peripheral location, which was also true in the raccoon. The mean percentage expansion data suggested that there might be differences in the extent of RF expansion in different regions (distal pad, mean expansion = 202%, proximal pad, mean expansion = 168% and palm, mean expansion = 390%). However, this conclusion was not supported by an analysis of variance of the percentage expansion for the three zones.

In this study, the average RF expansion measured as a result of BMI application was 38.8 mm<sup>2</sup> or 224% in control animals. In the primate, Alloway and Burton (1991) found an average increase in RF area of 231% at RA neurons that had RFs on glabrous skin. In the cat, changes in RF size were not quantified in terms of the area but by changes in one of the radii of the RF. Alloway and Burton (1989) showed that BMI produced a 149% average increase in the length of the RF of neurons representing glabrous and a 141% increase for RFs on the hairy skin on the forepaw. However, these changes cannot be compared directly as measurements based on the radius only capture changes in one dimension, whereas changes in area represent changes in two dimensions.

It is interesting that percentage expansion was similar for the control condition in the primate and raccoon, 231% and 224%, respectively. However, an important difference in these two experiments was that in the primate, RF expansion revealed multi-digit RFs, but in the raccoon, expansion was restricted to the on-focus digit. These data raise questions as to whether the same proportion of expansion occurs with either suprathreshold and peri-threshold stimuli provided the intensity of stimulation is consistent throughout the mapping procedure and if BMI produces a consistent percentage RF expansion across different species.

RF expansion with BMI application is more commonly seen at rapidly-adapting neurons and less commonly found at slowly-adapting neurons (Hicks and Dykes 1983). The present study was restricted to an exploration of rapidly-adapting neurons. In the normal raccoon, BMI caused expansion in 65/102 cells or 64% of the neurons tested. This number was lower than the percentage of RA neurons that expanded with BMI application in the cat, which was 85%. Alloway and Burton (1991) did not report a value for the number of RFs expanded with BMI in the primate, but indicated that BMI expanded RFs at "most neurons". The lower relative number of cells that underwent RF expansion with BMI in the present experiment could be explained by several methodological differences including anesthetic planes of the subjects, intensity of mechanical stimulation and different strengths of ejection current.

#### 4.1.b Disinhibition versus excitation

It is possible that increased RF size with BMI was due to non-specific lowering of thresholds for all inputs rather than to a disinhibition revealing subthreshold inputs. To test this hypothesis, glutamate has often been used to directly increase the excitability of neurons, making them more responsive to the full extent of their anatomical connectivity. In general, glutamate application has altered the threshold without significant changes in RF size (Hicks and Dykes 1983; Dykes et al. 1984; Alloway et al. 1989). This finding was confirmed in the control raccoons: the effects of glutamate on RF expansion were tested at 47 neurons and in no case did it produce RF expansion. Therefore, our hypothesis (#5), that the effects of glutamate and BMI application would produce different effects on RF organization was confirmed.

### **4.2 The effect of GABA<sub>A</sub> antagonism on deafferented neurons depends on time after amputation.**

#### 4.2.a Reactivation of the gyrus

One important feature of reorganization is that the probability of finding a neuron with a cutaneous receptive field increased with time after deafferentation. The earliest recordings were made 2 weeks after digit amputation and the average number of cells per penetration was 0.4. By 40 weeks post-amputation, the average number of cells per

penetration had increased to 1. However, this value was considerably below the average number of cells per penetration in control cortex (1.7). Neither glutamate nor BMI application could be used to reveal RFs at functionally "silent" neurons (with no apparent RF) in reorganized cortex, which suggested that the circuitry which supported the new RF might not have been developed at silent cells.

#### 4.2.b Pre-drug RFs in deafferented cortex

The size and shape of RFs for neurons in the deafferented cortical region were categorically different from those found in control cortex. The terms used to describe these RFs throughout this thesis were joined, split and confined. An example of each RF type can be seen in Figure 7. Reorganized cortical neurons often had thresholds that were higher than those found in control regions, and unlike the control animals, in addition, the threshold in the reorganized animal was often not uniform throughout the RF.

The patterns of new RFs and the time course for their reappearance following reorganization were initially described by Rasmusson (1982). In that study, RFs were categorized as large (which correspond to split or joined fields in the present thesis) or small (confined) fields. Approximately equal numbers of large and small RFs were identified in the rostral and caudal divisions of the deafferented gyrus. By 16 weeks post-amputation 35 RFs were small and 18 large, but 17 of these 18 large fields were found in the caudal half of the gyrus. These findings indicated a slight trend where increased time

after amputation was associated with an increase in the numbers of cells in the deafferented gyrus that had small RFs, but this was not statistically significant ( $r=0.15$ ). Furthermore, the appearance of smaller RFs coincided with a reduction in RF thresholds (Rasmusson 1982). In the paper by Kelahan and Doestch (1984) changes in RF area, threshold and RF location were reported with increased time after amputation for RFs mapped with a threshold level stimulus. These authors identified low threshold RFs that were larger than RFs in control cortex during the period immediately after digit amputation and at long periods of reorganization. The weeks in between the immediate period and the late period of reorganization were associated with very small RFs around the wound.

Many of the conclusions from Rasmusson (1982) as well as Kelahan and Doetsch (1984) also applied in the present study. Large RFs were more common in the early period of reorganization and confined RFs in the late period. In experiments performed 2 – 8 weeks after amputation, the greatest percentage of RFs were split fields (56%). Confined RFs were found at 28% of the cells and 17% were joined RFs. The animal studied at 11 weeks post-amputation had a large number of small RFs around the wound. By 15 weeks post-amputation 62% of the neurons had confined fields, 21% joined and 17% split. The greatest number of joined fields (35%) was found between 19-24 weeks; however, the highest percentage of RFs found at this time were confined fields (53%). In experiments that were performed 34 to 37 weeks post-amputation, the greatest percentage

of RFs were confined (67%), with only 15% being joined RFs and 19% split RFs. As was previously reported by Rasmusson, the appearance of smaller RFs was associated with RFs having lowered thresholds.

The average size of the confined RFs found in reorganized neurons was smaller than the average RF size in the control animal. These findings are in contrast with the report by Kelahan and Doetsch et al. (1984) who found that the average RF size was the same before and after amputation. A decrease in the average RF size for corresponding regions on the digit in control and reorganized cortex has been reported for primates by Merzenich et al (1984) and was postulated to result from the increase in cortical territory that has come to represent the remaining skin (Sur et al. 1980; Merzenich et al. 1984). Several factors could contribute to the differences in the two studies in raccoon but the most logical explanation would be methodological differences as a source of sampling bias in terms of either the number of neurons studied at different post-amputation times or the spatial distribution of sampling across the reorganized gyrus.

#### 4.2.c BMI induced changes in RFs in the amputated animal

Approximately the same ratio of neurons underwent RF alterations in the control and deafferented cortex, a finding which supports the hypothesis that BMI would influence the spatial organization of neurons in the deafferented region (#6). In the control animal 65/102 cells had RF expansion with BMI application whereas in the



reorganized animal BMI altered RF organization in 61/103 neurons. The average increase in area for all reorganized neurons that expanded with BMI was 26.7 mm<sup>2</sup> or 400% which was almost double the percentage expansion seen in controls animals. The average absolute expansion in the control animal (38.8 mm<sup>2</sup>) was greater than the average expansion seen in reorganized neurons. However, RFs found on the palm in the control animal were generally larger than those found on the digit and in reorganized animal, RFs were usually located on the digits.

When the RF sizes and expansions were compared for control and amputated animals using only confined RFs that were located on a digit, no statistically significant differences were found. However, mean RF expansion for the control population was 32.0 mm<sup>2</sup> with a percentage expansion of 210%, whereas in reorganized cortex it was 32.7 mm<sup>2</sup> and 344%. The difference in relative expansion is likely explained by the RF size in the pre-drug condition in the reorganized animal, which was an average of 4 mm<sup>2</sup> smaller than the corresponding RFs in control animals.

In addition to the diversity of the pre-drug RFs seen at reorganized neurons, the effects of BMI application were also highly varied. In some cells (n=39), BMI produced a simple expansion of the RF that reflected the original RF shape in the expanded state. In 22 neurons BMI resulted in complex changes in RF organization that have been termed RF transitions. We did not demonstrate a "greater" effect of BMI in neurons with

smaller RFs in the pre-drug condition. The two types of RF changes that were produced with GABA<sub>A</sub> antagonism will be discussed separately.

#### **4.2.c.1 Simple expansion**

The term simple expansion was used to emphasize the preservation of the original RF shape despite an expansion of the RF area. Of the 39 cells that showed a simple RF expansion in response to BMI application, the clearest examples were associated with confined RFs (n=29). Although BMI also induced expansion in the other two classifications of RF (3 joined and 7 split RFs), the boundaries of the RF at the joined fields were less well-defined, when compared with confined RFs, both before and after RF expansion with BMI. RF expansion produced with BMI application at split fields was often selective for one or two subfields. Frequently a simple expansion was detected at one of two subfields on the digits, although a couple of the cells underwent expansion of both digital subfields.

#### **4.2.c.2 Transitions**

The second type of BMI-induced change was a drastic alteration in the spatial qualities of the RF. Often the new expanded RF included skin from a different functional region of the forepaw, such as a subfield on an adjacent digit. These changes in RF shape always resulted in a RF that could be described within another category. RF transitions have been regarded as a special classification of expansion as BMI never resulted in a RF

that was smaller than the RF in the pre-drug condition (Fig. 17 – 20). The most common form of transition was found in the joined RF where subfields were revealed by BMI within the original RF boundary (n=8). The new subfields were regions where the threshold was reduced to levels that are characteristic of control RFs (Fig. 16). The second most common type of transition was from a split field to a joined field (n=7). These cases are interesting given that only 25 joined fields and 24 split fields were found in reorganizing cortex. On the contrary, 59 neurons in reorganizing cortex were identified as having confined fields but BMI only caused RF transition at 7 of these neurons. In two cases, a confined field was reclassified as a split field following BMI application and in three neurons the confined RF resembled a joined RF. The two remaining transitions converted a confined RF into a multi-claw RF.

#### 4.2.d The interaction of time and the role of the GABA<sub>A</sub> receptor in RF expansion

There were no pronounced differences in the frequency with which BMI produced RF expansions or transitions for early and late post-amputation recording times (Table 4). However, in all experiments performed more than 15 weeks post-amputation, the greatest proportion of neurons sampled had confined RFs. Of all the cells recorded later than 34 weeks post-amputation, there was only one example of a confined RF that underwent a transition into a larger category of RF with BMI application.

#### 4.2.e Disinhibition versus excitation

The excitation with glutamate application and the disinhibition with BMI application resulted in different responses at 43/68 cortical neurons, which confirmed our hypothesis regarding the different effects of these two drugs on reorganizing cortical neurons. In nine other neurons each drug affected a different region of the forepaw. These findings may be the most puzzling outcome of this thesis. It was proposed in a previous paragraph that GABA was functionally reducing the abnormally large RFs found in reorganizing cortex, in which case BMI would be exposing inputs from regions of the field that were behaviorally or biologically less relevant to the organism. The unexpected finding was that glutamate lowered the threshold to portions of the RF in or near the wound in 12 cases, and that BMI only had this effect on one cell. One interpretation for these findings is that BMI reveals the extent to which active connections are suppressed in the cortex, whereas glutamate facilitates the cell's response to a weak input. Since the appearance of RFs near the wound decreased with time, it would also appear that this input is attenuating rather than actively suppressed by inhibitory mechanisms.

#### 4.2.f GABA and the reorganization process

##### **The reorganization process: A proposed role for GABA in reshaping of RFs**

The ability of GABA<sub>A</sub> antagonism to expose large RFs within reorganizing cortex supports the hypothesis that reorganization involves the division of large fields into subfields that are subsequently reduced in size and number (Figure 26). According to this interpretation of the reorganization process, the latter stages of reorganization would be accompanied by the reduction of the RF area to a single functional zone (i.e. a digit). The data in this thesis suggest not only that this reduction in RF area occurs at longer times after the amputation but that this inhibition may lead to a permanent reduction of RF area. The RF transitions produced with BMI in these experiments demonstrate the capacity for GABA to reduce the area of the RF. However, in the majority of examples, chemical unmasking did not result in massive changes in RF size that encompassed the skin of multiple digits, as was described in primate (Alloway and Burton 1991).

#### **4.3 Other Drug Effects**

Glutamate, rather than BMI, was associated with exposing RFs near the wound. This effect was greatest for animals studied between 11 and 19 weeks post-amputation. The ability to use glutamate to facilitate responsiveness near the wound area decreased with longer post-amputation times and did not occur in animals that were studied later

than 24 weeks post-amputation. This situation suggested that at early post-amputation times RF stimulation near the wound could activate the normal pathway by direct stimulation of the nerve stumps. One implication of this finding is that the ascending pathway must still have been intact in order to activate the primary somatosensory cortical neuron despite the loss at the receptor level. The return of cortical organization after a peripheral nerve crush injury supports this idea. Likewise, a restructuring of the new pathway that is in progress might account for the appearance of new RFs, which were being reduced to a size that was functionally meaningful for the somatosensory system. It has been well established from research in the cat that iontophoretic application of glutamate, GABA or BMI does not alter the modality of the neuron being tested. In cat, this preservation of modality has been demonstrated for cortical neurons (Dykes et al. 1984; Hicks et al. 1986; Alloway et al. 1989), thalamic neurons (Hicks et al. 1986) and in the dorsal column nuclei (Schwark et al. 1999). Likewise, drug application had no effect on the submodality of cortical neurons in the primary somatosensory cortex.

Table 3 lists the effects of the two chemicals tested in the present experiment on neuronal activity. As expected, glutamate and BMI predominantly had excitatory effects on cortical neurons. GABA was frequently inhibitory but had an excitatory effect on a small number of cells.

Glutamate increased spontaneous firing and/or decreased the threshold to mechanical stimulation of both control and reorganizing neurons. Comparisons between

the effects of BMI and glutamate in control and amputated animals revealed a significant difference between the drugs, with glutamate increasing neuronal excitability at more neurons than BMI, but there was no difference in the effectiveness of the same drug in control versus amputated animals.

BMI also increased neuronal activity in both control and amputated animals. At cortical neurons, BMI application increased neuronal firing, which often appeared as bursts of 3 or 6 spikes. This result was slightly different than the values reported by Dykes et al., (1984) where BMI application caused bursts of 3 to 15 spikes in certain cells. BMI lowered the neuronal threshold to activation by cutaneous receptors for neurons in the control (21%) and amputated animal (42%). Small increases in spontaneous firing were detected in cortical neurons in the control condition (41%) and in the amputated animal (20%) which suggested that even with the removal of a considerable amount of fast inhibitory input, the remaining excitatory input may have been insufficient to cause these cells to fire. Since RF expansion and increased neuronal excitability coincided in only 6/88 neurons in the amputated animal, the effects of increased neuronal excitability as a potential cause of RF expansion can be ruled out.

Given that both glutamate and GABA<sub>A</sub> receptors are likely present on every cell in the neocortex, these drugs might be expected to alter cell activity everywhere they were applied. However, in this study, not every cell responded to drug application. This

**Figure 26**

Opposite effects of GABA<sub>A</sub> antagonism and reorganization of cortical neurons. The results of the present experiment indicated a trend whereby the effects of reorganization, reduced RF area, could be reversed with BMI application, at certain cortical neurons.



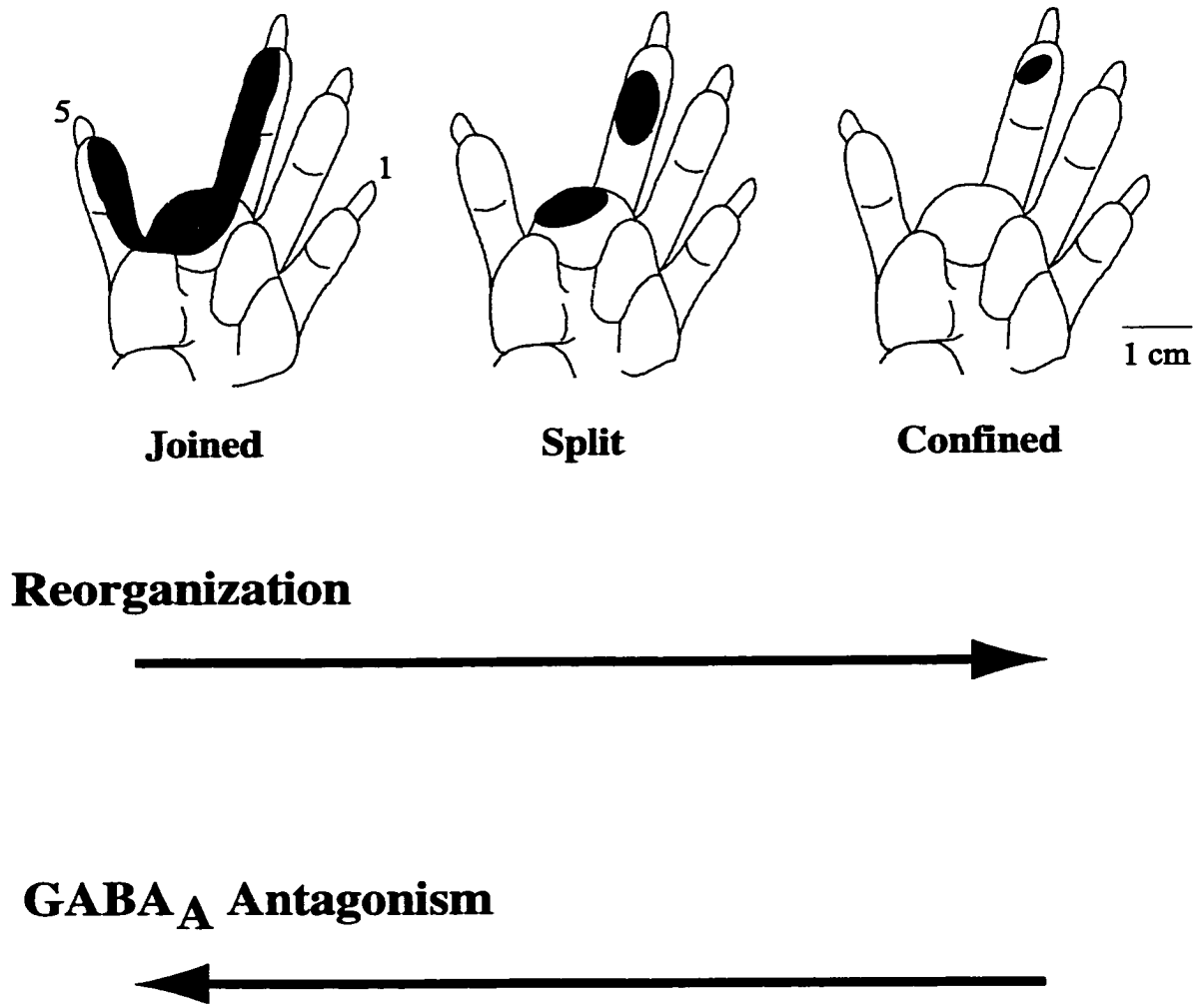


**Figure 26**

finding reveals one of the technical difficulties of using the microiontophoretic technique of in vivo drug application. At present, there are no adequate descriptions of the spatial extent of BMI diffusion in the cortex. In one study (Hupe et al., 1999), it has been demonstrated that GABA can diffuse up to 300  $\mu\text{m}$  from the ejection pipette, however, the currents used to inject this volume of drug were above the range used in the present experiment. Furthermore, it is inappropriate to base estimations of drug diffusion on the effects produced with GABA, as this molecule is likely to be identified and destroyed by endogenous enzymes, unlike the alkaloid, BMI, for which there is no known endogenous, degradative enzyme in the brain.

In total, glutamate altered activity in 74%, BMI at 53% and GABA at 78% of the cells tested. These ratios are somewhat higher than corresponding values reported by Hicks et al. (1983), however, the difference is not likely due to poor electrode function, as two of the criteria for including this data were that the pipettes conducted current normally and the drug had been effectively delivered to other neurons. Furthermore, the proportion of neurons influenced by the application of drug in this thesis may have been underestimated. When the number of action potentials was compared before and during GABA application using a window discriminator with a constant threshold, a greater number of cells were recorded as having altered activity (9/10).

The majority of neuronal recordings in the present experiment were made at depths  $< 500\mu\text{m}$  or  $> 500\mu\text{m}$ , and were most likely made from a sub-class of small

pyramidal neurons (Towe and Harding 1970). Cortical neurons at sub-granular cortical layers were not as easily influenced with the microiontophoretic technique, a finding that has been previously reported by Kyriazi et al. (1998) and Hicks (personal communication).

#### **4.4 Progression of reorganization at cortical neurons**

A common theme in CNS reorganization literature is that cortical neurons initially acquire wide, multi-digit fields and that the process of reorganization involves the reduction in area of these abnormally large fields to a single functional region (Rasmusson 1982; Merzenich et al. 1983b; Kelahan and Doetsch 1984; Merzenich et al. 1984; Calford and Tweedale 1990a; Rasmusson et al. 1991). According to this theory of reorganization, the three classes of RF used in the raccoon might represent progressive stages within reorganization. In this section the process of cortical reorganization is discussed and specific roles for GABA within this hypothesis are proposed.

##### **4.4.a The generation of new RFs**

After amputation, the denervated cortex is unresponsive to mechanical stimulation for approximately two months in the raccoon. Indications of CNS reorganization within this early period of reorganization are related to the progressive reactivation of functionally silenced neurons.

The literature on cortical reorganization in the raccoon has favored two sources for the new excitatory drive that would generate new activity in the deafferented cortical region. One possible source of new excitatory afferent input comes from the thalamus and cuneate. There is no evidence for altered thalamocortical connectivity (Rasmusson and Nance 1986). However, thalamic neurons also undergo reorganization (Rasmusson 1996). Like cortical reorganization, thalamic reorganization is associated with activation from adjacent digits and decreased thresholds for mechanical stimulation; yet, the appearance of small, confined RFs is much less common in the thalamus. The appearance of new RFs in the cortex may reflect these changes at the thalamic level. Likewise, changes in the thalamus are likely to reflect changes in the cuneate nucleus (Northgrave and Rasmusson 1996). In both the raccoon and primate, reorganization of the cuneate nucleus following denervation has been postulated as the primary site of new excitatory inputs which are relayed to thalamic and cortical RFs and provide the basis for the formation of new excitatory RFs at these levels (Rasmusson and Northgrave 1997; Xu and Wall 1999).

A second potential source for new afferent input to cortical neurons is from a neighboring region of cortex called the heterogeneous zone (Johnson et al. 1982). This region of cortex contains neurons that respond to several submodalities, including hair, joint and glabrous skin. Doetsch et al. (1988b) has proposed the heterogeneous zone is a candidate for the source of excitatory activity for neurons that formerly represented

glabrous skin, based on anatomical connectivity between these regions. Using intracellular recordings of neurons in the fourth digit representation, Smits et al. (1991) demonstrated that some neurons that respond to mechanical stimulation of the glabrous skin also have excitatory postsynaptic potentials (EPSPs) in response to electrical stimulation of hairy skin (10 of 98), vibrotactile stimulation (31 of 39), and electrical stimulation of adjacent digits (22 of 103). They also can produce mono- and polysynaptic EPSPs following intracortical microstimulation of the heterogeneous zone. Zarzecki et al. (1993) subsequently showed that these corticocortical connections may be strengthened during reorganization resulting from digit amputation.

While some neurons in the reorganized region respond to new inputs that are not strictly glabrous, the majority of new RFs are glabrous (Rasmusson 1982; Kelahan and Doetsch 1984; present thesis). Furthermore, RFs that appear in early stages of reorganization do not have the same spatial organization or mix of submodalities that characterize the RFs found in heterogeneous cortex. Therefore, although some pre-existing connectivity between these regions does exist, it is unlikely that this connectivity explains the appearance of new RFs within reorganized cortex.

The major changes seen in reorganized cortex in the late period of reorganization are related to the appearance of smaller RFs. A role for GABA in reshaping the RFs of cortical neurons has been heavily suggested in previous literature but is explicitly confirmed in the present study. The ability of BMI to unmask large RFs from confined

RFs provides critical evidence in support of the hypothesis that GABA regulates the size and shape of reorganized RFs in cortical neurons.

Interestingly, a large number of cortical neurons with confined fields underwent simple expansion after BMI. This result suggested either that RF narrowing by GABAergic inhibition is only part of a greater process which causes a permanent reduction in RF size or that the inputs to these cortical neurons are relaying information from a confined RF. However, another possible explanation for the new small RFs within the reorganized region may be that increased stimulation of certain regions of skin, that are made more accessible to touch following an amputation, for example skin on the sides of the adjacent digits, leads to invasion into the denervated zone. The evidence to support this hypothesis comes from the work of Recanzone et al. (1990) who demonstrated that increased stimulation of a peripheral nerve produced an expansion of the corresponding cortical representation. A similar acquisition of new cortical territory has been shown to result from the increased activity of a body part associated with the completion of a stereotyped behavioral task (Jenkins et al. 1990; Recanzone et al. 1992).

## ***5.0 Conclusions***

The major conclusion of the present study is that the GABA<sub>A</sub> receptor regulates RF size in normal somatosensory cortex and in reorganized cortex following digit amputation.

In the normal animal, RF expansion with BMI is limited to a single digit, or if the RF is on the palm, there is no expansion onto the digits. Therefore, the pharmacological blockade of this receptor did not mimic RFs seen in reorganized cortex and could not explain the appearance of RFs on adjacent digits following amputation. The magnitude of RF expansion induced by GABA<sub>A</sub> antagonism was not related to the neuron's laminar depth within the cortex. However, relatively less expansion was seen for RFs of neurons below 800µm. This indicated that BMI might have different effects on neurons in the supragranular and granular layers than it does in infragranular; these data confirm an earlier similar conclusion in the rat. The effects of disinhibition produced with BMI were not functionally equivalent to increased excitation as glutamate failed to produce RF expansion. These findings suggest that in the cortex, GABA may have a unique role in determining the impact of viable inputs on the target neuron.

In amputated animals, GABA<sub>A</sub> receptor antagonism also caused RF expansion for many neurons in reorganized cortex at all post-amputation times. RF expansion was produced with BMI in neurons RFs of all categories (joined, split and confined RFs)

which suggested that even when GABA appears to be down-regulated, GABA<sub>A</sub> antagonism can still modify the RF. However, BMI did have more pronounced effects with increased time after amputation, suggesting that recovery of inhibition is likely to be part of the reorganization process. RF expansion induced by GABA<sub>A</sub> antagonism did not differ according to the laminar location of the neuron but differed according to post-amputation time. This effect was closely related to the increased proportion of confined RFs seen at longer post-amputation times. Since GABA<sub>A</sub> antagonism at neurons with confined RFs did not always result in the appearance of abnormally large, joined or split RFs, it would appear that the appearance of smaller RFs at longer post-amputation times is not strictly regulated by local inhibitory mechanisms dependent on this GABA receptor.



## **6.0 Appendix**

Activity dependent decreases in cytochrome oxidase (CO), GAD and GABA have been reported following ablation of a vibrissal follicle in the rodent (Land and Akhtar 1987; Akhtar and Land 1991) and monocular deprivation in adult monkeys (Benson et al. 1994). It was possible that amputation would result in the decrease in labeling of GAD or CO in the gyrus that represented the fourth (amputated) digit. Therefore, comparisons were made between the normal and deafferented cortex for CO and GAD histological profiles in normal and deafferented cortex. Our hypotheses are:

- Decreased metabolic activity in the denervated gyrus will result in decreased cytochrome oxidase staining within the gyrus that represents the fourth digit.
- The number of GAD immunoreactive cell bodies and/or terminals per unit area will be decreased in amputated animals relative to controls. If this hypothesis is supported, a secondary hypothesis is that the greatest relative decrease will be seen at post-amputation periods that correspond to the early stages of reorganization, the first four months after amputation.
- The density of cell bodies will not be altered in the deafferented gyrus.

## **Methods**

At the end of the recording session each animal was euthanized with a dose of more than 50 ml of  $\alpha$ -chloralose or sodium pentobarbital (Somnotol, 65 mg/ml). When

the animal was used for histology, it was perfused transcardially with 1000 ml of 0.9% saline followed by the same volume of 4% paraformaldehyde. The brain was removed from the skull and immersion fixed for 12 hours in 4% paraformaldehyde. Following this period, the brain was cut in half at the midline and S1 cortex was cut into large blocks. This tissue was cryoprotected by placing it into 30% sucrose until it equilibrated.

The tissue was sectioned on a freezing microtome at either 20 or 30  $\mu\text{m}$  thickness and placed into 0.01 M phosphate buffered saline (PBS). The sections were reacted with one of three types of histological protocols. Tissue was processed with to see the density of cells and the extent of damage around an electrode track. Alternatively, the activity level was assessed with a mitochondrial stain, cytochrome oxidase c. In addition, immunocytochemistry was performed using three different antibodies, as well as different cell visualization techniques.

### **Thionine Stain**

Sections were mounted and dried onto chrome-alum-subbed slides and placed into a series of alcohols to rehydrate the tissue. Nissl staining was performed with 0.05% thionine. The sections were subsequently dehydrated, exposed to xylenes and then coverslipped with a resin mountant (Entellan, BDH, Darmstadt, Germany).

## Cytochrome Oxidase

The tissue was mounted from 0.01M PBS onto chrome-alum-subbed slides and allowed to dry. These slides were immersed in cold acetone for 5 minutes. Acetone was rinsed away with three changes of 10% sucrose in 0.1M PBS. The slides were placed in a solution containing 0.01M TBS, 0.028% cobalt chloride, 10% sucrose and 0.5% dimethylsulphoxide (DMSO) for 15 minutes. After a brief rinse in the sucrose solution, the slides were set into a reaction medium containing 0.1M TBS, 0.05% diaminobenzidine (DAB) tetrahydrochloride, 0.0075% cytochrome c, 5% sucrose, 0.002% catalase and 0.25% DMSO. Oxygen was bubbled through this reaction medium and the temperature was maintained at 40° C throughout the experiment. Sections were air dried, dehydrated and coverslipped as described above.

## Immunocytochemistry

Sections were incubated in an antibody to glutamic acid decarboxylase (GAD) (AB108 or AB1511, Chemicon, Temecula, California). The procedure began by washing the sections in 0.01M PBS. Sections were then placed in 0.3% hydrogen peroxide and agitated for 30 minutes. They were then washed in three changes of PBS for ten minutes each and placed into a blocking serum (10 - 20% normal goat serum (NGS) in PBS) for 1 hour. Sections were incubated in primary antibody for 72 hours at 40° C. AB108, AB1511 or AB143 antibodies were diluted with PBS and 2% NGS. The sections were

removed from the primary antibody and washed in PBS for 3 x 10 minutes. Sections were subsequently incubated in biotinylated secondary antibody at a 1:100 dilution for two hours. They were then washed for 3 x 10 minutes (PBS) and placed into avidin-biotin complex (ABC) solution made with the Elite kit from Vectastain (Vector Laboratories, Burlingame, CA). The concentration was 5  $\mu$ l of each solution per ml of 2% NGS. Sections were left in the ABC solution for 2 hours. The sections were reacted according to the "double-bridging" protocol detailed in the Vectastain Elite kit. Sections were subsequently washed 3 x 10 minutes in PBS and placed into solution containing 50 mg DAB (Sigma, St. Louis, MO). Visualization of the DAB reaction was carried out in fresh DAB solution with 0.3% hydrogen peroxide. To stop the reaction sections were placed in PBS. After all sections were reacted they were stored overnight in PBS at 4°C. Sections were mounted onto chrome alum subbed slides from 0.005M PBS or distilled water and allowed to air dry. Slides were dehydrated in an alcohol series (5 min @ 50%, 2 min @ 70%, 2 min @ 95%, and twice for 2 min @ 100%) and cleared in xylenes for at least 5 min. Slides were coverslipped with the synthetic resin, Entellan (BDH, Darmstadt, Germany).

### Photomicrographs

Images were captured as colored images using a JVC TK-F7300U color frame capture video camera mounted on a Leitz Orthoplan microscope. The image was also sent

to a Power Macintosh 7100/80 computer with a NuVista frame grabber board. These images were processed using Photoshop (version 3 or 4, Adobe Systems, San Jose) or Canvas (version 5.0 Deneba Systems Inc., Miami). The “levels and curves” commands were used to match background levels for the grayscale images contained in the present thesis.

## **Results**

### **Histological changes after amputation**

Tissue from animals that had amputations 2, 15 and 23 weeks prior to euthanasia was reacted for cytochrome oxidase (CO) activity. The deafferented fourth digit gyrus was compared with cortex representing intact regions of the hand. No obvious differences were seen in the tissue taken from the 2 week and 23 week post-amputation animals. However, in the animal that had an amputation 15 weeks earlier there was a subtle difference in the density of CO. Figures A1 presents low (A,B) and high (C,D) magnification photomicrographs of the same cortical section reacted for CO and photographed at equal levels of illumination. In this specimen, control regions of cortex are characterized by patches of dark staining (B,D). Alternatively, no CO rich patches were detected in the deafferented gyrus (A,C). This absence of CO patches in the deafferented region was found consistently in all sections from this animal.

Two different antibodies directed against GAD were employed in the current study. No obvious differences were detected in the IR profiles for the antibody directed against the 65 kD isoform of the GAD molecule versus the antibody raised to detect both the 65 and 67 kD isoforms of GAD. Therefore, the GAD-IR presented in this section will refer to findings obtained with the antibody that identifies both types of GAD. This reaction was robust with or without the enhancing effects of nickel ammonium sulfate.

Labeling of cells and puncta was evident throughout the primary somatosensory cortex as well as the caudate nucleus and white matter. The small round neurons in the superficial layers of cortex were the most clearly labeled cell bodies. There were fewer IR neurons within cortical layers 3 and 4 than in layer 2, and the lowest concentrations of GAD-IR positive cells were detected in cortical layers 5 and 6. Figure A2 shows examples of the IR profile in cortical layer 3. Figure A2 A and B are photographed in the same animal showing deafferented and non-deafferented regions of the forepaw representation, respectively. Regions are enlarged by 25% in Figure A2 C and D in order to reveal more clearly the relationship between the pattern of puncta and the cell morphology of the putative target neurons. While the superficial half of cortical layer 3 had few GAD IR, there was a field of dense labeling of fibers and puncta in the lower half of cortical layer 3. The photographs revealed no pronounced difference between deafferented and non-deafferented cortex.

As previously reported (Doetsch et al. 1983), the majority of GAD-IR neurons were small, round and approximately 10  $\mu\text{m}$  in diameter across the major axis. In the deeper layers larger round GAD-IR interneurons (25  $\mu\text{m}$ ) were also encountered. The number of large GAD-IR cells was small and they were always encountered below cortical layer 3. The shape, size and orientation of the soma indicated that these cells were likely basket or chandelier cells. In addition, some bipolar neurons were revealed in cortical layers 5 and 6, as well as in the white matter.

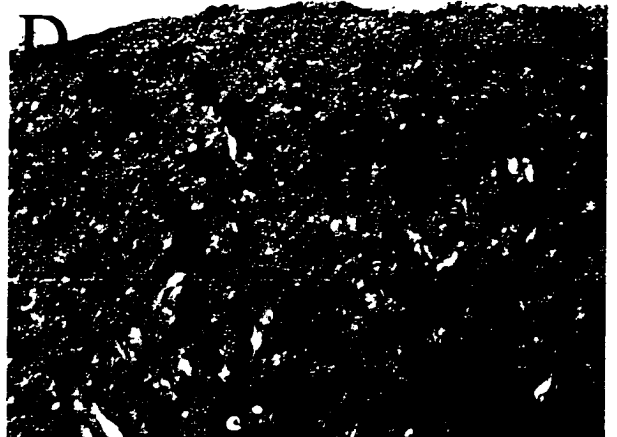
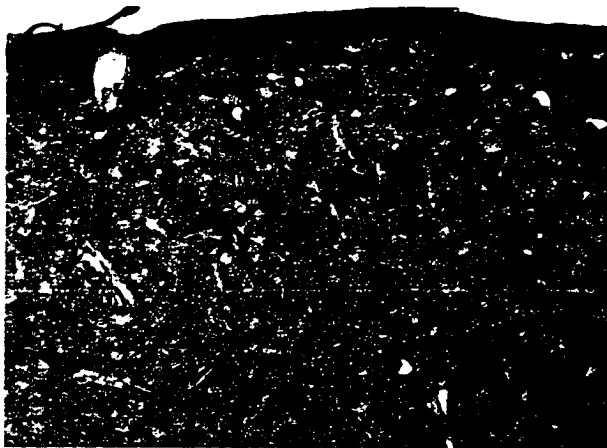
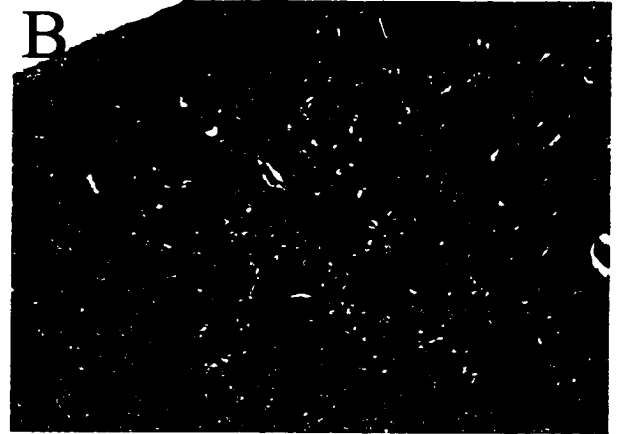
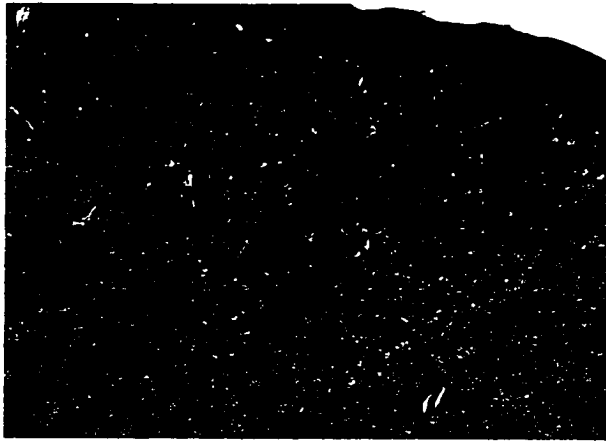
It was possible to detect IR fibers coursing over short distances; these often had several enlarged regions. These fibers were most easily detected within two dense bands of IR puncta previously described by Doetsch et al. (1993) as a bi-laminar pattern of GAD label. Relative to the cell labeling and the background, these puncta were intensely labeled and are therefore likely axon terminals. A superficial band of puncta was usually encountered at approximately 250  $\mu\text{m}$  below the pial surface and the deep band began at a depth of 1000  $\mu\text{m}$  ( $\pm$  200  $\mu\text{m}$ ).

One characteristic feature of GAD-IR labeling that appeared in the present study was the outlining of IR negative cells with IR positive puncta, sometimes referred to as “ghost cells”. When these cells were heavily surrounded by GAD-IR puncta it was possible to speculate on the morphology of the encapsulated neuron. This effect was most pronounced at large cells such as the pyramidal neuron shown in Figure A2(A). In

**Figure A1**

Cytochrome oxidase reactivity in control and deafferented cortex. All sections were photographed at the same illumination levels. (scale bar = 200  $\mu\text{m}$  for A,C and 100  $\mu\text{m}$  for B,D). CO rich patches are apparent in control tissue (A,B). This tissue was obtained from an animal sacrificed at 15 weeks after amputation.





other examples where both the cell and the puncta were labeled by GAD-IR, these were probably small interneurons (Fig A2D).

No pronounced differences were found in the density or distribution of GAD IR neurons in deafferented tissue when compared with control tissue. In many regions of the deafferented cortex as well as adjacent gyri, the size of the puncta in cortical layer 3 appeared to be approximately half the size ( $0.6\mu\text{m}$ ) of the puncta in control tissue ( $1.2\mu\text{m}$ ). However, this was not true for the puncta that outlined the large classes of pyramidal neurons found in and below cortical layer 5 that had an average size of  $1\mu\text{m}$ . There was no GAD IR fiber labeling in the 2-week animal. In the 15-week animal there appeared to be a reduction in both the frequency of encountering labeled fibers and the intensity of IR at the fiber. Preliminary attempts to calculate optical density measures were not successful.

### **Cytoarchitectonics**

The thionine stain was used to identify gross cytoarchitectural changes and/or changes in cell density between deprived and control cortex (Fig. A2(E)). No obvious differences were detected.

### **Conclusions**

The findings in this preliminary histological study show that the gyrus corresponding to the amputated digit had decreased histological reactivity for CO but not

GAD. Based on the work in other species, amputation was expected to produce a clear decrease in the number of cell bodies labeled with GAD. However, no clear decrease in GAD IR cells occurred in the deafferented gyrus in raccoon cortex. One possible explanation for these findings is that by 16 weeks, the GAD activity had been reinstated but the CO activity had not; a pattern of reactivation that has been previously reported in rats by Welker et al. (1989b).

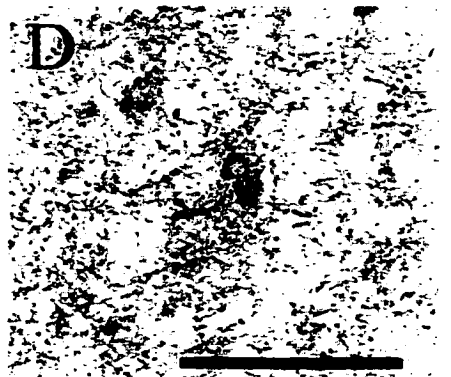
**Figure A2**

IR profiles for GAD and an example of somatosensory cortical layers.

Immunoreactive profiles for an antibody directed against the 65 and 67 kD isoforms of GAD. Photomicrographs were taken in cortical layer 3 in deprived (A) and control (B) cortex. No obvious differences can be seen in the IR profiles at these two conditions. Enlarged samples from both photomicrographs facilitate the identification of non-specific cell labeling, commonly seen in GAD IR profiles, from IR puncta (C,D). In some cases it is possible to identify the morphology of the “ghost cell” that is dotted with GAD IR puncta. Photomicrograph of a thionine stained section of somatosensory cortex from the fourth digit region in a control (E).



I  
II  
III  
IV  
V  
VI  
WM



## **7.0 Bibliography**

- Akhtar, N. D. and Land, P. W. (1991). Activity-dependent regulation of glutamic acid decarboxylase in the rat barrel cortex: Effects of neonatal versus adult sensory deprivation. J. Comp. Neurol. **307**: 200-213.
- Allard, T., Clark, S., Jenkins, W. and Merzenich, M. (1991). Reorganization of somatosensory area 3b representations in adult owl monkeys after digital syndactyly. J. Neurophysiol. **66**: 1048-1058.
- Alloway, K. and Burton, H. (1991). Differential effects of GABA and bicuculline on rapidly- and slowly-adapting neurons in primary somatosensory cortex of primates. Exp. Brain. Res. **85**: 598-610.
- Alloway, K. D. and Burton, H. (1986). Bicuculline-induced alterations in neuronal responses to controlled tactile stimuli in the second somatosensory cortex of the cat: a microiontophoretic study. Somatosens. Res. **3**: 197-211.
- Alloway, K. D., Rosenthal, P. and Burton, H. (1989). Quantitative measurements of receptive field changes during antagonism of GABAergic transmission in primary somatosensory cortex of cats. Exp. Brain Res. **78**: 514-532.
- Batuev, A. S., Alexandrov, A. A. and Scheynickov, N. A. (1982). Picrotoxin action on the receptive fields of the cat sensorimotor cortex neurons. J. Neurosci. Res. **7**: 49-55.

- Benson, D. L., Huntsman, M. M. and Jones, E. G. (1994). Activity-dependent changes in GAD and preprotachykinin mRNAs in visual cortex of adult monkeys. Cereb. Cortex **4**: 40-51.
- Brandenberg, G. A. and Mann, M. D. (1989). Sensory nerve crush and regeneration and the receptive fields and response properties of neurons in the primary somatosensory cerebral cortex of cats. Exp. Neurol. **103**: 256-266.
- Burt, A. M. (1993). Textbook of Neuroanatomy. Toronto, Saunders.
- Byrne, J. and Calford, M. (1991). Short-term expansion of receptive fields in rat primary somatosensory cortex after hindpaw digit denervation. Brain Res. **565**: 218-224.
- Calford, M. B. and Tweedale, R. (1988). Immediate and chronic changes in responses of somatosensory cortex in adult flying-fox after digit amputation. Nature **332**: 446-448.
- Calford, M. B. and Tweedale, R. (1990a). The capacity for reorganization in adult somatosensory cortex. Information processing in mammalian auditory and tactile systems. Rowe, M. and Aitkin, L. New York, Alan R. Liss: 221-236.
- Calford, M. B. and Tweedale, R. (1990b). Interhemispheric transfer of plasticity in the cerebral cortex. Science **249**: 805-807.
- Calford, M. B. and Tweedale, R. (1991a). Acute changes in cutaneous receptive fields in primary somatosensory cortex after digit denervation in adult flying fox. J. Neurophysiol **65**: 178-187.

- Calford, M. B. and Tweedale, R. (1991b). C-fibres provide a source of masking inhibition to primary somatosensory cortex. Proc. R. Soc. Lond. B Biol. Sci. **243**: 269-275.
- Calford, M. B. and Tweedale, R. (1991c). Immediate expansion of receptive fields of neurons in area 3b of macaque monkeys after digit denervation. Somatosens. Motor Res. **8**: 249-260.
- Carson, L. V., Kelahan, A. M., Ray, R. H., Massey, C. E. and Doetsch, G. S. (1981). Effects of early peripheral lesions on the somatotopic organization of the cerebral cortex. Clinical Neurosurgery **28**: 532-46.
- Churchill, J. D., Muja, N., Myers, W. A., Besheer, J. and Garraghty, P. E. (1998). Somatotopic consolidation: a third phase of reorganization after peripheral nerve injury in adult squirrel monkeys. Exp Brain Res **118**: 189-196.
- Clarey, J. C., Tweedale, R. and Calford, M. B. (1996). Interhemispheric modulation of somatosensory receptive fields: evidence for plasticity in primary somatosensory cortex. Cerebral Cortex **6**: 196-206.
- Connors, B. W., Malenka, R. C. and Silva, L. R. (1988). Two inhibitory post-synaptic potentials and GABA<sub>A</sub> and GABA<sub>B</sub> receptor-mediated responses in neocortex of rat and cat. J. Physiol. Lond. **40**: 443-468.



- Costanzo, R. M. and Gardner, E. P.. (1980). A quantitative analysis of responses of direction-sensitive neurons in somatosensory cortex of awake monkeys. J. Neurophysiol. **43**: 1319-1341.
- Cusick, C. G. (1996). Extensive cortical reorganization following sciatic nerve injury in adult rats versus restricted reorganization after neonatal injury: implications for spatial and temporal limits on somatosensory plasticity. Prog. Brain Res. **108**: 379-390.
- Doetsch, G. S., Harrison, T. A., MacDonald, A. C. and Litaker, M. S. (1996). Short-term plasticity in primary somatosensory cortex of the rat: rapid changes in magnitudes and latencies of neuronal responses following digit denervation. Exp. Brain Res. **112**: 505-512.
- Doetsch, G. S., Norelle, A., Mark, E. K., Standage, G. P., Lu, S. M. and Lin, R. C. S. (1993). Immunoreactivity for GAD $\delta$  and three peptides in somatosensory cortex and thalamus of the raccoon. Brain Res. Bull. **31**: 553-563.
- Doetsch, G. S., Standage, G. P., Johnston, K. W. and Lin, C.-S. (1988). Intracortical connections of two functional subdivisions of the somatosensory forepaw cerebral cortex of the raccoon. J. Neurosci. **8** : 1887-1900.
- Dykes, R. W., Landry, P., Metherate, R. and Hicks, T. P. (1984). Functional role of GABA in cat primary somatosensory cortex: shaping receptive fields of cortical neurons. J. Neurophysiol. **52**: 1066-1093.

- Dykes R.W., Avendano, C., Leclerc S.S., (1995). Evolution of cortical responsiveness subsequent to multiple forelimb nerve transections: an electrophysiological study in adult cat somatosensory cortex J. Comp. Neurol. **354**: 333-44
- Feldman, R. S., Meyer, J. S. and Quenzer, L. F. (1997). Principles of Neuropharmacology. Sunderland, MA, Sinauer Associates Inc., Publishers.
- Florence, S. L., Garraghty, P. E., Wall, J. T. and Kaas, J. H. (1994). Sensory afferent projections and area 3b somatotopy following median nerve cut and repair in macaque monkeys. Cereb Cortex **4**: 391-407.
- Florey, E. (1961). Comparative physiology: Transmitter substances. Ann. Rev. Neurosci. **23**: 501-528.
- Freund, T. F. and Meskenaite, V. (1992). Gamma-Aminobutyric acid-containing basal forebrain neurons innervate inhibitory interneurons in the neocortex. Proc Natl Acad Sci USA **89**: 738-42.
- Fugleholm, K., Schmalbruch, H. and Krarup, C. (1994). Early peripheral nerve regeneration after crushing, sectioning, and freeze studied by implanted electrodes in the cat. J. Neurosci. **5**: 2659-73.
- Gardner, E. P. and Costanzo, R. M. (1980). Spatial integration of multiple-point stimuli in primary somatosensory cortical receptive fields of alert monkeys. J. Neurophysiol. **43**: 420-443.

- Garraghty, P. E., Hanes, D. P., Florence, S. L. and Kaas, J. H. (1994). Pattern of peripheral deafferentation predicts reorganizational limits in adult primate somatosensory cortex. Somatosens. Motor. Res. **11**: 109-117.
- Garraghty, P. E. and Kaas, J. H. (1991). Large-scale functional reorganization in adult monkey cortex after peripheral nerve injury. Proc. Natl. Acad. Sci. USA **88**: 6976-6980.
- Hallin, R. G., Wiesenfeld, Z. and Lindblom, U. (1981). Neurophysiological studies on patients with sutured median nerves: faulty sensory localization after nerve regeneration and its physiological correlates. Exp. Neurol. **73**: 90-106.
- Harding, G. W., Stogsdill, R. M. and Towe, A. L. (1979). Relative effects of pentobarbital and chloralose on the responsiveness of neurons in sensorimotor cerebral cortex of the domestic cat. Neuroscience **4**: 369-378.
- Hicks, T. P. and Dykes, R. W. (1983). Receptive field size for certain neurons in primary somatosensory cortex is determined by GABA-mediated intracortical inhibition. Brain Res. **274**: 160-164.
- Hicks, T. P., Metherate, R., Landry, P. and Dykes, R. W. (1986). Bicuculline-induced alterations of response properties in functionally identified ventroposterior thalamic neurones. Exp. Brain Res. **63**: 248-264.
- Hupe J.M., Chouvet G., Bullier J. (1999). Spatial and temporal parameters of cortical inactivation by GABA. J Neurosci Methods **86**:129-43.

- Jenkins, W. M., Merzenich, M., Ochs, M. T., Allard, T. and Guic-Robles, E. (1990). Functional reorganization of primary somatosensory cortex in adult owl monkeys after behaviorally controlled tactile stimulation. J. Neurophysiol. **63**: 82-104.
- Johnson, J. (1990). Comparative development of somatic sensory cortex. Cerebral Cortex. Jones, E., Peters, A. New York, Plenum. **8**: 335-449.
- Johnson, J. I., Ostapoff, E. M. and Warach, S. (1982). The anterior border zones of primary somatic sensory (S1) neocortex and their relation to cerebral convolutions, shown by micromapping of peripheral projections to the region of the fourth forepaw digit representation in raccoons. Neuroscience **4**: 915-936.
- Jones, E. G. (1993). GABAergic neurons and their role in cortical plasticity in primates. Cereb Cortex **3**: 361-372.
- Kaas, J. (1991). Plasticity of sensory and motor maps in adult mammals. Annu. Rev. Neurosci. **14**: 137-167.
- Kaas, J. H., Merzenich, M. M. and Killackey, H. P. (1983). The reorganization of somatosensory cortex following peripheral nerve damage in adult and developing mammals. Ann. Rev. Neurosci. **6**: 325-356.
- Kalaska, J. and Pomeranz, B. (1979). Chronic paw denervation causes an age-dependent appearance of novel responses from forearm in "paw cortex" of kittens and adult cats. J. Neurophysiol. **42**: 618-633.

- Katz, D. B., Simon, S. A., Moody, A. and Nicolelis, M. A. L. (1999). Simultaneous reorganization in thalamocortical ensembles evolves over several hours after perioral capsaicin injections. J. Neurophysiol **82**: 963-977.
- Kelahan, A. M. and Doetsch, G. S. (1984). Time-dependent changes in the functional organization of somatosensory cerebral cortex following digit amputation in adult raccoons. Somatosens. Res. **2**: 49-81.
- Kelahan, A. M., Ray, R. H., Carson, L. V., Massey, C. E. and Doetsch, G. S. (1981). Functional reorganization of adult raccoon somatosensory cerebral cortex following neonatal digit amputation. Brain Res. **223**: 152-159.
- Kitchell, R. L., Canton, D. D., Johnson, R. D. and Maxwell, S. A. (1982). Electrophysiologic studies of cutaneous nerves of the forelimb of the cat. J. Comp. Neurol **10**: 400-410.
- Korodi, K. and Toldi, J. (1998). Does the cortical representation of body parts follow both injury to the related sensory peripheral nerve and its regeneration? Neuroreport **9**: 771-774.
- Kravitz, E., Kuffler, S. W. and Potter, D. D. (1963). Gamma-Aminobutyric acid and other blocking compounds in crustacea III. Their relative concentrations in separated motor and inhibitory axons. J. Neurophysiol. **26**: 739-751.

- Kyriazi, H., Carvell, G. E., Brumberg, J. C. and Simons, D. J. (1998). Laminar differences in bicuculline methiodide's effects on cortical neurons in the rat whisker/barrel system. Somatosens. Mot. Res. **15**: 146-156.
- Land, P. W. and Akhtar, N. D. (1987). Chronic sensory deprivation affects cytochrome oxidase staining and glutamic acid decarboxylase immunoreactivity in adult rat ventrobasal thalamus. Brain Res. **425**: 178-181.
- Land, P. W., de Blas, A. L. and Reddy, N. (1995). Immunocytochemical localization of GABAA receptors in rat somatosensory cortex and effects of tactile deprivation. Somatosens. Mot. Res. **12**: 127 - 141.
- Laskin, S. E. and Spencer, W. A. (1979). Cutaneous masking. II. Geometry of excitatory and inhibitory receptive fields of single units in somatosensory cortex of the cat. J. Neurophysiol. **42**: 1061-1082.
- Li, C. X., Waters, R. S., Oladehin, A., Johnson, E. F., McCandlish, C. A. and Dykes, R. W. (1994). Large unresponsive zones appear in cat somatosensory cortex immediately after ulnar nerve cut. Can. J. Neurol. Sci. **21**: 233-247.
- Lundy-Ekman, L. (1998). Neuroscience: Fundamentals for Rehabilitation. Toronto, Saunders.
- Macdonald, R. L. and Olsen, R. W. (1994). GABAA receptor channels. Annu. Rev. Neurosci. **17**: 569-602.

- McCandlish, C. A., Li, C. X., Waters, R. S. and Howard, E. M. (1996). Digit removal leads to discrepancies between the structural and functional organization of the forepaw barrel subfield in layer IV of rat primary somatosensory cortex. Exp. Brain Res. **108**: 417-426.
- Merzenich, M. M. and Jenkins, W. M. (1993). Reorganization of cortical representations of the hand following alterations of skin inputs induced by nerve injury, skin island transfers, and experience. J. Hand Ther. **6**: 89-104.
- Merzenich, M. M. and Kaas, J. H. (1982). Reorganization of mammalian somatosensory cortex following peripheral nerve injury. Trends Neurosci. **5**: 434-436.
- Merzenich, M. M., Kaas, J. H., Wall, J., Nelson, R. J., Sur, M. and Felleman, D. (1983). Topographic reorganization of somatosensory cortical areas 3b and 1 in adult monkeys following restricted deafferentation. Neuroscience **8**: 33-55.
- Merzenich, M. M., Kaas, J. H., Wall, J. T., Sur, M., Nelson, R. J. and Felleman, D. J. (1983b). Progression of change following median nerve section in the cortical representation of the hand in areas 3b and 1 in adult owl and squirrel monkeys. Neuroscience **10**: 639-665.
- Merzenich, M. M., Nelson, R. J., Stryker, M. P., Cynader, M. S., Schoppmann, A. and Zook, J. M. (1984). Somatosensory cortical map changes following digit amputation in adult monkeys. J. Comp. Neurol. **224**: 591-605.

- Mountcastle, V. B. (1957). Modality and topographic properties of single neurons of cat's somatic sensory cortex. J. Neurophysiol. **20**: 408-434.
- Mountcastle, V. B. and Powell, T. P. (1959). Neural mechanisms subserving cutaneous sensibility with special reference to the role of afferent inhibition in sensory perception and discrimination. Bull. of the John Hopkins Hospital **105**: 201 - 232.
- Munger, B. L. and Pubols, L. M. (1972). The sensorineural organization of the digital skin of the raccoon. Brain, Behav. Evol. **5**: 367-393.
- Northgrave, S. A. and Rasmusson, D. D. (1996). The immediate effects of peripheral deafferentation on neurons of the cuneate nucleus in raccoon. Somatosens. Motor Res. **13**: 103-113.
- Otsuka, M., Kravitz, E. and Potter, D. D. (1967). Physiological and chemical architecture of a lobster ganglion with particular reference to gamma-aminobutyrate and glutamate. J. Neurophysiol. **30**: 725 - 752.
- Patel, I. M. and Chapin, J. K. (1990). Ketamine effects on somatosensory cortical single neurons and on behavior in rats. Anesth. Analg. **70**: 635 - 644.
- Pons, T. P., Garraghty, P. E., Ommaya, A. K., Kaas, J. H., Taub, E. and Mishkin, M. (1991). Massive cortical reorganization after sensory deafferentation in adult macaques. Science **252**: 1857-1860.
- Rasmusson, D. D. (1982). Reorganization of raccoon somatosensory cortex following removal of the fifth digit. J. Comp. Neurol. **205**: 313-326.



- Rasmusson, D. D. (1996). Changes in the organization of the ventroposterior lateral thalamic nucleus after digit removal in adult raccoon. J. Comp. Neurol. **364**: 92-103.
- Rasmusson, D. D., Louw, D. and Northgrave, S. A. (1993a). The immediate effects of peripheral denervation on inhibitory mechanisms in the somatosensory thalamus. Somatosens. Motor Res. **10**: 69-80.
- Rasmusson, D. D. and Nance, D. (1986). Non-overlapping thalamocortical projections for separate forepaw digits before and after cortical reorganization in the raccoon. Brain Res. Bull. **16**: 399-406.
- Rasmusson, D. D. and Northgrave, S. A. (1997). Reorganization of the raccoon cuneate nucleus after peripheral denervation. J. Neurophysiol. **78**: 2924-2936.
- Rasmusson, D. D., Northgrave, S. A. and Louw, D. F. (1996). Changes in the organization of the Ventroposterior Lateral thalamic nucleus after digit removal in adult raccoon. J. Comp. Neurol. **364**: 92 - 103.
- Rasmusson, D. D. and Turnbull, B. G. (1983). Immediate effects of digit amputation on SI cortex in the raccoon: unmasking of inhibitory sites. Brain Res. **288**: 368-370.
- Rasmusson, D. D., Webster, H. H. and Dykes, R. W. (1992). Neuronal response properties within subregions of raccoon somatosensory cortex one week after digit amputation. Somatosens. Mot. Res. **9**: 279-289.

- Rasmusson, D. D., Webster, H. H., Dykes, R. W. and Biesold, D. (1991). Functional regions within the map of a single digit in raccoon primary somatosensory cortex. J. Comp. Neurol. **313**: 151-161.
- Recanzone, G. H., Allard, T. T., Jenkins, W. M. and Merzenich, M. M. (1990). Receptive-field changes induced by peripheral nerve stimulation in SI of adult cats. J. Neurophysiol. **63**: 1213-1225.
- Recanzone, G. H., Merzenich, M. M., Jenkins, W. M., Grajski, K. A. and Dinse, H. R. (1992). Topographic reorganization of the hand representation in cortical area 3b of owl monkeys trained in a frequency-discrimination task. J Neurophysiol **67**: 1031-1056.
- Rice, F. L. and Rasmusson, D. D. (2000). Innervation of the digit on the forepaw of the raccoon. J. Comp. Neurol. **41**: 467-490.
- Schwark, H. D., Tennison, C. F., Ilyinsky, O. B. and Fuchs, J. L. (1999). Inhibitory influences on receptive field size in the dorsal column nuclei. Exp Brain Res **126**: 439-442.
- Sillito, A. M. (1975a). The contribution of inhibitory mechanisms to the receptive field properties of neurones in the striate cortex of the cat. J Physiol (Lond) **250**: 305-329.
- Sillito, A. M. (1975b). The effectiveness of bicuculline as an antagonist of GABA and visually evoked inhibition in the cat's striate cortex. J Physiol (Lond) **250**: 287-304.

- Smits, E., Gordon, D. C., Witte, S., Rasmusson, D. D. and Zarzecki, P. (1991). Synaptic potentials evoked by convergent somatosensory and corticocortical inputs in raccoon somatosensory cortex: substrates for plasticity. J Neurophysiol **66**: 688-695.
- Sur, M., Merzenich, M. M. and Kaas, J. H. (1980). Magnification, receptive-field area, and "hypercolumn" size in areas 3b and 1 of somatosensory cortex in owl monkeys. J Neurophysiol **44**: 295-311.
- Towe, A. L. and Harding, G. W. (1970). Extracellular microelectrode sampling bias. Exp Neurol **29**: 366-381.
- Turnbull, B. G. and Rasmusson, D. D. (1990). Acute effects of total or partial digit denervation on raccoon somatosensory cortex. Somatosens. Mot. Res. **7**: 365-389.
- Turnbull, B. G. and Rasmusson, D. D. (1991). Chronic effects of total or partial digit denervation on raccoon somatosensory cortex. Somatosens. Mot. Res. **8**: 201-213.
- von Békésy, G. (1967). Sensory Inhibition. Princeton, New Jersey, Princeton University Press.
- Wall, J. T. and Cusick, C. G. (1984). Cutaneous responsiveness in primary somatosensory (S-I) hindpaw cortex before and after partial hindpaw deafferentation in adult rats. J. Neurosci. **4**: 1499-1515.
- Wall, J. T., Felleman, D. J. and Kaas, J. H. (1983). Recovery of normal topography in the somatosensory cortex of monkeys after nerve crush and regeneration. Science **221**: 771-773.

- Wall, J. T. and Kaas, J. H. (1986). Long-term cortical consequences of reinnervation errors after nerve regeneration in monkeys. Brain Res **372**: 400-404.
- Warren, R., Tremblay, N. and Dykes, R. W. (1989). Quantitative study of glutamic acid decarboxylase-immunoreactive neurons and cytochrome oxidase activity in normal and partially deafferented rat hindlimb somatosensory cortex. J Comp Neurol **288**: 583-592.
- Welker, E., Soriano, E., Dorfl, J. and van der Loos, H. (1989a). Plasticity in the barrel cortex of the adult mouse: transient increase of GAD-immunoreactivity following sensory stimulation. Exp. Brain Res. **78**: 659-664.
- Welker, E., Soriano, E. and Van der Loos, H. (1989). Plasticity in the barrel cortex of the adult mouse: effects of peripheral deprivation on GAD-immunoreactivity. Exp Brain Res **77**: 441-52.
- Welker, W. I. and Seidenstein, S. (1959). Somatic sensory representation in the cerebral cortex of the raccoon (*Procyon lotor*). J. Comp. Neurol. **111**: 469-501.
- Wong-Riley, M. T. (1989). Cytochrome oxidase: an endogenous metabolic marker for neuronal activity. Trends Neurosci. **12**: 94-101.
- Wong-Riley, M. T. T. and Welt, C. (1980). Histochemical changes in cytochrome oxidase of cortical barrels after vibrissal removal in neonatal and adult mice. Proc. Natl. Acad. Sci. USA **77**: 2333-2337.

Xu, J. and Wall, J. T. (1999). Functional organization of tactile inputs from the hand in the cuneate nucleus and its relationship to organization in the somatosensory cortex. J Comp Neurol **411**: 369-389.

Zarzecki, P., Witte, S., Smits, E., Gordon, D. C., Kirchberger, P. and Rasmusson, D. D. (1993). Synaptic mechanisms of cortical representational plasticity: somatosensory and corticocortical EPSPs in reorganized raccoon SI cortex. J. Neurophysiol. **69**: 1422-1432.